Development of a Novel Active Muzzle Brake for an Artillery Weapon System

BY

D. J. Downing **B. Eng Mechanical**
Post Graduate Diploma Aeronautical

Dissertation presented in partial fulfillment of the requirements for the degree Master of Engineering at the Potchefstroomse Universiteit vir Christelike Hoër Onderwys.

Promoter: **Prof E.H. Mathews**

November 2002

CONFIDENTIAL

Abstract

A conventional muzzle brake is a baffle device located at some distance in front of the muzzle exit of a gun. The purpose of a muzzle brake is to alleviate the force on the weapon platform by diverting a portion of the muzzle gas resulting in a forward impulse being exerted on the recoiling parts of the weapon. A very efficient muzzle brake unfortunately gives rise to an excessive overpressure in the crew environment due to the deflection of the emerging shock waves.

The novel active muzzle brake of this dissertation is based on a concept developed by Qinetiq. The novel technique involves the main brake chamber being closed for a very short period of time after the projectile has uncorked from the barrel eliminating the main emerging shock wave from developing to full strength with the result that the novel muzzle brake gives rise to a very low overpressure. This has the advantage that the gun crew suffers from less strain to the ears and vulnerable organs. Inherently the novel brake suffers a loss in efficiency due to the chamber being closed for a while and a method had to be developed to improve the efficiency of the conventional part.

This dissertation deals with the development of a novel active muzzle brake intended for a 155 mm artillery weapon, but scaled to an 88 mm 25 pounder G1 as an interim phase. Several constraints and requirements have been set regarding the physical properties and performance criteria of the prototypes. The interim phase of the project was executed within three years in which six prototypes were developed and evaluated. Major challenges in the development were to design a control and restoring mechanism that would survive the harsh conditions at muzzle exit and to enhance the efficiency. The establishment of linear movement of the closure mechanism and friction springs as the restoring mechanism was a major breakthrough in this respect. The first four prototypes were designed using empirical data and first order modeling as background while a CFD technique was used to refine the last two prototypes.

Of the six prototypes developed, the first two were unsuccessful in demonstrating the novel technique. The one was unable to survive the muzzle exit conditions and the control mechanism on the second muzzle brake opened too soon. Of the remaining four, the last prototype passed all the specified constraints and proved to be a candidate for the 155mm upgrade. Not only was the structure robust enough, the general appearance of the novel muzzle brake is futuristic. This prototype is also a candidate if a much more efficient muzzle brake, with similar overpressure characteristics of a less efficient muzzle brake, is needed.

Samevatting

'n Konvensionele tromprem is 'n wapen komponent bestaande uit een of meer skotte wat op'n vasgestelde afstand voor aan 'n loop geheg word. Die doel van 'n tromprem is om die kragte wat oorgedra word na die wapen platform te verlig deurdat 'n gedeelte van die ontsnappende gas gedeflekteer word met die gevolg dat 'n voorwaartse impuls krag op die teruglopende gedeelte van die wapen uitgeoefen word. Ongelukkig het die gebruik van 'n baie effektiewe tromprem 'n oormaat oordruk in die bemanning gebied tot gevolg weens die defleksie van die skokgolwe.

Die aktiewe tromprem is gebaseer op 'n konsep wat deur Qinetiq ontwikkel is. Die aktiewe tegniek behels dat die tromprem kamer afgesluit word vir 'n baie kort tydpose nadat die projektiel die tromp verlaat het. Dit veroorsaak dat die skokgolf verhoed word om tot volle sterkte te ontwikkel met die gevolg van 'n laer oordruk. Dit het die voordeel dat die wapen bemanning se ore en organe aan 'n laer drukpeil blootgestel word. Ongelukkig word die effektiwiteit van die aktiewe tromprem nadelig beïnvloed deur die afsluiting van die tromprem kamer en 'n metode moes ontwikkel word om die effektiwiteit van die konvensionele gedeelte van die aktiewe tromprem te verhoog.

Hierdie verhandeling behels die ontwikkeling van 'n aktiewe tromprem afgestem vir 'n 155 mm artillerie wapen afgeskaal na 'n 88 mm 25 ponder G1 wapen as 'n interim fase. Verskeie beperkings is op die fisiese en werkverrigting eienskappe van die prototipes geplaas. Die interim fase van die projek is binne 'n bestek van drie jaar afgehandel waartydens ses prototipes ontwikkel en getoets is. Die ontwerp van die beherende en terugkerende meganisme om die fel omstandighede by trompverlating te deurstaan asook om die effektiwiteit te verhoog was die vernaamste uitdagings in die ontwikkeling. 'n Belangrike deurbraak was die gebruik van weerstands ("Friction") vere as terugkerende meganisme en deur die afdigtings meganisme as 'n gly bewegende item te monteer. Die eerste vier prototipes is ontwerp vanuit empiriese data sowel as deur van eerste orde modellering gebruik te maak. Rekenaargesteunde vloeisimulasies is gebruik om die laaste twee prototipes mee te optimeer.

Die eerste twee prtotipes wat ontwikkel is, was onsuksesvol om die aktiewe beginsel mee te demonstreer. Die een prototype het nie die toestande by trompverlating deurstaan nie, terwyl die beheer meganisme van die ander een te vroeg oopgemaak het. Die laaste prototipe van die oorblywende vier het al die beperkings en vereistes wat gestel is, geslaag en is 'n sinvolle kandidaat vir opgradering na 155 mm. Die struktuur was nie net sterk genoeg nie, maar het 'n

futuristiese voorkoms. Hierdie prototype is ook 'n kandidaat indien 'n baie effektiewe tromprem met vergelykende oordruk eienskappe as 'n minder effektiewe tromprem benodig word.

Acknowledgements

I would like to express my gratitude to:

- Prof E.H. Mathews and D.T. Claassen for guidance and support.
- Dr K.C. Phan as originator of the novel active theory and for his valuable contribution on the project as technical manager and specialist scientist of Qinetic.
- T. Nieuwoudt for his contribution on concept designs, concepts illustrations and general project support.
- My wife Petra for the moral support and encouragement.

Special circumstances

It was requested that this dissertation be classified as "Confidential". The development of a novel active muzzle brake is unique in the world and may prove to have great financial benefits if successful as it can be retro–fitted on existing artillery weapons. The development of a conventional muzzle brake involves complex technology that is not freely available. Due to that fact the amount of references available is also limited. Any more references if possible to be obtained on this technology may be a benefit for this dissertation.

List of Figures

List of Tables

Table of Contents

Nomenclature

A list of all principal symbols is given below.

ΔP	Peak overpressure level (kPa)
E	Recoil energy (J)
E_k	Kinetic energy (J)
F_{FS}	Impulse force on friction spring (kN)
P	Breech or muzzle pressure (MPa)
M	Mass of recoiling parts (kg)
M_{prop}	Propellant mass (kg)
M_{proj}	Projectile mass (kg)
M_{DB}	Dynamic body mass (kg)
V_t	Internal volume of barrel and chamber (m^3)
A	Cross sectional area of barrel (m^2)
a_0	Velocity of sound (m/s)
R	Average specific energy of propellant (kJ/kg/K)
S	Spring travel (mm)
T	Muzzle temperature (K)
$\dot{m}$	Mass flow (kg/s)
n	modified speed-up factor
t	Time at any instant (s)
V_0	Gas velocity (m/s)
V_{DB}	Dynamic body velocity (m/s)

W	Spring work (J)

Greek symbols

β	Peak overpressure ratio
η_M	Muzzle brake efficiency
γ	Specific heat
η	Covolume (m^3/kg)
ρ	Density (kg/m^3)
α	Baffle exit angle (deg)
τ	B-duration (s)

Footnotes

i	any instant
0	at the instant of shot ejection
B	with a muzzle brake
NB	without a muzzle brake

Abbreviations

CFD	Computational fluid dynamics
HEBSIM	High enthalpy blast simulator
FCT	Flux Corrected Transform
FEA	Finite element analysis
PPL	Peak pressure level
SANDF	South African National Defense Force
FS	Friction spring

Chapter 1

Introduction

The reader is familiarized with the general purpose of a muzzle brake, the principle of a novel muzzle brake and how it differs from a noise suppressor. The objective for this project as well as the possible benefits is described. The technical capability of Qinetiq on CFD simulations and the use of the HEBSIM gun tunnel are also described.

1. INTRODUCTION

1.1 General purpose of a muzzle brake.

When a weapon is fired, there are two events contributing to the total recoil force acting on the recoiling parts of the weapon. These are the impulses due to acceleration of the projectile while in bore and the discharge of the propellant gas from the barrel after the projectile has uncorked from the muzzle exit.

There are two methods that are commonly used to lessen the effect of the recoil forces on the weapon platform. One of these is achieved by using a hydraulic-pneumatic system as the recoil mechanism to distribute the response of the recoil impulse over a longer time span. The other method of reducing the maximum recoil force is by a gas dynamics means using a muzzle device commonly known as a muzzle brake.

Essentially, a muzzle brake is a baffle device located at some distance in front of the muzzle exit. It is attached to the muzzle and has a centre opening to allow the passage of the projectile. During the gas ejection phase, a portion of the exhausting propellant gas interacts with the baffle surface and is diverted from the axial direction. The deflection of the gas flow produces a forward impulse on the muzzle brake, thus reducing the net recoil impulse on the weapon platform. By increasing the forward impulse by using a more efficient muzzle brake, a greater reduction in the net recoil impulse can be achieved. It is possible to design a highly efficient muzzle brake by manipulation of the geometric parameters of the muzzle brake device. However, an efficient muzzle brake often produces a severe blast overpressure in the region behind the muzzle exit including the crew area. This leads to severe strain to the ears and vulnerable organs of the crew.[1] It is therefore necessary to compromise between efficiency and blast overpressure and it is not uncommon to accept a reduced muzzle brake performance to allow for an acceptable overpressure.

1.2 Objective for this research

The design of a conventional muzzle brake suffers inherently from the need to balance muzzle brake performance and blast overpressure. With the development of weapons with extended ranges, more effective muzzle brakes are required as the increased chamber pressures result in higher recoil forces. The more efficient muzzle brakes result in a more severe blast overpressure that is hazardous in especially a weapon without a turret. The development of a

novel active muzzle brake with the same performance characteristics of an efficient conventional muzzle brake, but with greatly reduced overpressure characteristics will therefore be a valuable advantage with the result that the gun crew will suffer less strain to the ears and vulnerable organs and it will lead to improved communication between the gun crew and fire control personnel.

A novel muzzle brake, with active elements to prevent the main emerging shock wave from developing to full strength and being deflected by the brake surface, was experimentally proven conceptually at Qinetiq (Originally RARDE and then DERA – Defense Research Agency in the UK) using a blast simulator or HEBSIM (High enthalpy blast simulator). It was the purpose of this project to extend this novel technology and to develop an active muzzle brake for a real weapon. A joint project designated Powhan started in 1996 by LIW (a division of Denel) with Qinetiq and LIW as the collaborative companies to develop this novel active muzzle brake over a period of three years.

This development will prove a financial advantage if successful as there are many weapons with overpressure hazards in the world that can be retro-fitted with such a device. Using this novel technique it will also be possible to design a much more efficient muzzle brake with similar overpressure characteristics of a less efficient muzzle brake permitted that the overpressure definition within the gun crew area is according to acceptable limits.

1.3 Technical background

The ballistic cycles during the launching of a projectile include the internal ballistic cycle, the intermediate ballistic cycle, the flight ballistic cycle and the terminal ballistic cycle.[2] The internal ballistic cycle relates to the movement of the projectile after the combustion of the charge until muzzle exit. The intermediate ballistic cycle is short lived by definition and relates to the uncorking of the projectile and the discharge of the barrel. The flight and terminal ballistic cycles are of less importance to the content of this dissertation.

The flows around the muzzle brake are associated with the intermediate ballistic cycle. The flows in this area are very complex and highly unsteady. Several computational techniques have been developed to simulate these types of fluid dynamics. The work in the next two paragraphs was undertaken by Qinetiq as specialist support for this project.

1.3.1 Computational simulation - CFD

Computational Fluid Dynamic techniques had been developed through the 60's and 70's and by the early 1980's were being exploited for shock tube applications. The UK, US and Canada developed the capability to compute muzzle brake flows as part of The Technical Co-operation Program. The joint study was led by Qinetiq and an axis-symmetric version of a single baffle version was completed in 1986 and computed by ten different codes in the three countries. This code has since been developed in three dimensions. The 3-D code, the Flux Corrected Transport algorithm was used to calculate the fluid forces on the active elements and aid in the design of the novel muzzle brake. The code is a fully dynamic 3D Euler solver which uses cell blocking and has a reliable and robust anti-diffusion routine [3].

This computational technique will be supplemented with empirical calculations and first order modeling.

1.3.2 HEBSIM simulation

The high enthalpy blast simulator was developed in the early eighties. This simulator was the first of its kind in the world. Essentially, the simulator is made up of the high pressure elements of a hypersonic gun tunnel. The layout is illustrated in figure 1. It consists of a breech, a double diaphragm block, a piston, a compression barrel, an end cap and a 25.4 mm diameter blast tube. The end cap is closed by a thick diaphragm between the blast tube and the compression barrel.

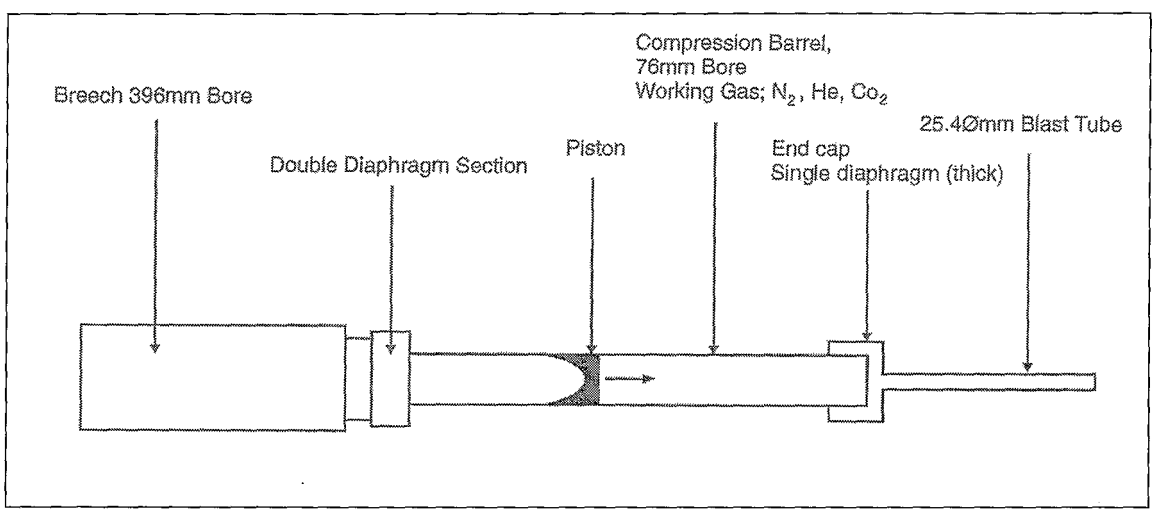

Figure 1. Schematic of HEBSIM facility.

The operating principle of HEBSIM is similar to that of a hypersonic gun tunnel. Initially the breech is filled with a high pressure gas. Following the rapture of the double diaphragms, the

piston accelerates along the compression barrel producing a series of compression waves ahead of the piston. These waves coalesce to form a shock wave which compresses and heats the working gas. As the volume between the end cap and the moving piston decreases and the pressure increases rapidly, the thick diaphragm bursts. This gas propagates into the blast tube and is released into the surrounding area as an expanding blast wave. Nitrogen or helium is normally employed as the working gas in the compression barrel.

To facilitate the muzzle brake type of work, a recoil rig was designed for the HEBSIM. There had been two studies using this test setup. The one was an empirical attempt to evaluate the design variables and their effect on the muzzle brake performance.[4] These variations were the geometric angle of the baffle, the stand off distance from the muzzle and a two baffle configuration. The second study was done to add the novel type of control surfaces and restoring mechanism to the muzzle brake of the first test setup.[5] Upon using these simulations the concept of the novel technique was proven. The prototype that was evaluated on the HEBSIM is illustrated as figure 3 in paragraph 2.2.1.

1.4 The principle of the novel active muzzle brake.

The designing of the novel muzzle brake involves the understanding of the muzzle gas phenomena in the intermediate ballistic region previously described in paragraph 1.3.

The projectile compresses the ambient air in front of it to form a weak shock that ends as a bow shock when the projectile emerges from the barrel. This shock is known as the precursor, is spherical in shape and has a weak intensity that is quickly diminished. As the projectile uncorks from the barrel, it is followed by a violent eruption of propellant gases. This process may be thought of as a three dimensional fluid piston expanding in air. The propellant gas forms the muzzle blast that is a system of normal and oblique shock waves that form the boundaries of the region that is known as the shock bottle. The main traveling shock is formed in the air by the released propellant gases when they flow past the projectile and induce a succession of shocks behind the first, but weaker projectile induced shock. This shock grows in strength as more gas is fed into the shock bottle. The initial stage of all of these phenomena is illustrated in figure 2.

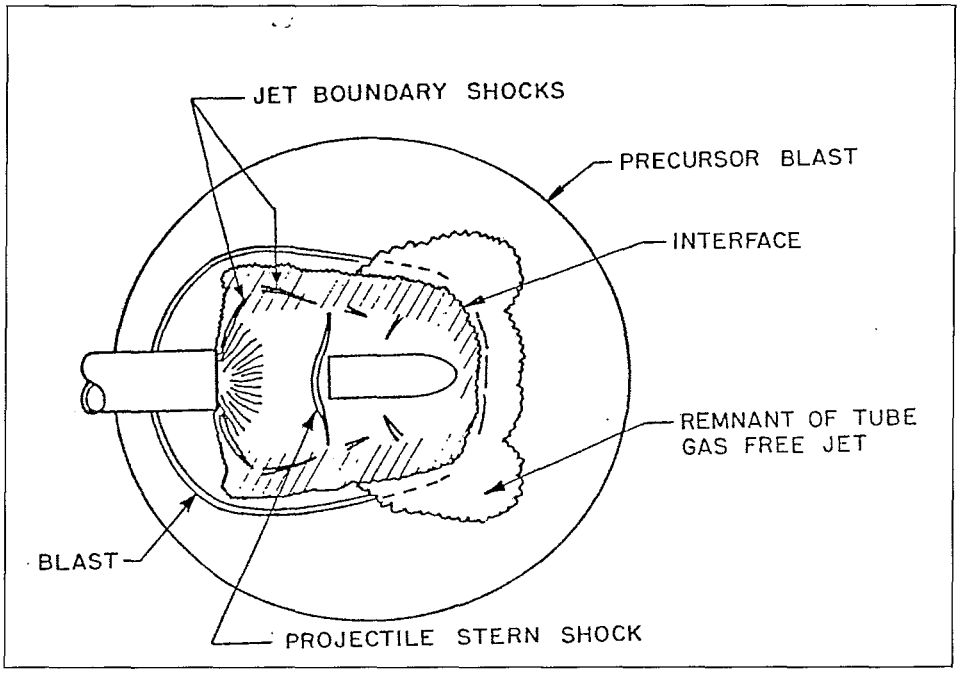

Figure 2. Initial stage of shock bottle formation.

As the projectile travels through the air the shock bottle expands rapidly. An observer (typical one of the crew) will experience the overpressure effect when the shock wave passes him.

The introduction of a muzzle brake to the scenario described above alters the distribution of mass flow from the muzzle brake. Schlenker[6] assumes that the muzzle brake causes two distinct shock spheres to be developed, each of which propagates with an independent decay rate until coalescence. Constructive interference within the crew area is assumed. This relates to an increase of the overpressure at the crew positions.

The novel technique revolves around the principle of retaining the main shock wave inside the muzzle brake until the shock strength has been diminished and to prevent it from being deflected to the rear. The end result needs to be that the same effect regarding overpressure is experienced as when firing without a muzzle brake attached to the muzzle end, but without compromising on the efficiency.

1.5 The novel brake versus noise suppressors.

The use of noise suppressors or silencers on small hand weapons to alleviate the intense noise of firing the guns is quite common. Such devices are most uncommon to large weapons like artillery due to the dimensions required. A noise suppressor for artillery weapons is sometimes

used at test ranges where the blast will cause damage to surrounding structures or cause discomfort to people living within the close vicinity like Europe and the United Kingdom with dense population. The typical dimensions of a noise suppressor for a 155 mm artillery weapon are a few meters in diameter and several meters long. This device is not part of the weapon, but placed around the muzzle end during trials while the novel active muzzle brake will be an integral part of the weapon.

The following four operations determine the effectiveness of a noise suppressor.

- It should cool the muzzle gas to the temperature that would prevent re-ignition.
- It should mix muzzle gas with air gradually to prevent atmospheric oxygen from supporting combustion.
- It should decelerate the muzzle gas to prevent shock front formation.
- It should retain the gas until they become relative cool through expansion and thus preventing shock front temperature increases.

Any one or a combination of the above operations must be incorporated in a noise suppressor design to be successful. The novel technique also incorporates the last operation as part of the method.

1.6 General overview of dissertation.

The arrangement of the rest of this dissertation is as follows:

Chapter 2: A technology overview is given of what the project entails regarding the fundamentals of the novel design. The requirements and constraints of the evaluation and design are addressed as well as the risks involved in achieving the goal.

Chapter 3: The theoretical approach to the design methodology is described. The development of the novel muzzle brake prototypes is described. The development is divided in three phases. The first phase served as a characterization phase of the scaled down version of the G5 muzzle brake to a caliber of 88 mm. Two initial prototypes of novel muzzle brakes were developed to gain insight in the structural strength required for the control surfaces and to demonstrate the novel principle. The second

and third phase entailed the development of four further generations of novel designs – being two per phase.

Chapter 4: The evaluation of the three phases is recorded. The conventional scaled down version of the G5 type of muzzle brake was also tested to serve as a reference for the novel designs. The results are given as tables and graphs where required.

Chapter 5: The conclusion of the study is presented. Recommendations for further work based on the final two prototypes that were developed are proposed. These include modifications on the desired prototypes before development and evaluation on the full scale 155 mm commenced.

Chapter 2

Novel muzzle brake technology overview

A technology overview is given of what the project entails regarding the fundamentals of the novel design. A conventional muzzle brake is selected as a baseline to reference the novel muzzle brake prototypes. The requirements and constraints that are placed on the novel muzzle brake are addressed as well as the risks involved in achieving the goal.

2. NOVEL MUZZLE BRAKE TECHNOLOGY OVERVIEW

2.1 *Introduction*

The project has been structured to develop a novel muzzle brake for the application to a 155 mm caliber weapon system. An interim phase on this project had been implemented before an attempt was made to evaluate the novel design on the 155 mm system. This dissertation deals with this interim phase. The interim phase being the development of a novel muzzle brake for an 88 mm weapon also known as the G1 or 25 ponder. This weapon is a pre World War II artillery field cannon designed by the British and was still used until a few years ago as the weapon to fire salutes on parades. The main reason for the choice of this particular weapon was the magnitude of ammunition and weapons freely available from the SANDF, the only disadvantage being the unknown properties of the charges.

2.2 *Concept description*

2.2.1 The novel muzzle brake

The prototype that was evaluated on the HEBSIM is illustrated in figure 3.

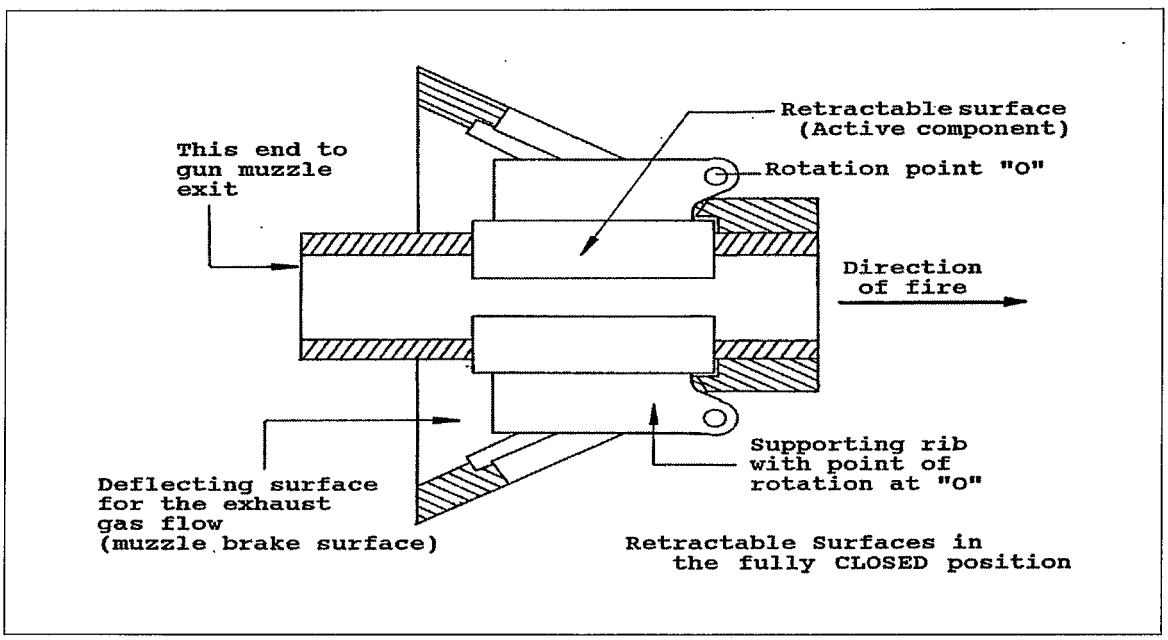

Figure 3. Illustration of earliest Qinetiq novel prototype.

It consists of a set of control surfaces implemented on an existing conventional muzzle brake design. The novel technique utilizes the energy from the propellant gas to operate the control surfaces. These surfaces remain inactive during the passage of the main shock wave allowing it to be discharged at the downstream end of the brake. It becomes active when the gas behind the projectile exerts pressure upon it. These surfaces must be coupled to a restoring mechanism to close the surfaces as soon as the exhaust gas conditions reach equilibrium with the ambient. It is required that the restoring mechanism must operate in a hostile environment and survive repetitive applications of the opening forces.

Several parameters influence the design of the novel muzzle brake. The time delay from the uncorking of the projectile from the baffle to the opening of the control surfaces is a very important factor. This time is governed by the stand-off distance of the baffle(s) from the muzzle exit, by the inertia of the control surfaces and by the return force of the restoring mechanism. This time is very crucial in the sense that it must be long enough to keep the shock wave inside the chamber until decay and short enough to maintain the efficiency needed. An ideal time of 1.5 to 2 ms is envisaged. As the muzzle brake only operates during the time of barrel discharge, much of the propellant gas may escape from the projectile aperture while the control surfaces are closed resulting in a decrease of the muzzle brake efficiency.

A way would have to be found to increase the efficiency of the conventional part of the novel muzzle brake to compensate for the loss during the closed part of the control surfaces. Three ways of doing such had been investigated during the design and evaluation phase of this project. The one method was to add more than one baffle to the conventional part of the muzzle brake. A second method was to change the baffle exit angle at 70 degrees to the bore axis instead of 90 degrees. The third method was to change the stand off distance and respective internal volume of the muzzle brake chamber. By increasing the internal volume of the muzzle brake, a more efficient muzzle brake is created.

2.2.2 Selection of a baseline muzzle brake.

There are several conventional types of muzzle brakes available in the world. The pepper pot types are found mostly on armor weapons and the type with baffles are more common to artillery weapons. The pepper pot types are mere extensions of the barrel with a series of holes with the advantage that fin stabilized projectiles with discardable sabots are supported by the bore, but these type of muzzle brakes are not as efficient as the baffle type.

The conventional configuration as fitted to the 155 mm G5 weapon is one the simplest forms of single baffle types available. The single baffle is mounted at approximate 1.5 calibers in front of the gun barrel exit and the baffle exit angle is at 90 degrees to the bore axis.

The selected configuration should resemble a real in service muzzle brake that has a good record of technical information. At the start of the project it was agreed between the technical managers of LIW and Qinetic that the G5 type of muzzle brake would serve as the standard for reference and comparison. A schematic of the G5 type with the caliber as reference for dimensions is shown in Appendix A.

2.3 Requirements

Two variables are required to assess the performance of a muzzle brake. These are the blast overpressure and muzzle brake efficiency.

For the blast overpressure measurement several parameters are important. The main blast is defined by the peak overpressure level (ΔP) and measured in kPa. From this the peak overpressure ratio (β) is derived.

$$\beta = \Delta P_B / \Delta P_{NB} \qquad (2.1)$$

For both the parameters of ΔP_B and ΔP_{NB} the kPa value is used. This non-dimensional value is useful for comparing results of different trials where the ΔP values could have been influenced by external factors beyond control. (For instance the effect of the main blast shield that was fitted on the G1 weapon in this project.)

Applicable impulse noise limits are set on the expected number of daily exposures the crew can withstand per day given a certain location and the type of hearing protection that is used. These limits are defined by MIL-STD 1474[7] and depend on the B-duration of the overpressure measurement and the peak pressure level.

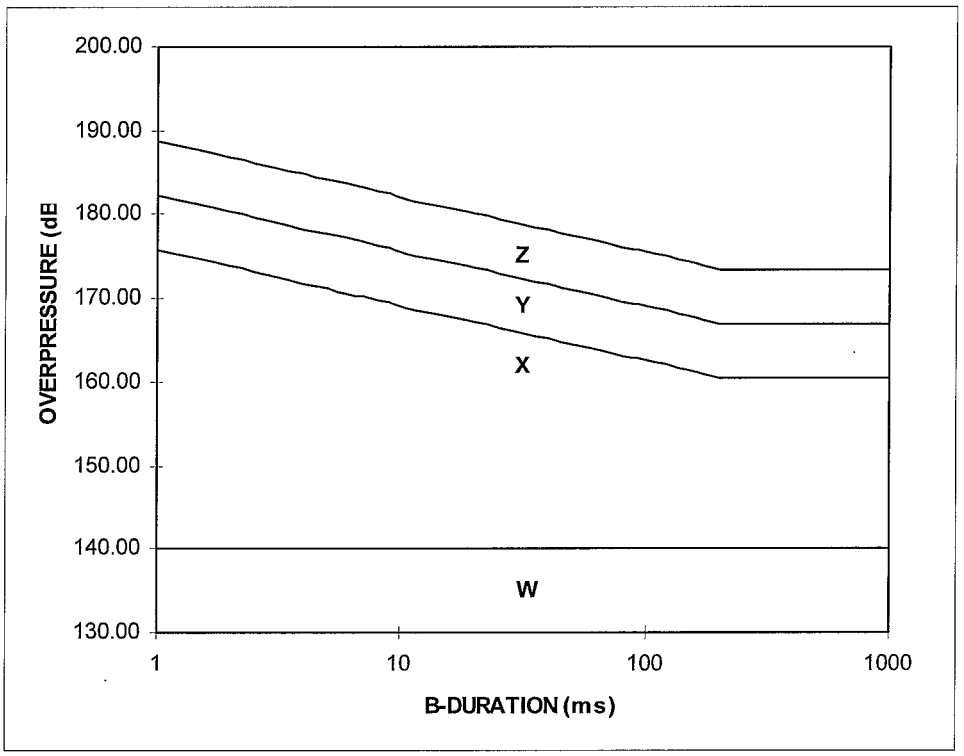

Figure 4. Peak pressure level and B-duration limits for impulse noise.

The B-duration or pressure envelope duration is the duration of the primary portion of impulse noise plus the duration of significant subsequent fluctuations. These durations are considered to be the time interval during which the envelope of pressure fluctuations (positive and negative) is within 20 dB of the peak pressure level.

For the purpose of this graph, the peak pressure level (PPL) is expressed in decibel (dB).

$$PPL = 20\log(\Delta P) + 153.98 \qquad (2.2)$$

The maximum number of exposures allowed per day is given in table 1.

Impulse noise limit range	No protection	Single protection	Double protection
W	Unlimited exposure		
X	0	2000	40000
Y	0	100	2000
Z	0	5	100

Table 1. Number of exposures per impulse noise limit range

Single protection can be either ear plugs or muffs whereas double protection is both ear plugs and muffs. The use of double protection is a disadvantage as the communication ability of the crew is impaired.

The muzzle brake efficiency is expressed world wide in several ways of which three are most commonly used.[8] The first one being propulsion index. Propulsion index relates to the total recoil momentum. A second one being performance index that relates to the momentum of the propellant gas. The third one being efficiency that relates to the recoil energy. The recoil energy is used as the basis for the assessment of the muzzle brake efficiency (η_M) of the novel muzzle brake. A muzzle brake that is added to a weapon system may affect either the recoil force or the recoil displacement or both. The recoil energy takes the recoil force and recoiling displacement of the recoiling parts of the weapon in consideration. The recoil energy is directly proportional to the mass of the recoiling parts as an increase in recoiling mass contributes to a lower recoil energy being measured. The G1 weapon was dismantled and each part that contributes to the recoiling mass was weighed. Due to the different muzzle brakes that needed to evaluated, each muzzle brake contributed a different mass to the recoiling parts of the weapon. The muzzle brake efficiency of each configuration needs to be corrected by the mass of the recoiling parts in relation to the no brake situation and is calculated by using the following formulae.

$$\text{Muzzle brake efficiency } (\eta_M) = 1 - (E_B / E_{NB}) * (M_B / M_{NB}) * 100\ \% \qquad (2.3)$$

A scaled down model of the 155mm G5 muzzle brake was manufactured for the 88 mm weapon. The characteristics of this conventional muzzle brake were used as the reference for the novel design. The weapon was also fired without a muzzle brake to serve as a baseline for the overpressure ratio and muzzle brake efficiency calculation. A dummy mass was added to the barrel when fired without a muzzle brake that partially compensated for the loss of recoiling mass.

2.4 Constraints

There are two types of constraints that have a major influence on the weapon system.

The first one is the physical constraint which is associated with the parameters such as mass, interchangeability and replaceability. The second is the operational constraint which is associated with the parameters such as overpressure and recoil efficiency.

The mass of the present 155mm G5 muzzle brake is 100 kg. This mass can be regarded as a point mass at the end of the barrel. A mass constraint of 120 kg for the point mass of the novel design was envisaged, but the closure mechanism may add more mass to the system if it is distributed over a longer length of the barrel. A mass constraint of 35 kg for the point mass of the 88 mm G1 was envisaged. The constraint regarding the closure mechanism mass as in the case of the 155mm G5 is also applicable. The individual components of the novel muzzle brake are to be interchangeable. If such a device goes into production, no matched components are envisaged. Ideally the device must also be replaceable on the standard weapon systems without replacing the barrel. Alternatively the barrel can be refashioned to accommodate the interfaces of the new device.

The second one is the operational constraint. There are two operational constraints. The one is the overpressure measurements at the crew operating positions and the second one being the efficiency of the novel muzzle brake.

The overpressure for the novel muzzle brake must be such that the protection of the crew must be alleviated with one level in relationship to the conventional muzzle brake (From double protection to single protection for a designated crew position) or alternatively must be alleviated from a higher impulse limit to a lower limit. (From Z to Y or from Y to X.). Refer to the graph in figure 4 and table 1 in paragraph 2.3. This change in overpressure relates to a difference of 6.5 dB. An increase of 6 dB in the PPL value is equivalent to double the intensity of the previous PPL value when evaluated as kPa.

The efficiency of the novel muzzle brake must not be less than 35%. This is equivalent to the efficiency of the present 155mm G5 muzzle brake that corresponds to a value of 32.1 % for the scaled down version on the G1.

2.5 *Risks*

The following risk elements have been identified for the development of this novel design.

- The design is not field proven. When this project started off no muzzle brake of this design was built anywhere in the world. The technology has only been tested on a

scaled down version in the laboratory on the HEBSIM at Qinetiq. Furthermore, the real hardware on a weapon system may give completely different results.

- The designed hardware may be unreliable. The control flaps and restoring mechanism are highly complex and may be fragile. A design of such nature may have high failure rates in the harsh environment that is found at the muzzle exit.

- It may be difficult to maintain the designed hardware. The weight and complexity of the hardware may result in the muzzle brake being difficult to maintain.

- The prototypes would only be evaluated at an elevation of 0 degrees. The introduction of evaluation at different elevation angles would place a too large burden on the ammunition budget and time allocated for the trials. It was decided that the evaluation at different elevation angles would only be addressed once a prototype was chosen as a candidate for the 155 mm G5. It may be that the chosen novel muzzle brake gives very good results on overpressure alleviation at a certain elevation, but poor results at a different angle.

Chapter 3

Development of the novel muzzle brake prototypes

The theoretical background to the design methodology is described. The development of the novel muzzle brake prototypes is described. The development is divided in three phases. The first phase served as a characterization phase of the scaled down version of the G5 muzzle brake to a caliber of 88 mm. Two initial prototypes of novel muzzle brakes were developed to gain insight in the structural strength required for the control surfaces and to demonstrate the novel principle. The second and third phase entailed the development of four further generations of novel designs – being two per phase.

3. DEVELOPMENT OF THE NOVEL MUZZLE BRAKE PROTOTYPES

3.1 Theoretical background

3.1.1 Charge characterization (Internal ballistic simulation)

The charges of the G1 25 pounder date back to the early 1960's and no data on the chemical composition of any nature exists. Somchem, (the division of DENEL that is responsible for charge development) was tasked to analyze one of the charges and to perform an internal ballistic simulation. The internal ballistic simulation is a computational simulation of the in bore conditions from shot start and up to muzzle exit. The conditions at muzzle exit are important for the design calculations of a muzzle brake and the parameters in table 2 were obtained from the internal ballistic simulation.

Muzzle velocity	470.1 m/s
Base pressure at muzzle exit	47.4 MPa
Time at muzzle exit	7.8550 ms

Table 2. Conditions at muzzle exit.

The important propellant gas parameter values that are needed as input to the discharge simulation are derived from the charge parameters of the internal ballistic program and are calculated on a mass base from the igniter and two propellant type characteristics. These values are presented in table 3.

Average specific energy of propellant	971000 J/kg
Flame temperature of propellant	2629 K
Gas temperature at muzzle exit	1652 K
Ratio of specific heats of gas	1.2587
CoVolume	1.1410e-3 m^3/kg

Table 3. Propellant gas parameters.

The computational results are presented in Appendix B.

3.1.2 Barrel discharge simulation

The muzzle brake utilizes the propellant gas to impose a forward impulse on the recoiling parts and is only operative in the time that the gas from the barrel is discharged. The discharging of the barrel has been simulated using a computational program developed by the author (programmed in Delphi). The output of this simulation gives the muzzle pressure, muzzle temperature, density and gas velocity as a function of time after shot ejection and this data served as inputs for the CFD simulations as done by Qinetiq. The maximum available impulse at the muzzle end is also calculated.

Several methods for calculation of the breech pressure when the projectile uncorks from the barrel are documented by Corner[9] namely.

- Hugeniot Method
- Corner Method
- Modified Rateau Method

The problem of the emptying of a reservoir of perfect gas by expansion through a nozzle was first treated by Hugeniot[9], by assuming that the state of flow at any instant was the same as would be set up eventually in steady flow with the reservoir pressure existing at that instant. This hypothesis of quasisteady flow is plausible, provided that the reservoir pressure is not falling too rapidly. Rateau[9] used the same assumption about quasi-steady flow and introduced the covolume term into the calculations. As the covolume is taken into account, the gas is thus not assumed to be a perfected gas anymore. Corner[9] assumes adiabatic expansion after the instant of shot ejection and introduces the effect of the rarefraction wave that enters the barrel after shot ejection and travels towards the breech.

The author investigates these three methods to calculate the breech pressure decay after shot ejection using the measured results from the 88 mm weapon as reference. None of these methods gave very accurate results. The author derived another method that gives very accurate values and refers to it as the Modified Hugeniot method. The graphical presentation of the simulated and measured values of the breech pressure decay is illustrated in figure 5.

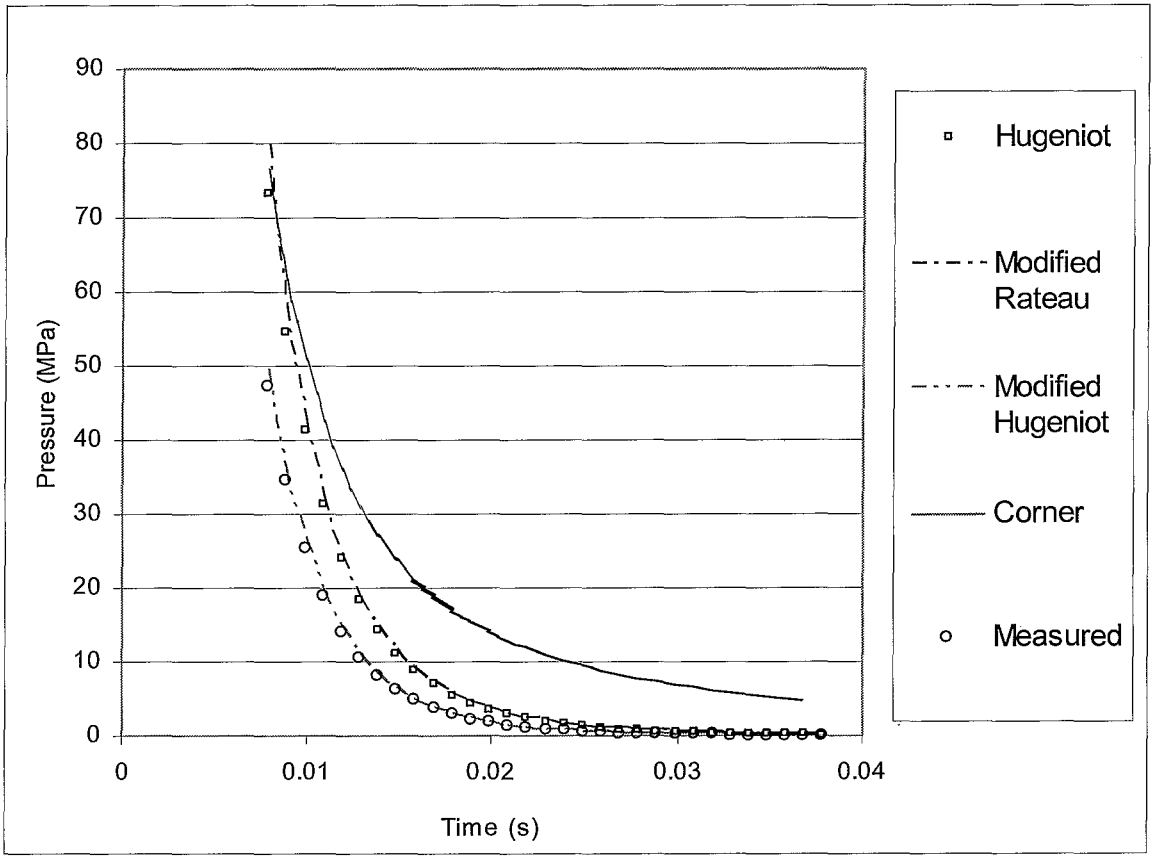

Figure 5. Graphical presentation of breech pressure decay.

Hugeniot[10] derived a formula to calculate the mass flow of the gas from the barrel and is calculated by.

$$\dot{m}_0 = \frac{M_{prop}.A}{V_t}\left(1+\frac{M_{prop}}{6.\gamma.M_{proj}}\right).\sqrt{\gamma.RT_0.\left[\frac{(\gamma-1).M_{prop}}{6.\gamma.M_{proj}}+1\right].\left(\frac{2}{\gamma+1}\right)^{\frac{\gamma+1}{\gamma-1}}} \qquad (3.1)$$

and

$$\dot{m}_i = \dot{m}_0.\left(1+\frac{t}{\theta}\right)^{\frac{1+\gamma}{1-\gamma}} \qquad (3.2)$$

where $$\theta = \frac{V_t}{6.A.(\gamma-1)}\sqrt{\frac{\left(\frac{\gamma+1}{2}\right)^{\frac{\gamma+1}{\gamma-1}}}{\gamma.RT_0.\left(1+\frac{(\gamma-1).M_{prop}}{6.\gamma.M_{proj}}\right)}} \qquad (3.3)$$

The pressure at the breech or muzzle and the muzzle temperature are a function of the mass flow rate as derived by the author and are calculated by.

$$P_i = P_0(\dot{m}_i / \dot{m}_0)^{\gamma} \quad (3.4)$$

$$T_i = T_0(\dot{m}_i / \dot{m}_0)^{\gamma/(\gamma-1)} \quad (3.5)$$

The values of P_0 and T_0 are obtained from the internal ballistic simulation results.

The density and gas velocity at the muzzle exit are governed by formulae (3.6) and (3.7) respectively. The formula denoting the density closely relates to the *Ideal Gas Law* and is corrected with the covolume parameter for the non ideal behavior of the propellant gas.

$$\rho_i = 1/(R.T_i / P_i + \eta) \quad (3.6)$$

$$V_0 = \dot{m}_i / (\rho_i . A) \quad (3.7)$$

Using this approach, the results attached as Appendix C were obtained and are illustrated in the accompanying graphs as depicted from figures 6 to 9.

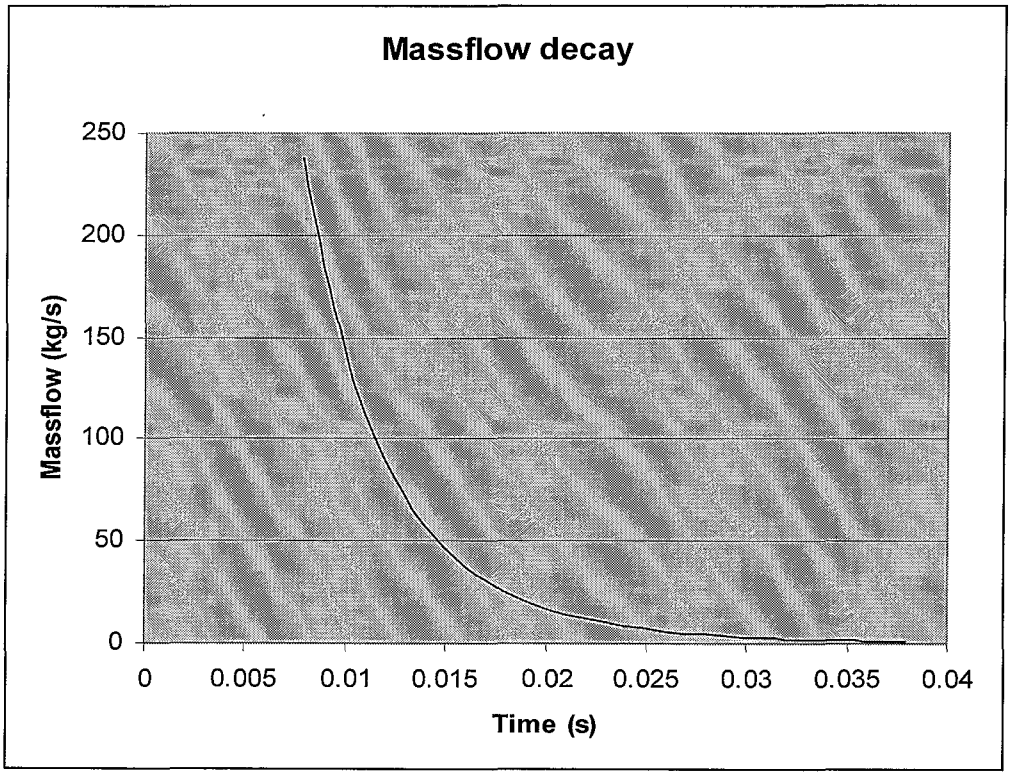

Figure 6. Graphical presentation of mass flow decay.

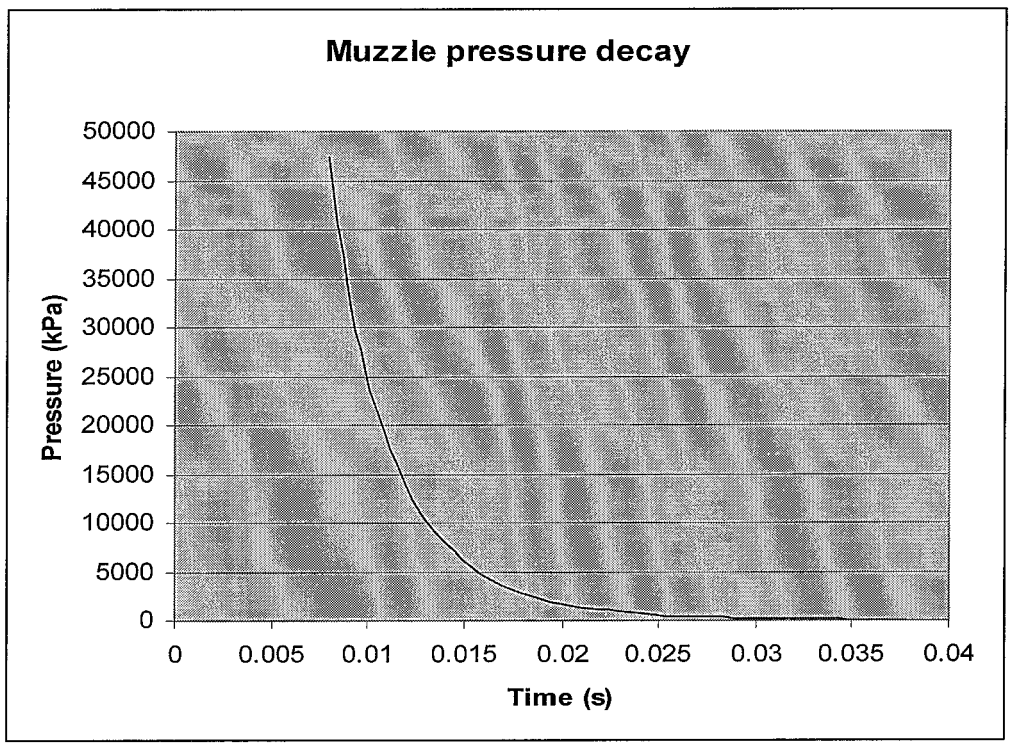

Figure 7. Graphical presentation of muzzle pressure decay

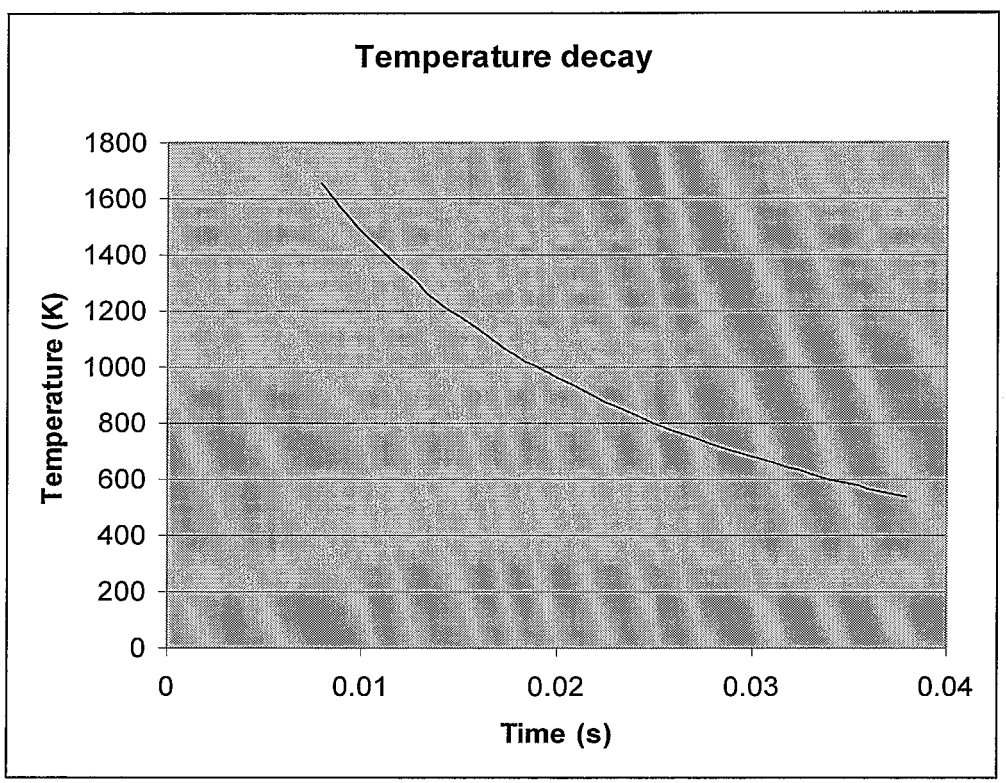

Figure 8. Graphical presentation of temperature decay

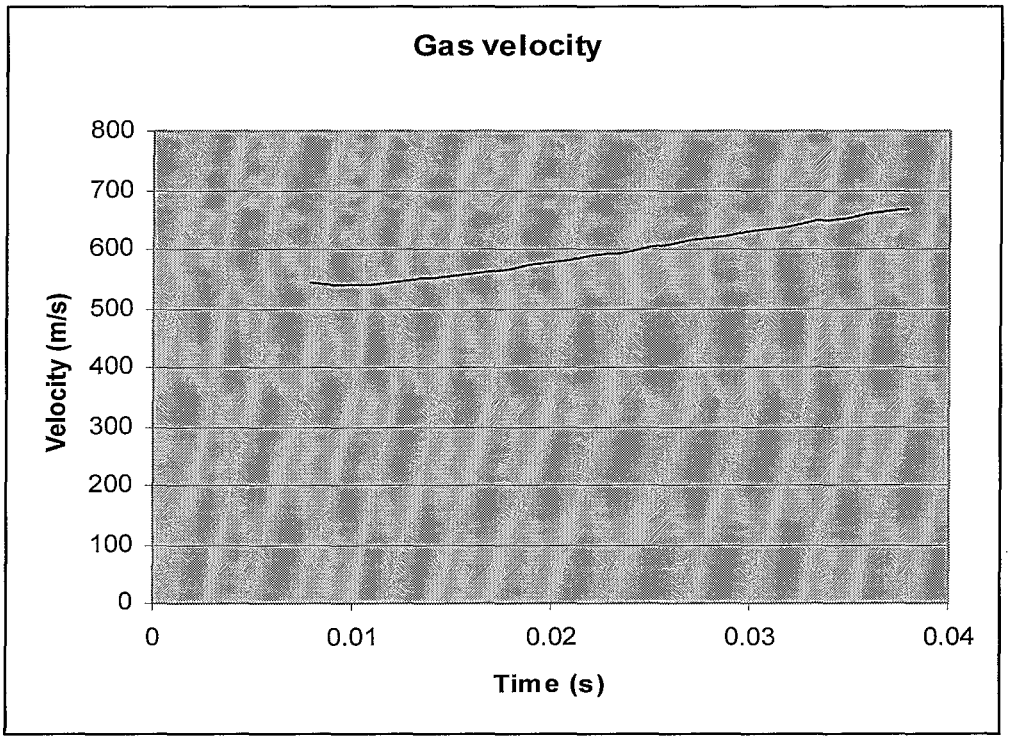

Figure 9. Graphical presentation of gas velocity.

3.1.3 Analysis of important parameters

Phan[4], Schmidt[11] and Salsbury[12] investigated the design variables and their effect on the muzzle brake performance and derived some empirical standards. The forward impulse force of a single baffle muzzle brake increases as the stand-off distance of the baffle to the muzzle exit is increased up to a certain value. The force decreases however if the stand-off distance is increased further. The stand-off value to give a maximum impulse lies between 1.5 and 2 calibers and depend on the size of the baffle. A larger baffle results in a larger stand off value needed to reach a maximum impulse. According to Salsbury this standoff distance can be even extended to 2.5 calibers. From 2 to 2.5 calibers the efficiency stays relatively constant while the overpressure produced is almost 16 percent less than at 1.5 calibers. The stand-off distance of the G5 and scaled down version at a value of 1.5 calibers can therefore still be increased to obtain a more effective muzzle brake with a benefit in overpressure according to Salsbury.

Hugenoit[10] defined two types of muzzle brakes. The one type is designated a closed type and relates typical to a muzzle brake where the exit ports for the gas is in the shape of nozzles and the gas is assumed to fill the nozzle completely. The second type is designated the open type

and is typically of the shape of the G5 type of muzzle brake. For the open type of muzzle brake the gas expands freely before it impinges upon the baffle/s.

The mathematical model that describes the mass flow through the nozzles of a closed muzzle brake resembles that being used to calculate the discharge from fume extractors or also known as bore evacuators.

A first order value of the impulse force generated by an open single baffle muzzle brake is given by.[10]

$$F_m = \dot{m}.a_0.n.r.(1-\cos\alpha)/f \tag{3.8}$$

where $$a_0 = \sqrt{\gamma.R.T_0} \tag{3.9}$$

These formulae relates to the momentum equation that governs simple mass addition as described by Zucrow & Hoffman[13] while in the case of a muzzle brake the mass is removed from the main stream flow.

The value of n is proportional to the exit speed of the gas from the baffle and is defined as a modified speed-up factor. The value of r relates to the amount of gas that is deflected and depends on the radius of the shock envelope. The value of r is always nearly equal or smaller than 1. The calculation of the shock front envelope radius was formulated by Soifer[14] using a cylindrical blast wave solution. The value of f is a fixed value of 1.33.

The author developed a first order mathematical model to determine the impulse force exerted by an open double baffle muzzle brake. When utilized as a conventional muzzle brake, version 3 as described in 3.2.3 resembles an open double muzzle brake. The total forward impulse is given by

$$F = \sum \dot{m}.a_0.n.r.(1-\cos\alpha)/f \tag{3.10}$$

An important part of this model resides in the mass flow distribution. A typical double baffle muzzle brake is illustrated in figure 10. The different flow rates are given by.

$$\dot{m}_3 = \dot{m}_{in} - \dot{m}_1 - \dot{m}_2 \tag{3.11}$$

and

$$\dot{m}_{uit} = \dot{m}_3 - \dot{m}_4 - \dot{m}_5 \tag{3.12}$$

The mass flow distribution is also dependent on the aperture sizes of the expansion holes. This resembles the flow through the stator blades of a turbine cascade. [15]

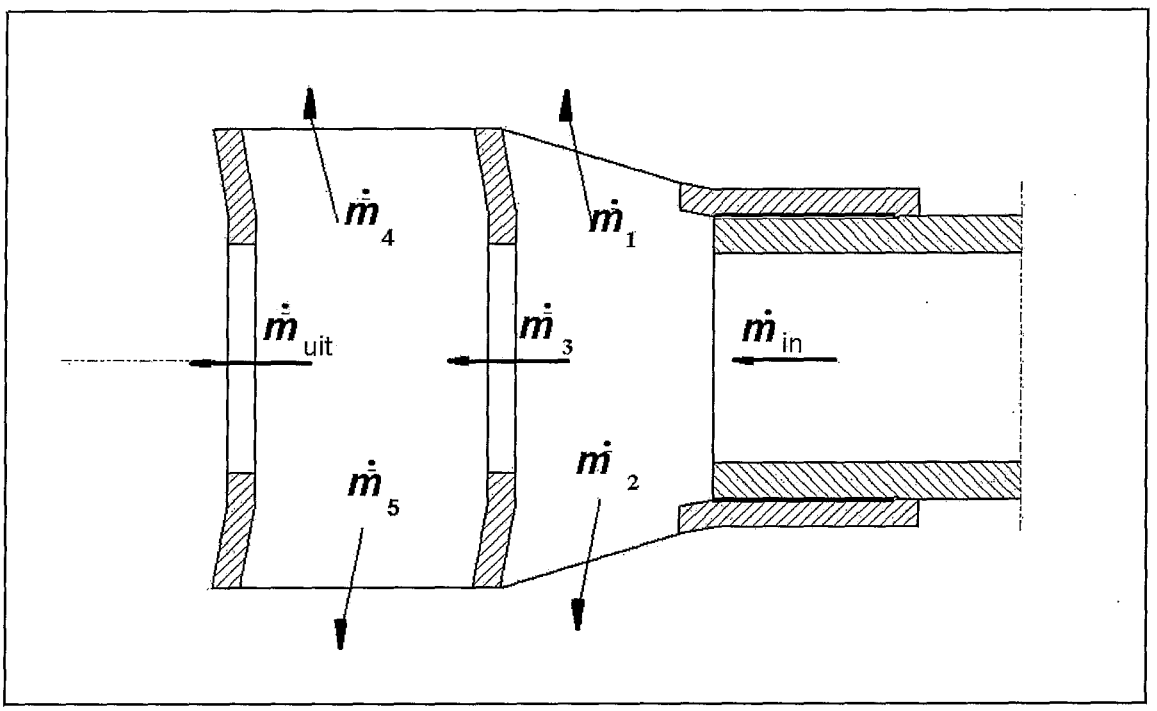

Figure 10. Mass flow distribution through baffles.

3.2 *Development of prototypes*

The development of the prototypes commenced chronographically over time and can be classified in three phases. The prototypes developed during a specific phase were evaluated at the end of that phase as described in the evaluation section or chapter 4 of this dissertation before commencing with the next phase. The limitations and advantages of every prototype were exploited and used as the drivers for the prototypes developed during the next phase. It was not envisaged on the offset of the project that there will be three phases. The designs of the prototypes from the first two phases were based on empirical data and basic modeling as described in paragraph 3.1.3. The two prototypes of the last phase were optimized with the aid of CFD modeling from Qinetiq and with inputs that were derived as described in paragraph 3.1.2.

3.2.1 **Phase 1 – Version 1**

The main purpose of the first design phase was to characterize the scaled down version of the G5 type of muzzle brake. A muzzle brake was manufactured in accordance to the G5 type as illustrated in Appendix A and scaled to the caliber value of the G1.

A second muzzle brake was manufactured to the same proportions, with a baffle stand off distance of 1.7 calibers. This prototype was fitted with active components and designated as version 1. This was done to demonstrate that the novel principle would be a useful application on a weapon system. The main body was a scaled down version of the G5 open type of brake as mentioned, while the control flaps were rotating doors that open to form a baffle with a 70° angle to the rear to form a stand off distance of 1.5 calibers. The control flap mechanism was designed based on the prototype that was tested by Qinetic on the HEBSIM. The restoring mechanisms were made up of several blade springs to form a torsion bar. Each control flap had its own torsion bar that was pre - tensioned to hold the flap in the closed position.

Version 1 with the control flaps in the open position and with the blade springs removed is shown in figure 11. A schematically view is shown in Figure 12 that illustrates a sectional view, with one flap in the closed position and the other in the open position.

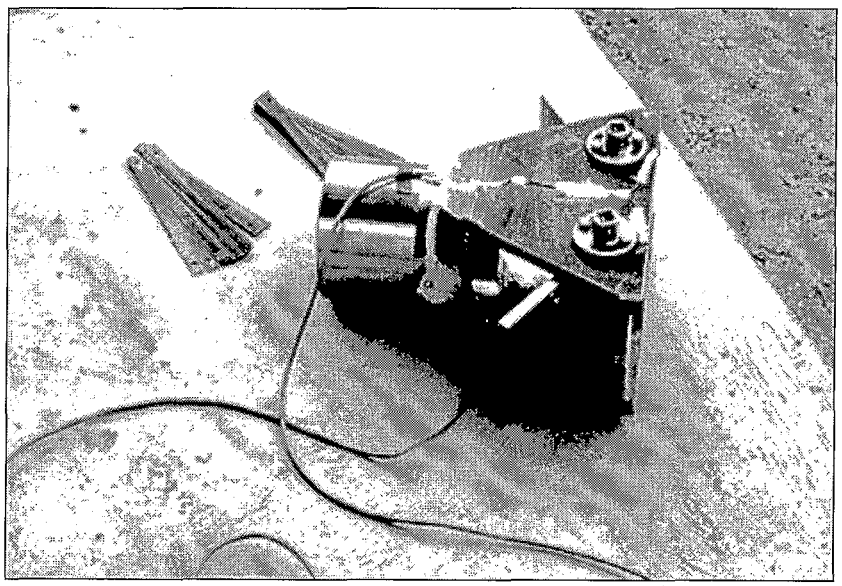

Figure 11. Version 1

The mass of the total muzzle brake was 31.7 kg that is well within the set constraint of 35 kg.

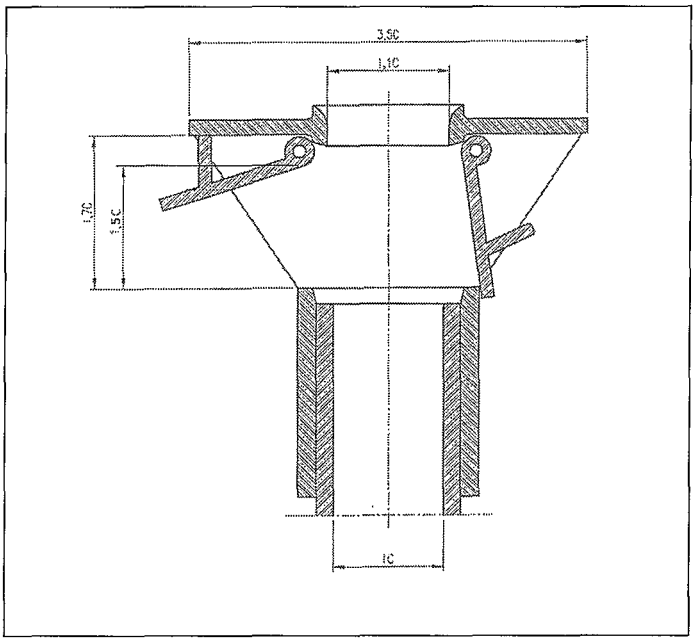

Figure 12. Sectional view, with one flap in the closed and the other in the open position.

i. Limitations of version 1.

- The control flaps could not withstand the harsh environment and were completely sheared off when tested on the G1.
- The internal volume of the muzzle brake was less than the initial scale down G5 type. Due to this the expected improved efficiency due to the increased return angle of 70 degrees for the gas flow did not materialize. (The stand off distance remained similar to 1.5 calibers with the flaps in the open position.)
- The novel principle could not be demonstrated when evaluated on the G1 due to the hardware failure.

3.2.2 Phase 1 – Version 2

Version 2 was a completely different type of muzzle brake and is an adaptation of a pepper pot type of muzzle brake that is used on armor weapons. The use of pepper pot type muzzle brakes are described in paragraph 2.1.2. This design was done as a fall back plan in case version 1 did not meet expectations. The apertures of the gas ports on the muzzle brake were five cylindrical slots and the control mechanism was an inner sleeve with five identical slots that is offset to close off the gas ports. This type of muzzle brake is a closed type as described in paragraph 3.1.3.

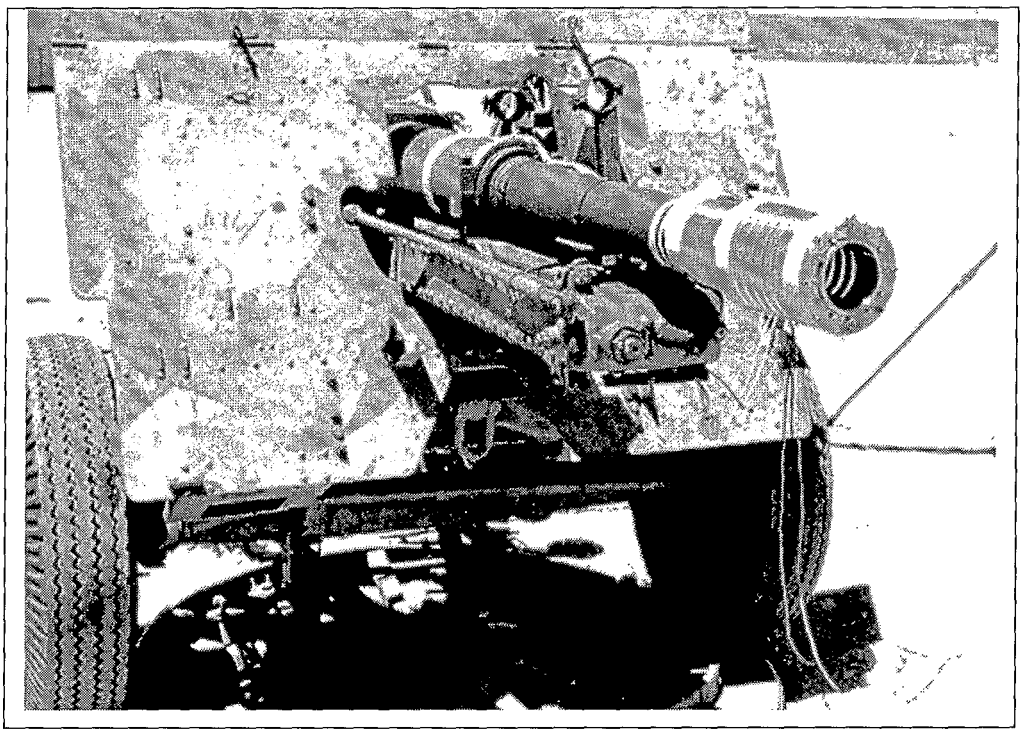

Figure 13. Version 2 mounted on a G1 gun.

Version 2 is shown mounted on the G1 weapon in figure 13. Version 2 is illustrated in figure 14 with the inner sleeve in the initial position before the projectile uncorks from the barrel when the inner sleeve closes off the gas exit ports.

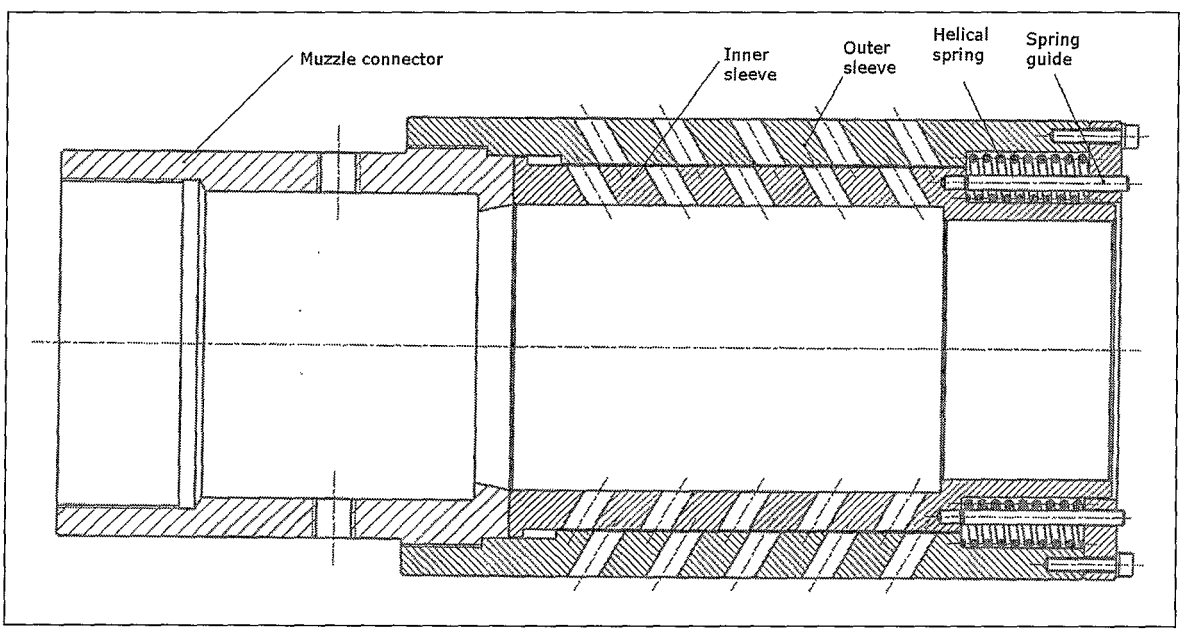

Figure 14. Illustration of sleeve in closed position – version 2.

In order to open the gas exit ports, the inner sleeve was moved axially by the acceleration of the recoiling parts of the weapon when it is fired to minimize the delay time. The restoring mechanism was seven helical springs that acts on the inner sleeve to close the apertures after the shot was fired. The springs were guided with rods that were screwed into the inner sleeve.

i. Limitations of version 2.

- The sleeve was activated by the acceleration, but unfortunately this happened before the projectile uncorked from the muzzle end, with the result that the muzzle brake operated as a conventional muzzle brake.
- The efficiency of the muzzle brake was low compared to the conventional baffle type of muzzle brake.
- The novel principle was not demonstrated due to the inner sleeve opening the gas ports too soon.

ii. Strong points of version 2.

- The muzzle brake suffered no structural damage to any of its components.
- The concept of linear movement in respect to rotational movement of the closure mechanism as in version 1 proved to be a much better solution.
- The muzzle brake had an aesthetical appearance on the weapon.

3.2.3 Phase 2 – Version 3

The muzzle brake was redesigned from version 2 to the following extent and was designated version 3:

- The opening direction of the sleeve was changed to open against the effect of acceleration. It was changed as such that the ports had to be activated by the pressure of the escaping gas rather than the acceleration. Refer to chapter 4.2 on evaluation of Phase 1.
- The multiple slots were replaced with only two slots of 0.6 calibers wide.
- Two baffles were added to increase the efficiency of the muzzle brake.

The muzzle brake type could now be described as an open type in comparison to the closed type of version 2 and a picture of version 3 is shown in figure 15.

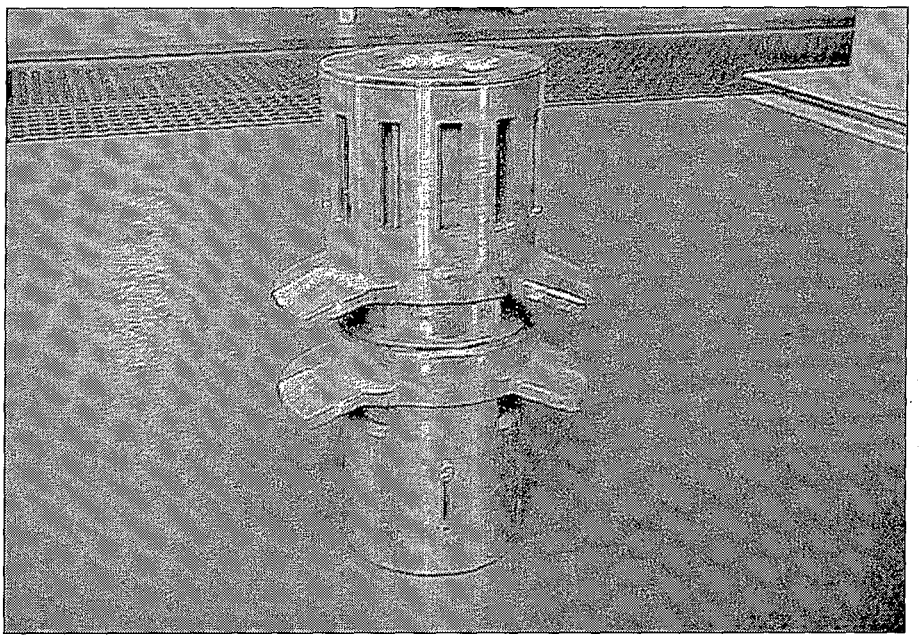

Figure 15. Version 3.

The total mass of the muzzle brake was 54 kg of which the dynamic body contributes a value of 15.7 kg. This total mass is seen as a point mass added in front of the barrel.

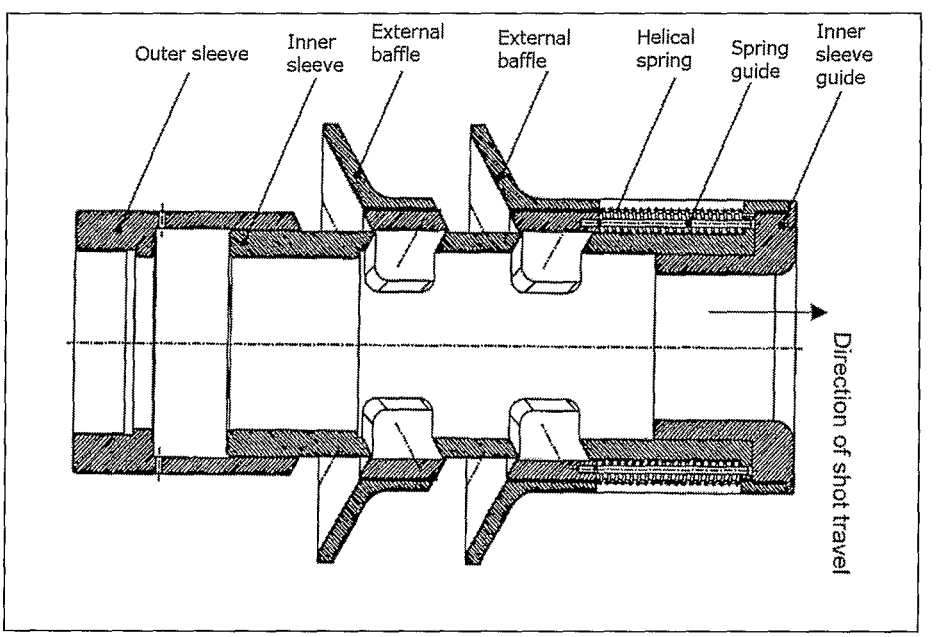

Figure 16. Illustration of sleeve in closed position – version 3

Version 3 is illustrated in figure 16 with the inner sleeve closing off the gas exit ports. This is the initial position before the projectile uncorks from the barrel.

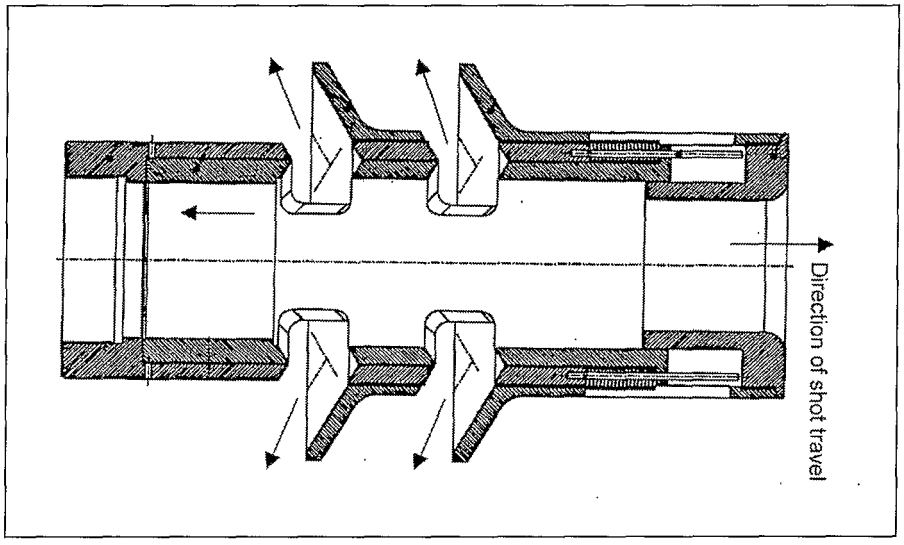

Figure 17. Illustration of sleeve in open position – version 3.

Version 3 is illustrated in figure 17 with the inner sleeve opened due to the differential in gas pressure.

Helical springs were used as the closing mechanism as with version 2. The springs were also guided with rods, but these were screwed into the outer sleeve. The external and internal baffles were screwed onto the outer sleeve and locked. The inner sleeve was guided by the spring rods that prevent it from turning and was supported with the inner sleeve guide that screws into the front portion of the external baffle.

The dimensions of the inner sleeve were optimized to achieve the lowest possible mass and inertia for the shortest delay time when the sleeve opens. A FEA method was used to evaluate the stress and displacement of the inner sleeve. The radial displacement of the sleeve was to be within a reasonable limit to prevent contact with the outer sleeve. A limit of 0.2 mm (0.1 mm on radius) was set and the sleeve designed to be within that limit. The initial design was done on first order principles (thick walled cylinder) without taking the stress concentration of the two holes into consideration. The FEA simulation of the displacement in the radial direction is shown in figure 18. It is evident from that figure that the sleeve will deform in access of 1 mm. The sleeve was optimized to a minimum volume as illustrated in figure 19 giving a displacement of only 0.002 mm.

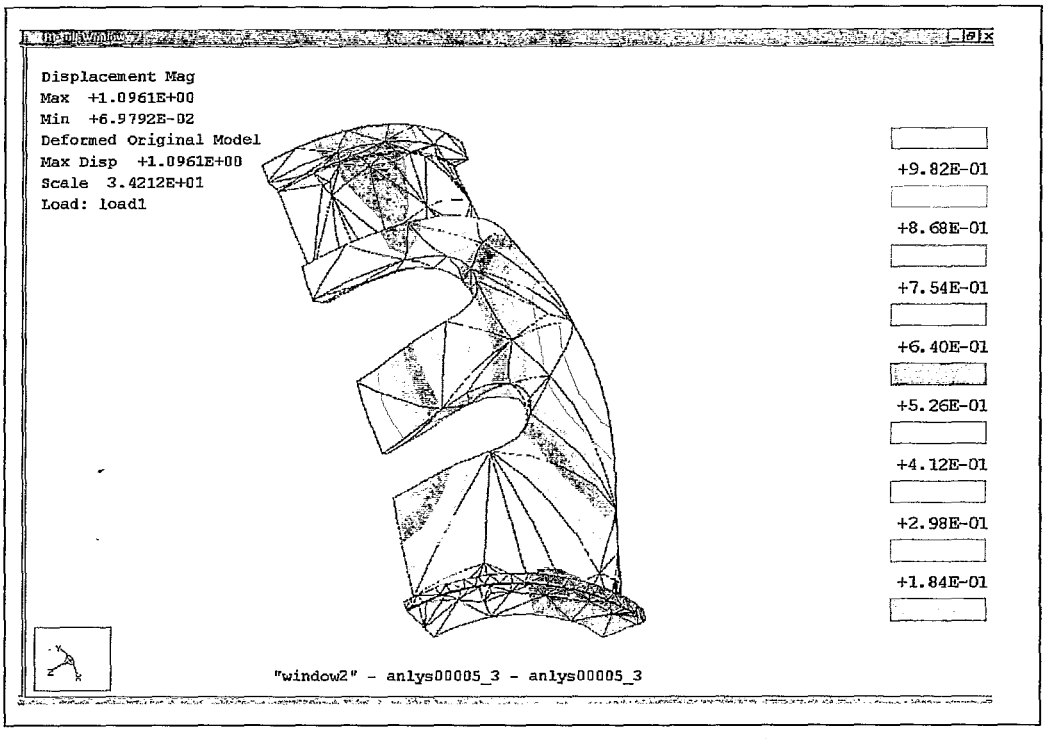

Figure 18. Residual displacement of inner sleeve. (Initial design)

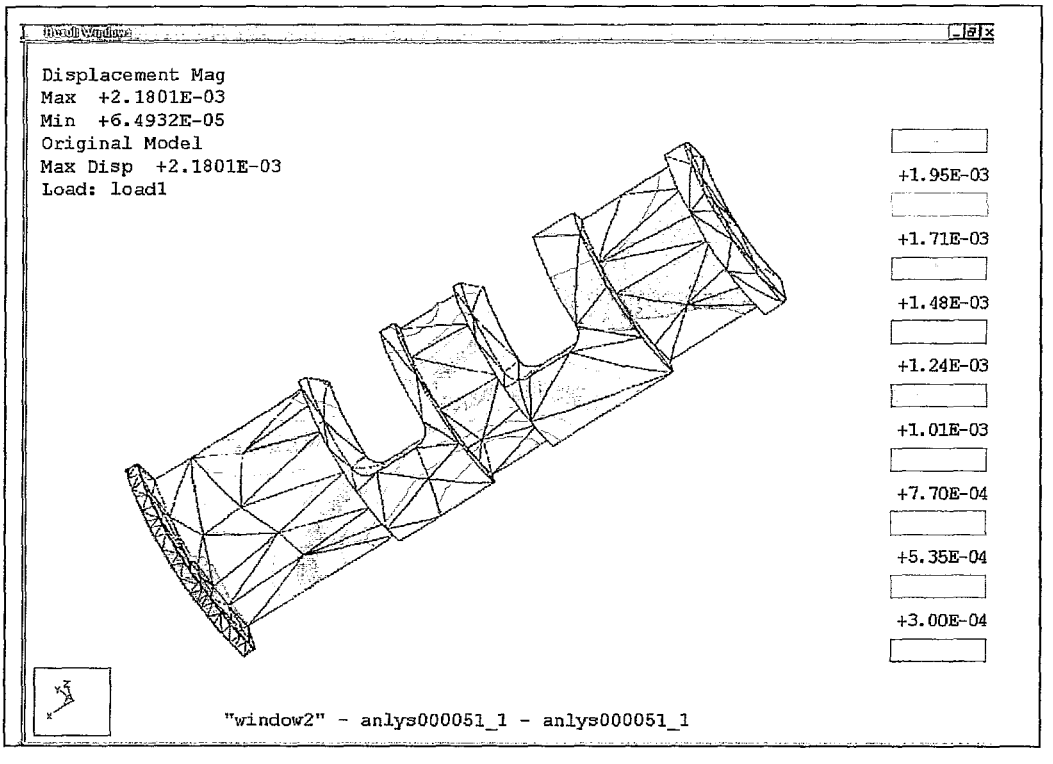

Figure 19. Residual displacement of inner sleeve. (Improved design)

i. Limitations of version 3.

- The helical springs were plastically deformed after the evaluation shots were fired.
- The double baffles increased the efficiency, but the blast overpressure also increased. This was probably due to the fact that the propellant gas was not adequately expanded and the shockwave had not been depleted before the sleeve opened. Due to this fact, the further upgrading and exploration of this concept was not concluded in phase 3.
- The point mass value of 54 kg exceeded the mass constraint of 35 kg.

ii. Strong points of version 3.

- The muzzle brake had an aesthetical appearance on the weapon.

3.2.4 Phase 2 – Version 4

This version is an adaptation of version 1 and the rotational movement of the control surface was replaced by linear movement. From this configuration and onwards the terminology of control surfaces was replaced with dynamic body due to the appearance of the structure.

The appearance of version 4 is shown in figure 20 and a sectional view with the dynamic body in the closed position in figure 21.

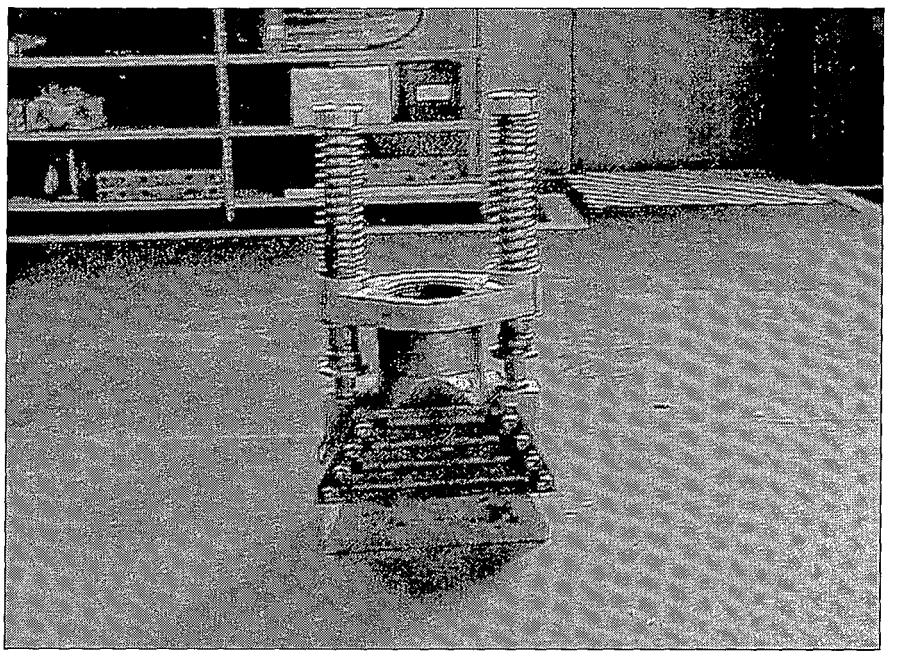

Figure 20. Version 4.

The total mass of the muzzle brake was 56 kg of which the dynamic body contributes a value of 15.9 kg. This total mass is seen as a point mass added in front of the barrel.

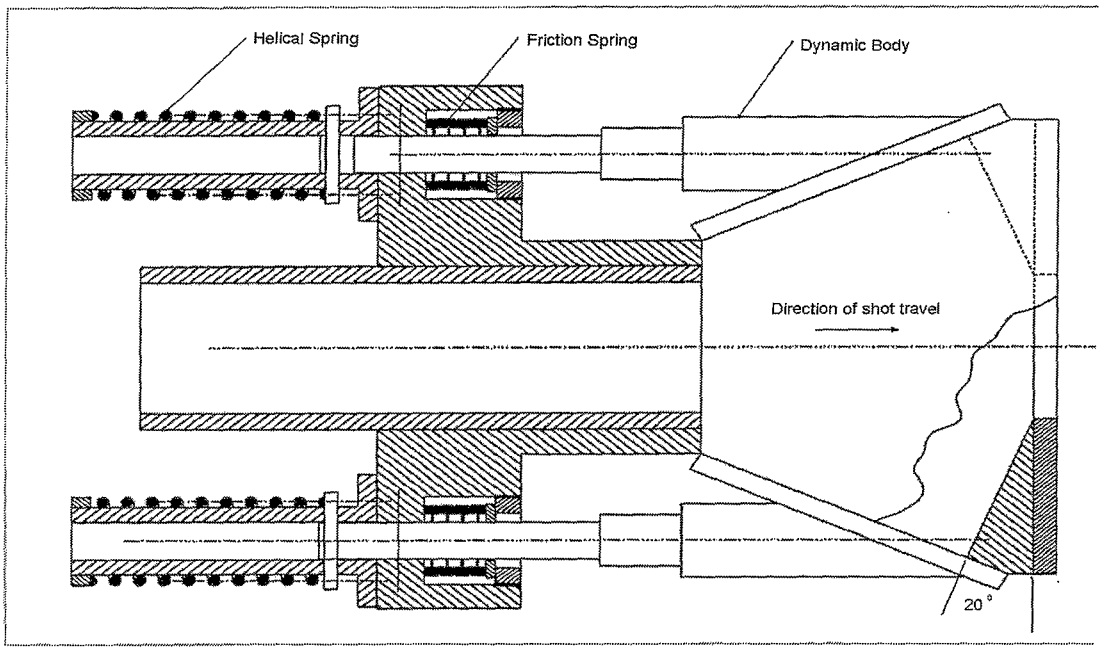

Figure 21. Illustration of version 4 with dynamic body in closed position.

A 20° wedge baffle (70° from the barrel centre line to the rear) was implemented on this design. The incorporating of the wedge helps to reduce the travel on the dynamic body resulting in a lower moving mass on the system. The linear movement of the dynamic body was restricted to one caliber. The dynamic body consisted of two flap portions with screw in pistons. These two flaps were held together with two breeching plates to counter the side loads on the flaps. The breeching plates were fastened by bolts onto the flaps. Helical springs were used as the restoring mechanism of the dynamic body assembly. The final damping mechanism of the dynamic body was accomplished using friction springs (Commonly known as RINGFEDERS from the company that did the development[16]).

The propellant gas actuates the flap parts of the dynamic body and set it in motion. The dynamic body moves with only the helical spring force restraining it until the shouldered part of the piston collides with the friction spring column. The compressed helical spring restores the dynamic body to the closed state.

i. Friction springs and their use.

Friction springs are used in cases where high amounts of kinetic energy of moving masses have to be absorbed and dampened. A secondary advantage is the fact that springs with relative small dimensions can be subjected to high forces resulting in occupying a minimum space with minimum weight. This is in contrast to Bellville type springs and helical springs. Friction springs are designed to block when maximum spring travel is reached. When this happens, the plane surfaces of the rings touch to form a rigid column. This ensures that the friction spring does not suffer any damage. The friction springs require relatively little maintenance. It needs only to be lubricated periodically and some systems have been known to function properly for over 25 years.

The springs consist of a series of separate inner and outer rings with mating taper faces. Under the application of axial load, the wedge action of the taper faces expands the outer rings and contracts the inner rings radially, allowing axial deflection. When the overload is removed, the spring returns to its pre-loaded condition. The spring is designed to absorb up to 2/3 of the impact load as heat and remove it from the impact system. In figure 22 the complete force-travel diagram of the friction spring is illustrated.

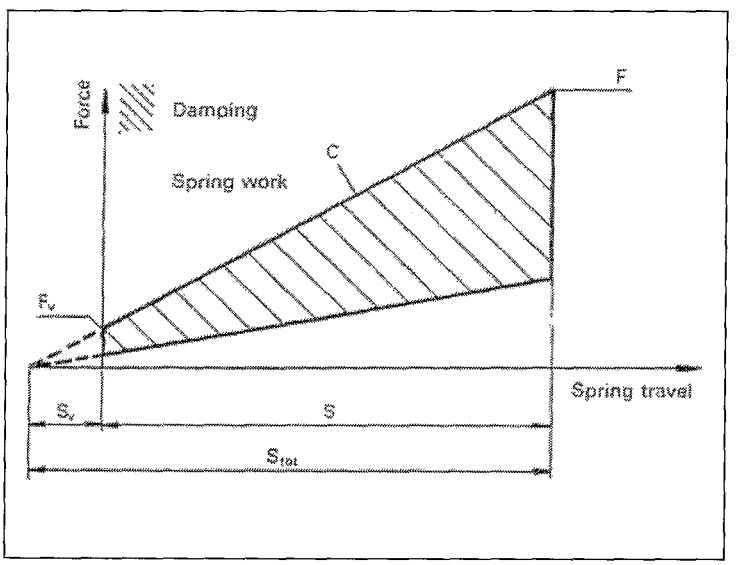

Figure 22. Force-travel diagram of a pre-tensioned friction spring.

The closed diagram is to be interpreted clock-wise. The area between the load curve and the travel axis is a criterion of the spring work absorbed, while the hatched hysteresis area represents the dampening. Friction springs should be pre-tensioned with at least 5 to 10 % of the spring travel. The pre-tension travel is presented by S_v in the figure.

ii. The design of the friction spring column.

The size and number of elements depend on the energy to be absorbed. The number of elements determines the spring travel whence each element contributes to a portion of the travel. The kinetic energy that needs to be absorbed due to the impact of the dynamic body would be:

$$E_k = M_{DB}.V_{DB}/2 \qquad (3.13)$$

The set of friction springs in each piston column would absorb half of that kinetic energy and that energy represents the spring work i.e.

$$W = F_{FS}.S/2 \qquad (3.14)$$

The contact velocity of the dynamic body with the friction springs was calculated with a simple mass-spring model where the dynamic body was actuated by an impulse force that accelerated the mass against the helical spring force over a distance of 1 caliber. The impulse force acting on the dynamic body was calculated from the muzzle exit pressure value.

From these calculations two friction spring columns with a capability of 34kN each consisting of 8 elements giving a total spring travel of 8.8 mm was derived. The design of the hardware also included a ring to pre-tension the column of friction springs.

iii. Limitations of version 4.

- Problems were encountered during the assembly of the muzzle brake due to out of alignment of the two rods, flaps and closing surface of the main muzzle brake body. The problem was solved by matching the flaps with the outer gas ports of the muzzle brake. If this muzzle brake was to achieve production status, this limitation would be a major disadvantage.
- The dynamic body started to deform plastic at the connection point of the rods onto the main structure due to the large side loads onto the flap part of the dynamic body. A fabricated welded construction rather than an assembled body would probably have overcome the problem. The helical springs were also plastic deformed after the evaluation shots were fired.
- The mass of 56 kg exceeded the mass constraint of 35 kg.
- An efficiency of only 12.9% was achieved when utilized in the active mode.
- The muzzle brake did not have an aesthetical appearance.

iv. Lessons learned from version 4.

- Friction springs as the damper element on the opening stroke of the dynamic body were a very positive contribution to the design.

3.2.5 Phase 3 – Version 5

Version 5 was a further improvement of version 4. It was evident from the evaluation data of version 4 that a more efficient muzzle brake was needed to achieve the constraint of 35% when utilized as active. The main brake body was redesigned to increase the internal chamber volume. The standoff distance was increased from 1.5 calibers to 1.75 calibers resulting in increasing the chamber volume by 24%.

It was evident from the evaluation of versions 3 and 4 that the use of helical springs as the closure mechanism is a wrong choice for the dynamic action that is bestowed upon the dynamic body. Due to the ruggedness and success with which the friction springs were applied to version 4, a solution was found in using friction springs as the sole component for the restoring mechanism.

The appearance of version 5 is shown in figure 23.

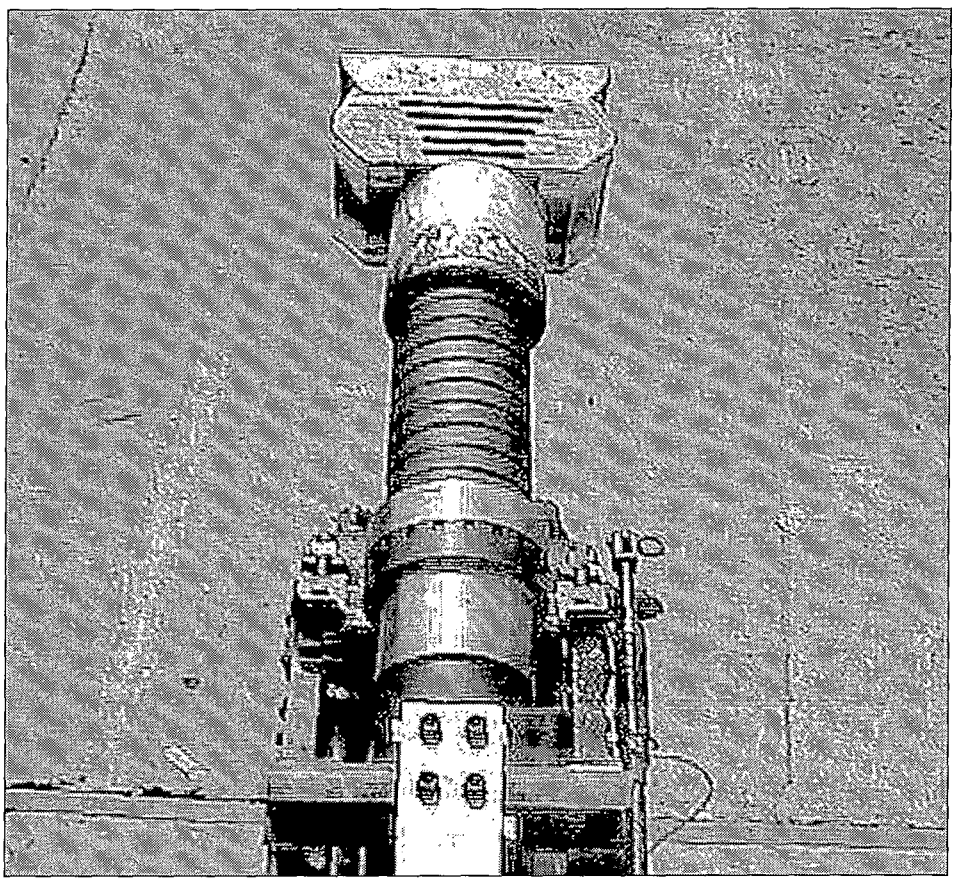

Figure 23. Version 5.

The total mass of version 5 was 57.3 kg of which 47 kg contributed to the point mass parts and 10.3 kg for the closure mechanism. The mass of the closure mechanism parts was evenly distributed on the front portion of the barrel. The G1 barrel was modified by shortening the barrel with 6.8 calibres. This was replaced by a screwed on tube that resembles the barrel over which the friction springs could slide. The conventional main brake body of version 5 screwed onto the front of this tube. This tube was smooth bored. No effect on the ballistic performance of the projectile due to the lack of grooves could be detected when tested with the pressure adaptor fitted as pictured in figure 23. The modification to the barrel also had the effect that the mass of the recoiling parts was reduced by two kilogram in relation to the previous mass of versions 1 to 4. This is evident from the recoiling mass data rendered in tables 10 and 14 of paragraphs 4.3.2 and 4.4.2 respectively.

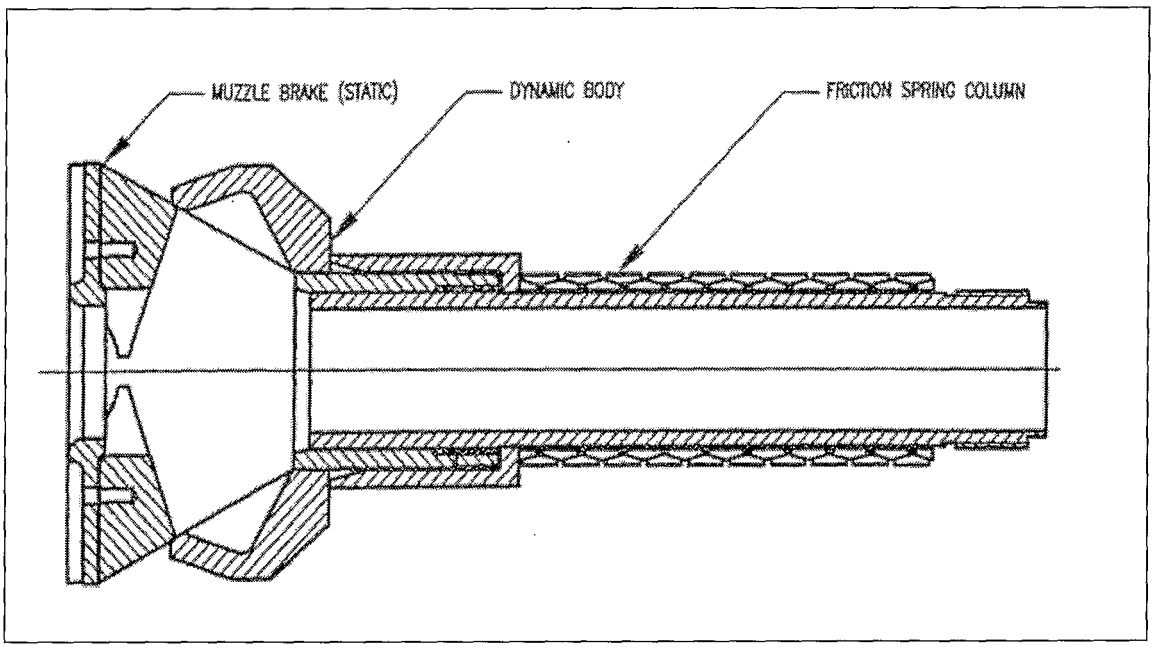

Figure 24. Illustration of version 5 with dynamic body in closed position.

The geometry of the dynamic body was of such a nature to lessen the force on the restoring mechanism and increased the internal brake volume. This was accomplished by the L - shape of the structure resulting in a much lower net force as the remainder of the rear and forward impulse force on the dynamic body. This whole structure was a welded fabrication as no close tolerances as with the case of version 4 were present. The dynamic body was made to slide over the side of the main muzzle brake body and a spacer between the body and friction springs transferred the motion and resultant force to the friction spring column. The length of the friction spring column was optimized by limiting the movement of the dynamic body to half a caliber.

i. CFD study of the flow through the muzzle brake.

A CFD simulation of the gas dynamic flow through this version was conducted by Qinetiq by means of the FCT algorithm as described in paragraph 1.3.1 over a time span of 3 ms. The muzzle exit conditions as derived and described in paragraph 3.1.2 were used as input values to the simulation. The muzzle exit pressure dropped from 47.4 MPa to 19.12 MPa during that duration. Version 5 was simulated with and without the dynamic body. The dynamic body started to move after 0.5 ms while a force of 86.2 kN was exerted on it. The resultant force on the baffle was 390 kN. The CFD study was carried out without the restrain of a friction spring column to the dynamic body and this can be seen as a shortfall. The pressure contour plots of the obtained flowfield are attached in Appendix D. The formation of the shock fronts and

corresponding Mach disc is clearly visible on the pressure contours. It is evident from the simulation of version 5 with the dynamic body that the shock strength had already decayed before the muzzle brake chamber had opened due to the movement of the dynamic body. It could also be derived from the CFD study that movement of the dynamic body in excess of half a calibre had little effect on the forward impulse of the muzzle brake. A force of 25 kN was exerted on the dynamic body after a movement of 44 mm while the forward impulse was still in excess of 150 kN. Friction springs of 125 kN in excess to the predicted 87 kN were fitted as the restoring mechanism.

ii. Limitations of version 5.

- The mass of 47 kg exceeded the mass constraint of 35 kg.
- An efficiency of only 24.4% was achieved when utilized in the active mode. That however is much better than the 12.9% achieved with version 4.

iii. Strong points of version 5.

- No structural damage occurred to any of the components when evaluated.
- The overpressure was alleviated to a lower level as when no muzzle brake was fitted to the gun.

3.2.6 Phase 3 – Version 6

Versions 5 and 6 had several commonalities in respect to the dynamic body and restoring mechanism. Friction springs were used as the sole members of the restoring mechanism and the dynamic body was a welded construction. The conventional part of the muzzle brake was a complete new design to achieve a very efficient muzzle brake. The baffle formed effectively an angle of 45° from the barrel centre line to the rear part of the baffle as illustrated in figure 26.

The appearance of version 6 is shown in figure 25.

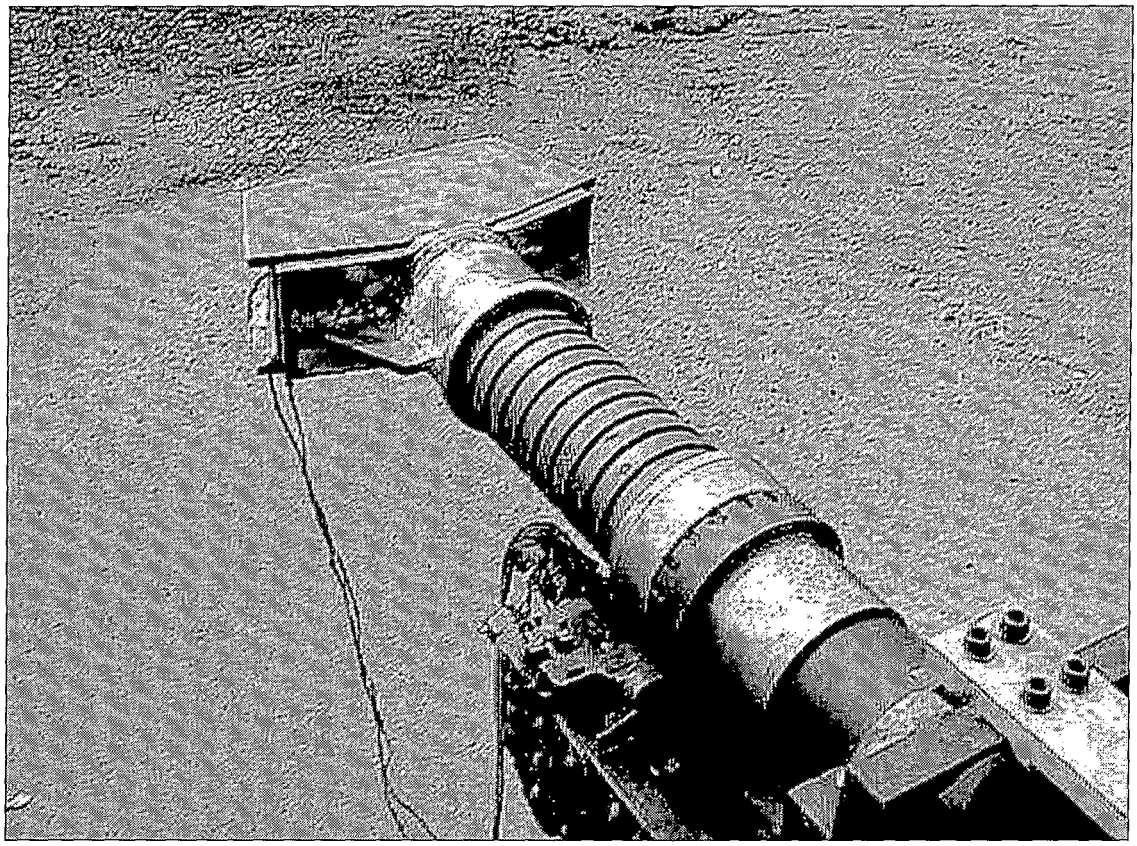

Figure 25. Version 6.

The total mass of version 6 was 37 kg for point mass parts and 10.3 kg for the restoring mechanism that was evenly distributed on front portion of the barrel. This corresponds favourable with the mass constraint of 35 kg for the point mass. With version 5 the front portion of the barrel was replaced by a tube onto which the main body of the muzzle brake was screwed. With version 6 this tube was an integral portion of the main muzzle brake body. A sectional view of version 6 is illustrated in figure 25.

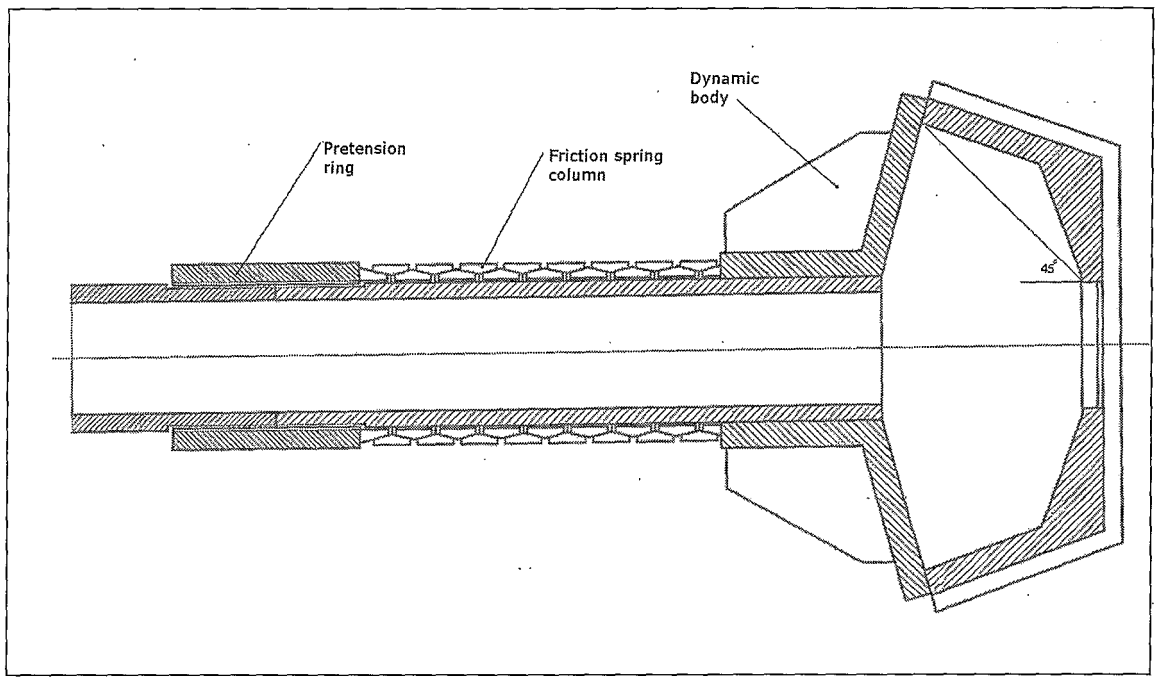

Figure 26. Illustration of version 6.

i. CFD study of the flow through the muzzle brake.

Version 6 was simulated with and without the dynamic body. Although the geometry of the baffle and dynamic body of version 6 differed a lot from version 5 very similar results were predicted with the CFD study. The dynamic body starts to move after 0.4 ms while a force of 84 kN was exerted on it. The resultant force on the baffle was 430 kN. The pressure contour plots of the obtained flowfield over a time span of 3 ms are attached in Appendix D.

ii. Limitations of version 6.

- The dynamic body had no aligning key to prevent it from turning while moving to the rear. The column of friction springs held the dynamic body in position up to a certain extent, but angular movement proved to be a problem.

iii. Strong points of version 6.

- No structural damage occurred to any of the components when evaluated.
- The total mass 37 kg corresponds favorable with the mass constraint of 35 kg.
- An efficiency of 34.8 was achieved that is very favorable with the constraint of 35 %.

3.3 *Risk mitigation.*

Several risks identified in paragraph 2.5 were addressed.

- The trials of the six prototypes were the first type of field tests of the novel active muzzle brake concept as the previous evaluation was only in the laboratory. The last two prototypes developed verified that this technology can be practically applied to a weapon.
- The principle of linear movement of the closure mechanism in respect to rotational as was evaluated in the laboratory established a practical and simple mechanism. Similar with the use of friction springs as the restoring mechanism that is robust and will survive the harsh conditions at muzzle exit.
- Versions 5 and 6 are rather simple prototypes that would be easy to maintain.
- One of the risks remains. As all the shots were fired at an elevation of zero degrees, the risk still exists that the muzzle brakes that perform well at zero degrees, may perform poorly at higher elevation angles.

Chapter 4

Evaluation

The evaluation of the three phases is recorded. The conventional scaled down version of the G5 type of muzzle brake was also tested to serve as a reference for the novel designs.

4. EVALUATION

The active muzzle brake designs as developed in the different phases as described in chapter 3 were evaluated during three trials.

4.1 Test overview for all three phases

The weapon was instrumented with sensors to measure the following dynamic variables as a function of time during all of the trials:

- Chamber pressure
- Muzzle exit pressure
- Axial acceleration of oscillating parts
- Recoil force
- Counter recoil force
- Recoil displacement as dynamic measurement.
- Maximum recoil displacement as a static measurement.
- Blast overpressure at aiming position. (Point G11)
- Blast overpressure aiming at muzzle. (Point G12)
- Blast overpressure at gunner. (Point G13)
- Blast overpressure beyond legs (Point G53)
- Open and closure positions of the closure mechanism (sleeve & flaps).

The weapon was fired at an elevation of 0 degrees for all of the three trials. It was decided that the evaluation at different elevation angles would only be addressed once a prototype was chosen as a candidate for the 155 mm G5.

The following instruments / techniques were used.

- The chamber and muzzle exit pressure were measured using Kistler gauges type 217 C.
- The axial acceleration of the oscillating parts was measured using an Entran type EGCS/DO/200 accelerometer.
- The recoil and counter recoil force were measured using strain gauges. These were installed on the recoil and counter recoil rods respectively.
- The dynamic recoil displacement can be obtained from the axial acceleration by integrating it twice. (From the first integral the recoil velocity is derived.) The dynamic

recoil displacement was physically measured on the last trial. A ramp was mounted at an angle of 1.03° on the recoiling parts of the weapon. A miniature LVDT was mounted on the stationary part of the weapon and the gap between the ramp and sensor was measured when the weapon recoiled. This gap is proportional to the displacement as a relation to the ramp angle. The trace obtained was unfortunately of a poor quality due to a stiffness problem of the ramp and the integration method was used again.

- The movement of the dynamic bodies was measured during the active application of the muzzle brakes using different techniques. Breaking contacts, micro switches and breaking wires were used to measure the opening cycle of the muzzle brakes. From the methods tested, the breaking wires were the most successful.

The positions of the overpressure measurement points are illustrated in the figure 27.

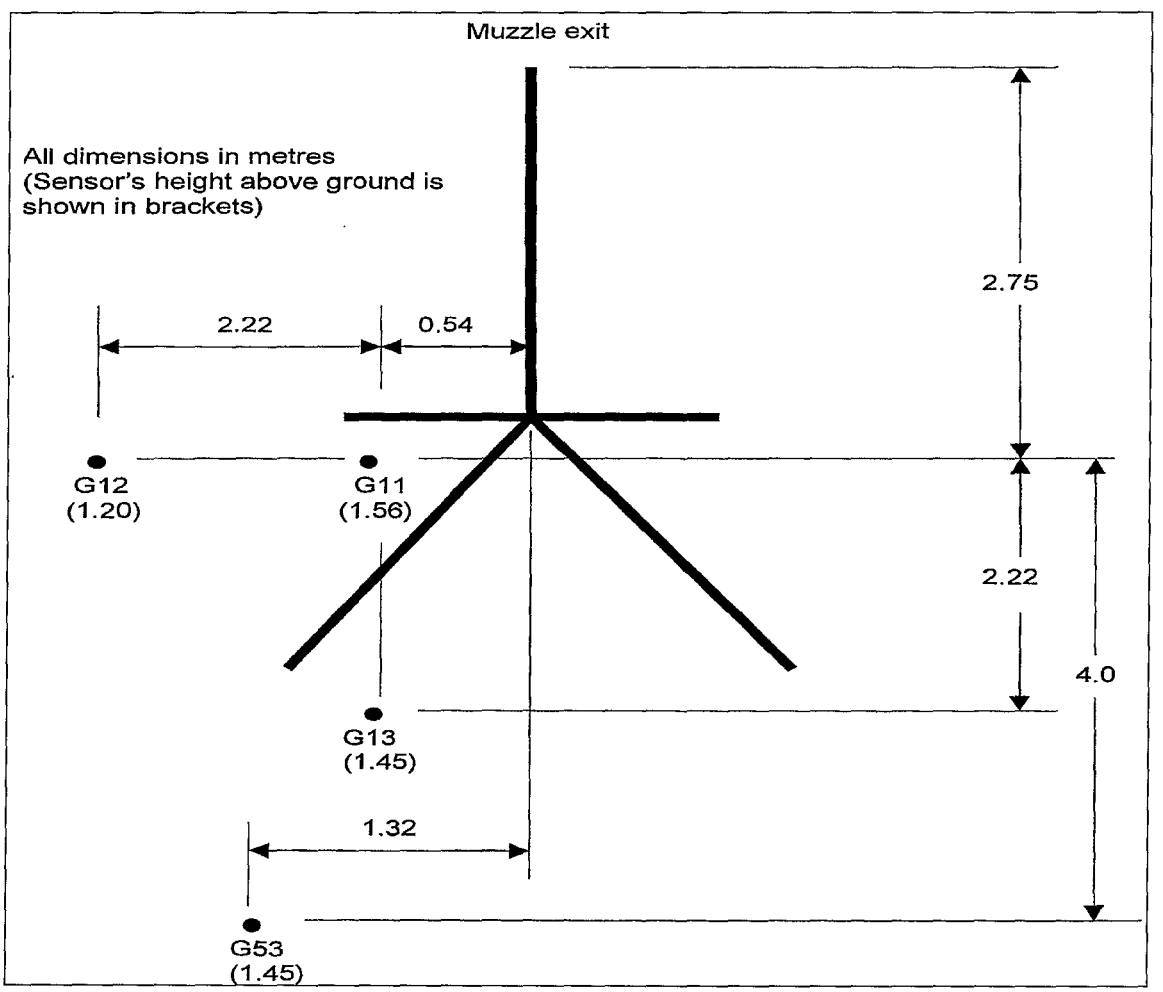

Figure 27. Positions of the overpressure measurement points.

Positions G13 and G53 are two crucial positions as this represents the positions where the gunners on the G1 and G5 operates. The position of point G53 was derived by scaling down the equivalent position when measured on the G5, using the caliber value as reference.

The weapon was fitted with a dummy piece of barrel at the muzzle exit when the reference shots without the muzzle brake were fired. The purpose of this component was to accommodate the pressure sensor for the measuring of the muzzle exit pressure and only partially compensated for the loss of mass on the recoiling parts of the weapon as the mass was only 10.9 kg. A mass correction was necessary when calculating the muzzle brake efficiency. Figure 28 shows the G1 weapon with the muzzle brake pressure adaptor fitted.

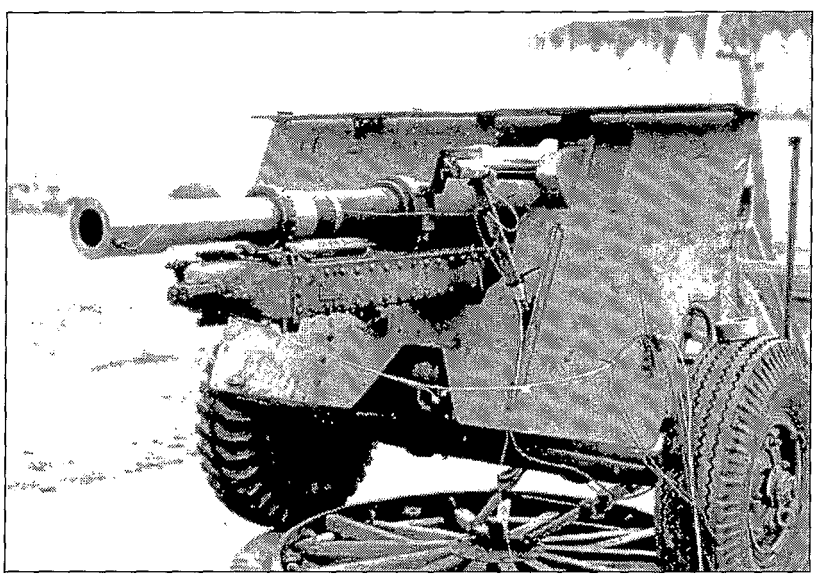

Figure 28. G1 with the muzzle brake pressure adaptor fitted. – Phase 3 configuration.

4.2 Test overview – Phase 1

The first trial was held from the 24th to the 28th of February 1997 at the test facility of Armscor at Alkantpan.

4.2.1 Test results :

The data for all the rounds that were fired on this trial is included in Appendix E. A representative value for each muzzle brake configuration is given in the main part of this dissertation.

The condensed impulse data is presented in table 4. The total recoil impulse and displacement is a good indication of the effect of the muzzle brake on the transfer of energy from the oscillating mass to the fixed platform of the weapon. The less the recoil impulse and recoiling displacement, the more efficient the muzzle brake. The total recoil impulse is the sum of the integrals of the recoil force and counter recoil force over time. The recoil energy is a good indication of the efficiency of the muzzle brake. The recoil energy takes the recoil force and recoil displacement into account.

Muzzle brake configuration	Chamber pressure (Mpa)	Recoil displacement (mm)	Total Impulse (kN.s)	Recoil Energy (kJ)
No muzzle brake	223	850	6.85	26.1
G5 scale down muzzle brake	235	760	5.62	17.3
G5 scale down muzzle brake Baffle 70° to rear. Version 1 with flap in open position	230	740	5.6	17.2
Slotted sleeve. Version 2 with sleeve fixed in open position	235	810	5.91	19.3

Table 4. Condensed impulse data – Phase 1

The condensed overpressure data is presented in table 5.

Muzzle brake configuration	Chamber pressure (MPa)	Overpressure (ΔP) in kPa and B-duration (τ_B) in ms					
		G11		G12		G13	
		ΔP	T_B	ΔP	T_B	ΔP	T_B
No muzzle brake	223	2.84	18.59	3.85	11.48	1.28	19.00
G5 scale down muzzle brake	235	17.79	8.31	18.43	12.28	8.23	14.53
G5 scale down muzzle brake. Baffle 70° to rear. Version1 with flap fixed in open position	230	22.56	8.23	17.81	11.85	10.26	11.82
Slotted sleeve version 2 with sleeve fixed in open position	235	11.35	14.08	12.78	13.15	6.88	10.62

Table 5. Condensed overpressure data – Phase 1

No data regarding the active application of versions 1 and 2 is presented in this dissertation. The reason for this being as follows:

The sleeve of version 2 was designed to open due to the acceleration of the weapon to minimize the delay time. Unfortunately this happened before the projectile uncorked from the muzzle end

resulting in similar results as when the shots were fired with the sleeve in the fixed open position.

Only one shot was fired with version 1 while the control flaps were active. The control flaps were completely sheared off and similar results as when the shot were fired with the control flaps in the fixed position were obtained. The remnants of the control flaps and closure mechanism are shown in figure 29.

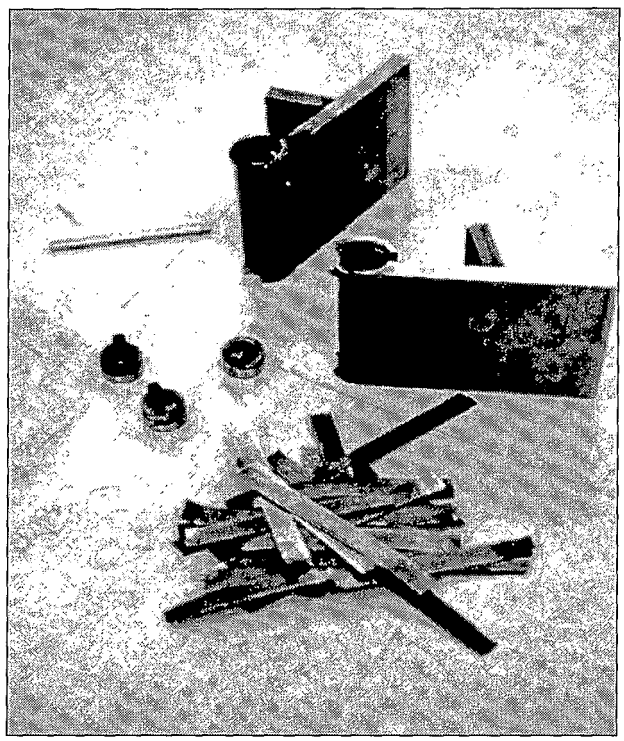

Figure 29. Remnants of control flaps and closure mechanism of version 1.

4.2.2 **Processed data :**

The muzzle brake performance is assessed by the efficiency that is given by :

$$\eta_M = 1 - (E_B / E_{NB} * M_B / M_{NB}) * 100\ \% \qquad (4.1)$$

The efficiency is compensated with the different values of the recoiling mass as presented in table 6.

Muzzle brake configuration	Recoiling mass kg	Efficiency (η_M) %
No muzzle brake	712.7	0
G5 scale down muzzle brake	729.8	32.1
G5 scale down muzzle brake. Baffle 70° to rear. Version 1 with flap in open position	733.5	32.2
Slotted sleeve. Version 2 with sleeve fixed in open position	746	22.6

Table 6. Efficiency data of muzzle brake configurations.

The muzzle brake performance is secondly assessed by using the peak overpressure ratio.

Peak overpressure ratio (β) = $\Delta P_B / \Delta P_{NB}$ (4.2)

Muzzle brake configuration	Peak Overpressure Ratio(β)		
	G11	G12	G13
No muzzle brake	1	1	1
G5 scale down muzzle brake	6.26	4.78	6.42
G5 scale down muzzle brake Baffle 70° to rear. Version 1 with flap fixed in open position	7.94	4.62	8.02
Slotted sleeve version 2 with sleeve fixed in open position	3.99	3.32	5.38

Table 7. Overpressure ratios.

4.2.3 **Data analysis :**

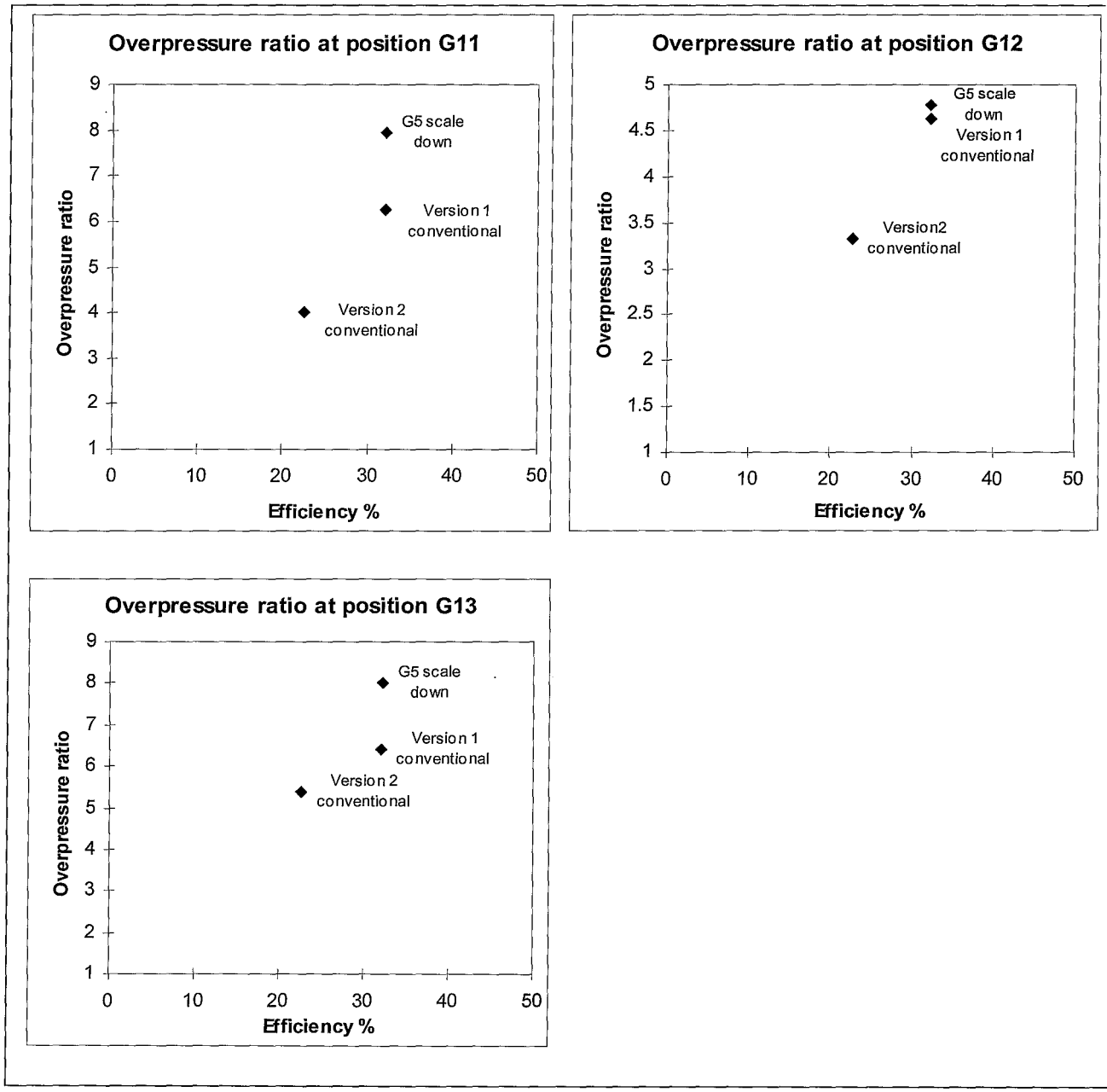

Figure 30. Graphs depicting the overpressure ratios

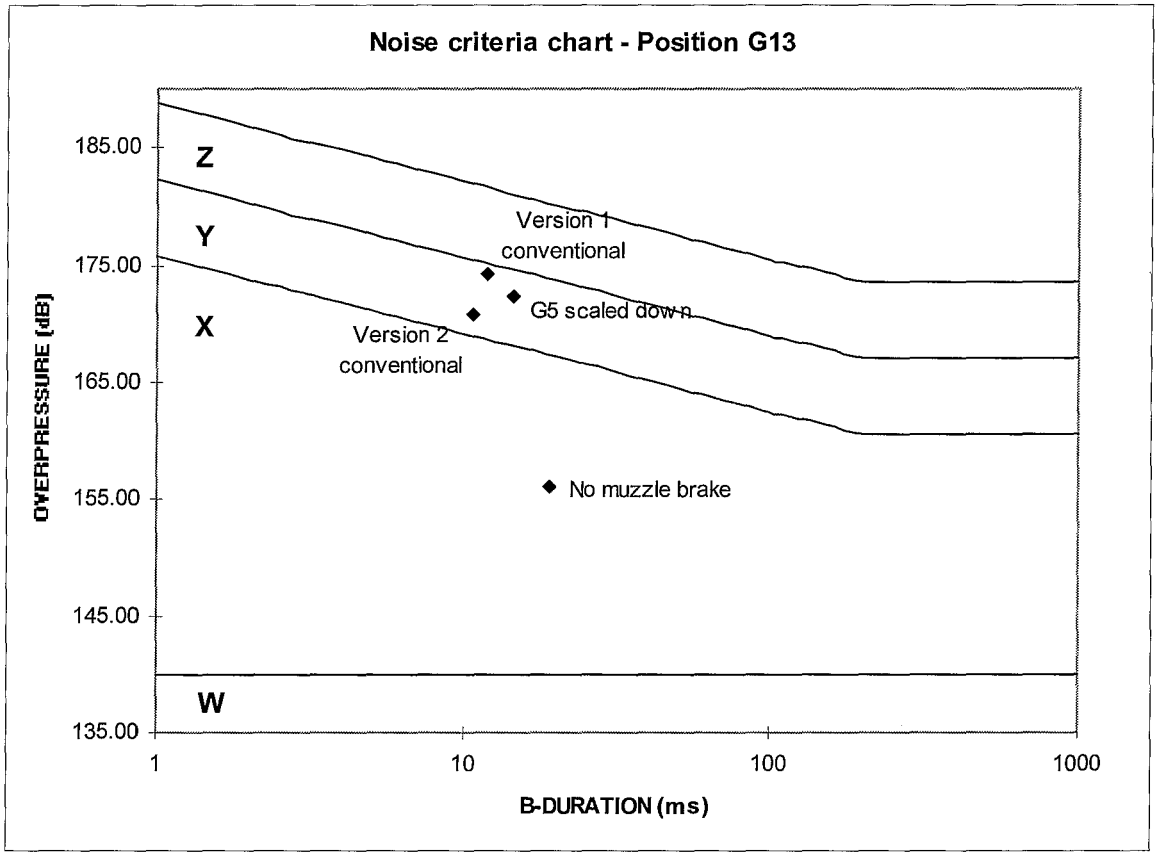

Figure 31. Noise criteria chart – Position G11.

4.3 *Test overview – Phase 2*

The second trial was conducted from the 19th to the 23rd of January 1998 at Alkantpan. A total number of 42 rounds were fired. From these amount a total of 24 rounds were fired using charge 2 and 18 rounds using charge 3. It was decided from the catastrophic results of version 1 when evaluated as an active muzzle brake on the first phase trial to apply a less severe impact to the muzzle brakes. The propellant in the cased ammunition is made up of different bags. One of these bags was removed to reduce the propellant weight and the charge belonging to that configuration was referred to as a charge 2. The first 4 rounds were fired to set up all the measuring equipment and to verify calibration of data.

4.3.1 **Test results :**

The complete data for all the rounds that were fired on this trial is included in Appendix E. A representative value for each muzzle brake configuration is given in the main part of this dissertation.

The condensed impulse and recoil energy data is presented in table 8. The data for the charge 2 configuration is also presented for the sake of completeness although the recoil energy was not calculated as the charge 2 configuration has no comparison value with the rest of the trials.

Muzzle brake configuration	Charge	Chamber pressure (MPa)	Recoil Displacement (mm)	Total Impulse (kN.s)	Recoil energy (kJ)
No Muzzle brake	2	158	580	3.89	-
	3	261	742	7.60	30.3
Version 3 Conventional	2	163	455	3.52	-
	3	246	595	5.23	17.5
Version 3 Active	2	159	512	4.14	-
	3	268	670	6.44	23.3
Version 4 Conventional	2	153	485	3.66	-
	3	238	636	5.56	19.8
Version 4 Active	2	153	522	3.93	-
	3	232	685	6.47	24.8

Table 8. Condensed impulse data – Phase 2.

Only two shots were fired with version 4 in the active mode using a charge 3 configuration, as the retainer block that houses the friction springs started to shear from the main body of the muzzle brake. The bushes that housed the piston rods also started to deform. The flaps still managed to close after the second shot.

The condensed data regarding the overpressure measurements is presented in table 9.

Muzzle brake configuration	Charge	Chamber pressure (MPa)	Overpressure (ΔP) in kPa and B-duration (τ_B) in ms							
			G11		G12		G13		G53	
			ΔP	τ_B	ΔP	τ_B	ΔP	τ_B	ΔP	τ_B
No muzzle brake	2	158	3.22	25.44	1.97	19.1	2.1	21.89	1.45	21.78
	3	261	4.92	18.59	1.96	20.71	2.66	16.59	1.73	20.32
Version 3 Conventional	2	162	15.85	17.32	7.68	14.21	7.46	16.21	5.63	11.85
	3	246	20.75	13.94	7.38	13.68	10.59	12.08	7.85	11.28
Version 3 active	2	159	4.56	16.85	3.27	14.12	3.52	16.23	2.59	11.32
	3	268	8.16	12.11	5.29	12.35	5.58	11.69	3.74	10.62
Version 4 Conventional	2	153	14	22.57	5.16	13.03	5.47	17.32	4.44	15.23
	3	238	17.64	13.90	6.13	13.28	8.37	12.22	5.78	14.87
Version 4 active	2	153	3.81	23.12	2.68	12.10	2.31	20.16	1.32	19.66
	3	232	5.08	15.94	5.27	12.61	3.2	15.14	1.98	18.58

Table 9. Condensed overpressure data – Phase 2

Wind with a velocity higher than 25 km/h (7 m/s) does have an influence on the overpressure. It is evident from the detail data as presented in Appendix E that the group of rounds fired with version 3 applied as active, falls outside that specification. It is very difficult to adjust the overpressure for the wind effect.

4.3.2 **Processed Data :**

The processed data for one shot per group of data for the charge 3 shots are included in Appendices F to J. These traces are added to give the reader information on the graphs that are expected for the different parameters. The shape of the traces is similar for the different phases.

- Appendix F – No muzzle brake.(Shot 26)
- Appendix G – Version 3 conventional (Shot 13).
- Appendix H - Version 3 active (Shot 22).
- Appendix I – Version 4 conventional (Shot 34).
- Appendix J – Version 4 active (Shot 42)

The parameters are shown in the following order :

- Chamber pressure.
- Recoil velocity.
- Recoil displacement.
- Recoil energy.
- Recoil force.
- Recoil impulse.
- Counter recoil force.
- Counter recoil impulse.
- Overpressure position G11.
- Overpressure position G12.
- Overpressure position G13.
- Overpressure position G53.

The different muzzle brake configurations are evaluated according to the efficiency, overpressure and dynamic motion performance parameters.

i. Muzzle brake efficiency:

The efficiency values of the different versions of the second trial are presented in table 10 and the values were again corrected with the mass of the recoiling parts as with the previous trial.

Muzzle brake configuration	Charge Conf.	Recoiling Mass (kg)	Efficiency (%)
No muzzle brake	3	712.7	0
Version 3 Conventional	2	-	-
	3	755.8	38.7
Version 3 Active	2	-	-
	3	755.8	18.5
Version 4 Conventional	2	-	-
	3	741.9	31.9
Version 4 Active	2	-	-
	3	757.8	12.9

Table 10. Muzzle brake efficiency.

ii. Overpressure ratio:

For the 88mm test the peak overpressure ratio is given in table 11.

Muzzle brake configuration	Charge Conf.	Peak Overpressure Ratio(β)			
		G11	G12	G13	G53
Version 3 Conventional	2	4.92	3.89	3.55	3.88
	3	4.21	3.76	3.98	4.53
Version 3 Active	2	1.42	1.66	1.68	1.79
	3	1.66	2.70	2.10	2.16
Version 4 Conventional	2	4.35	2.62	2.60	3.06
	3	3.58	3.12	3.15	3.34
Version 4 Active	2	1.18	1.36	1.10	0.91
	3	1.03	2.69	1.20	1.14

Table 11. Overpressure ratio – Phase 2

iii. Dynamic body motion:

The efficiency of the novel muzzle brake is partially governed by the time delay between the exit of the projectile and the opening of the dynamic body (sleeve or flap depending on the type

of muzzle brake). The second part of the motion being the start of movement up to the fully opened position is also of importance.

The graphs showing the opening time of the flap and sleeve with reference to the muzzle exit pressure decay are attached as Appendix K. The delay time for both active muzzle brakes is more or less the same, the flap type being a few microseconds faster. The delay time is 3.5 milliseconds were an ideal time of 1.5 milliseconds is anticipated.

4.3.3 **Data analysis :**

The overpressure ratios versus the efficiency are given in the following four graphs for the different positions measured for overpressure. The values are for the charge 3 scenario.

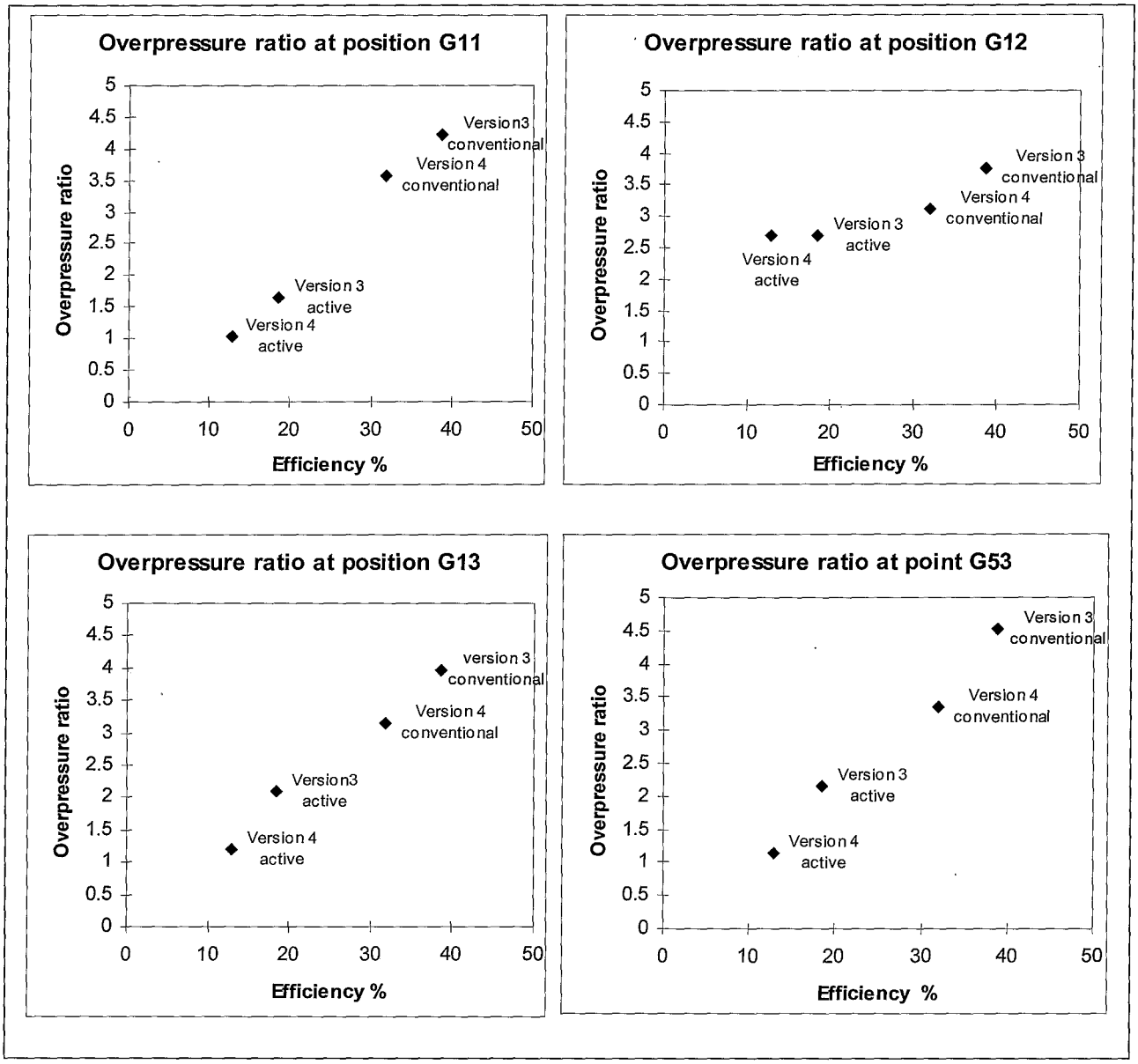

Figure 32. Graphs depicting the overpressure ratios.

All the points on the graph lie in a straight line when connected. This has the effect that the overpressure is proportional to the efficiency for all the prototypes. If the active muzzle brake had a positive contribution, it would have laid beyond that line.

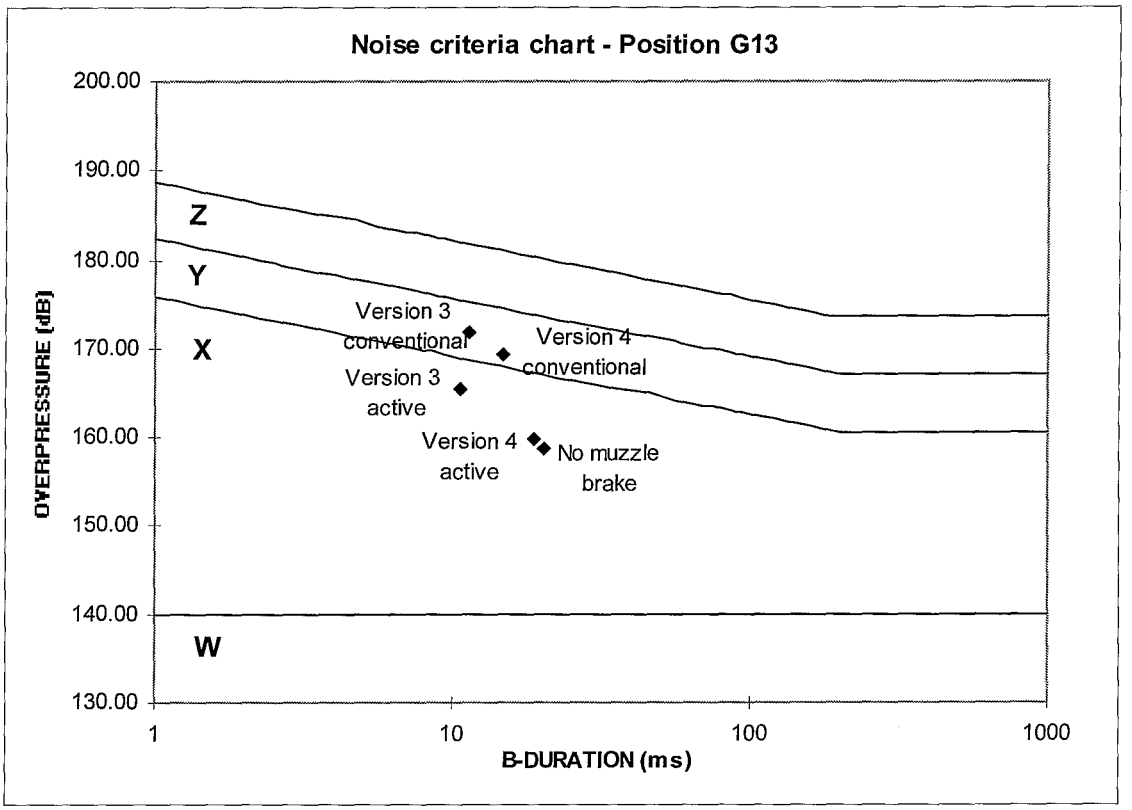

Figure 33. Noise criteria chart – Position G13 (Phase 2)

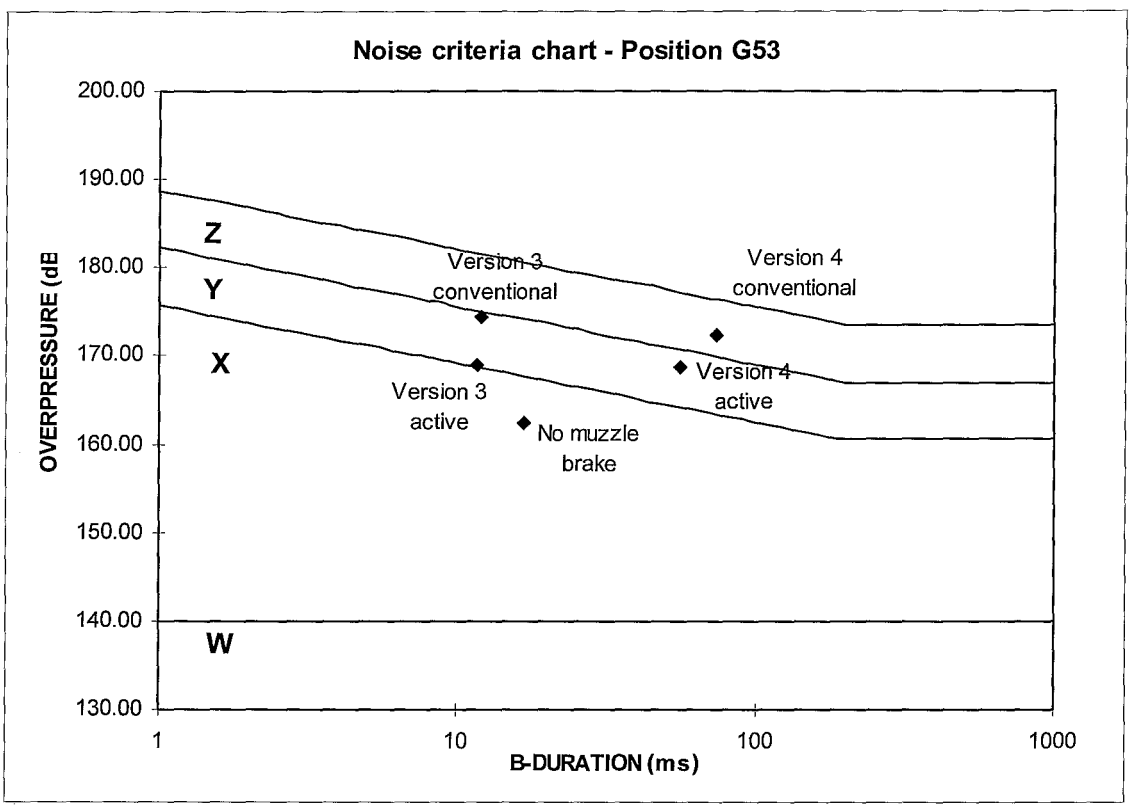

Figure 34. Noise criteria chart – Position G53 (Phase 2)

4.4 *Test overview – Phase 3*

The third 88 mm test was conducted from the 17th to the 21st of November 1999 at the test facility of Naschem at Potchefstroom. The reason for the change in venue was due to saving in overall cost of range and travel expenses. The weapon differed from the previous trial due to the blast reflect shield being removed. The overpressure measurements are higher and this gives better accuracy to the outcome of the blast overpressure referencing.

For this trial only charge 3 type of propellant was used. It was decided that the structural strength of the muzzle brakes was adequate and no need to apply a less severe impact to the muzzle brakes was necessary. The test schedule was adjusted during the trial as the need for the investigation of free movement of the dynamic body on version 5 arose.

4.4.1 **Test results :**

The complete data for all the rounds that were fired on this trial is again included in Appendix E and only a condensed set of data is presented. The condensed data for the impulse and recoil energy is presented in table 12.

Muzzle brake configuration	Chamber pressure (MPa)	Recoil displacement (mm)	Total Impulse (kNs)	Recoil Energy (kJ)
No muzzle brake	259.8	776	6.03	27.15
Version 5 conventional	261.4	682	4.26	16.28
Version 5 active with 20 elements Of 125 kN friction springs	260	756	4.44	19.12
Version 5 active with 17 elements Of 250 kN FS (38 mm free travel)	261.3	745	4.90	21.1
Version 5 active with 13 elements of 250 kN FS (94 mm free travel)	260.6	730	4.56	19.71
Version 6 conventional	261.3	647	3.43	13.62
Version 6 active with 20 elements of 125 kN friction springs	260	758	4.89	20.09
Version 6 active with 20 elements of 250kN friction springs	262.6	722	4.54	17.33

Table 12. Condensed data for recoil impulse & energy – Phase 3

The condensed data regarding the overpressure measurements is presented in table 13.

Muzzle brake configuration	Chamber pressure (MPa)	Overpressure(ΔP) in kPa and B-duration(τ_B) in ms							
		G11		G12		G13		G53	
		ΔP	τ_B	ΔP	τ_B	ΔP	τ_B	ΔP	τ_B
No muzzle brake	259.8	4.90	81.4	4.68	75.8	3.31	65.3	2.12	56.7
Version 5 conventional	261.4	16.33	30.8	14.17	35.6	8.56	59.6	5.43	55.2
Version 5 active with 20 elements of 125 kN FS	260	4.59	78.6	5.16	46.3	2.25	80.8	1.85	90.9
Version 5 active with 17 elements of 250 kN FS (38 mm free travel)	261.3	3.93	77.2	5.16	84.9	2.25	105	1.55	88.1
Version 5 active with 13 elements of 250 kN FS (94 mm free travel)	260.6	4.41	77.1	5.69	71.3	2.12	103.1	1.85	90
Version 6 conventional	261.3	32.26	-	15.23	30.1	13.64	20.4	9	37.9
Version 6 active with 20 elements of 125 kN FS	260	19.24	43.8	6.97	65.4	5.49	81.2	3.75	73.1
Version 6 active with 20 elements of 250 kN FS	262.6	9.93	26.5	10.33	35.8	4.86	31.3	3.53	56.1

Table 13. Condensed overpressure data– Phase 3

4.4.2 **Processed Data :**

i. **Muzzle brake efficiency:**

Muzzle brake configuration	Recoiling Mass (kg)	Efficiency (%)
No muzzle brake	710.7	0
Version 6 conventional	723.3	48.7
Version 6 active with 20 elements of 250 kN rating FS	752.4	34.8
Version 6 active with 20 elements of 125 kN rating FS	752.6	18
Version 5 conventional	728.3	40.4
Version 5 active with 20 elements of 125 kN rating FS	760.2	19.4
Version 5 active with 17 elements of 250 kN rating FS (38 mm free travel)	759.5	21.2
Version 5 active with 13 elements of 250 kN rating FS (94 mm free travel)	757.3	24.4

Table 14. Muzzle brake efficiency – Phase 3

ii. Overpressure :

Muzzle brake configuration	Overpressure ratio (β) and B-duration (τ_B) in ms							
	G11		G12		G13		G53	
	β	T_B	β	T_B	β	T_B	β	T_B
Version 6 conventional	7.17	-	3.41	29.6	4.59	21.6	5.08	46
Version 6 active with 20 elements of 250 kN rating friction springs	2.28	30.6	1.98	44.7	1.60	44.5	1.88	57.2
Version 6 active with 20 elements of 125 kN rating friction springs	4.22	43.8	1.61	66.5	1.67	68.7	1.84	70.5
Version 5 conventional	3.44	28.8	3.03	38.1	2.87	38.3	2.86	49.4
Version 5 active with 20 elements of 125 kN rating friction springs	0.99	76.9	1.11	65.3	0.72	94.5	0.89	92.1
Version 5 active with 17 elements of 250 kN rating friction springs (38 mm free travel)	0.9	77.4	1.09	78.7	0.73	101.5	0.79	93.4
Version 5 active with 13 elements of 250 kN rating friction springs (94 mm free travel)	1	76.8	1.14	68.8	0.71	105.8	0.91	96

Table 15. Overpressure ratio – Phase 3

iii. Dynamic body motion:

The dynamic body movement could only be determined by means of the "break wires" for version 5 with the free travel of 38 and 94 mm. The delay time is more or less the same for both with a value of 1.8 milliseconds. This is better than was achieved during phase 2 where a delay time of 3.5 milliseconds was measured.

4.4.3 Data analysis :

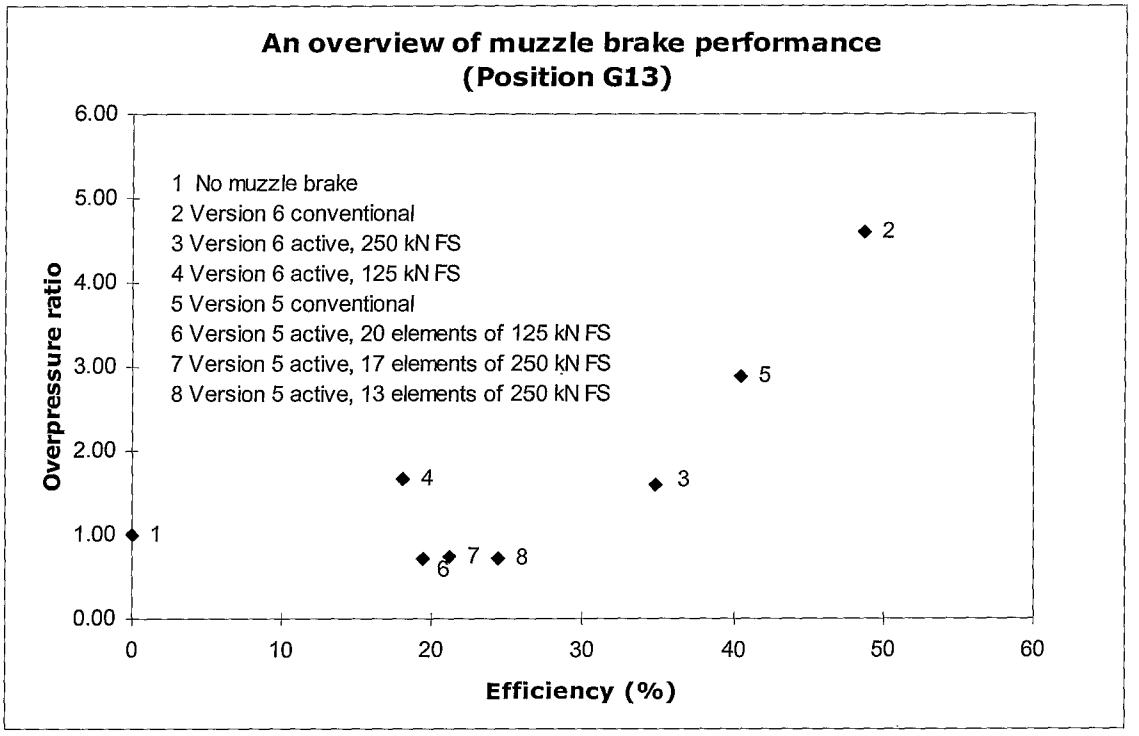

Figure 35. Graph depicting overpressure ratio – Position G13 (Phase 3)

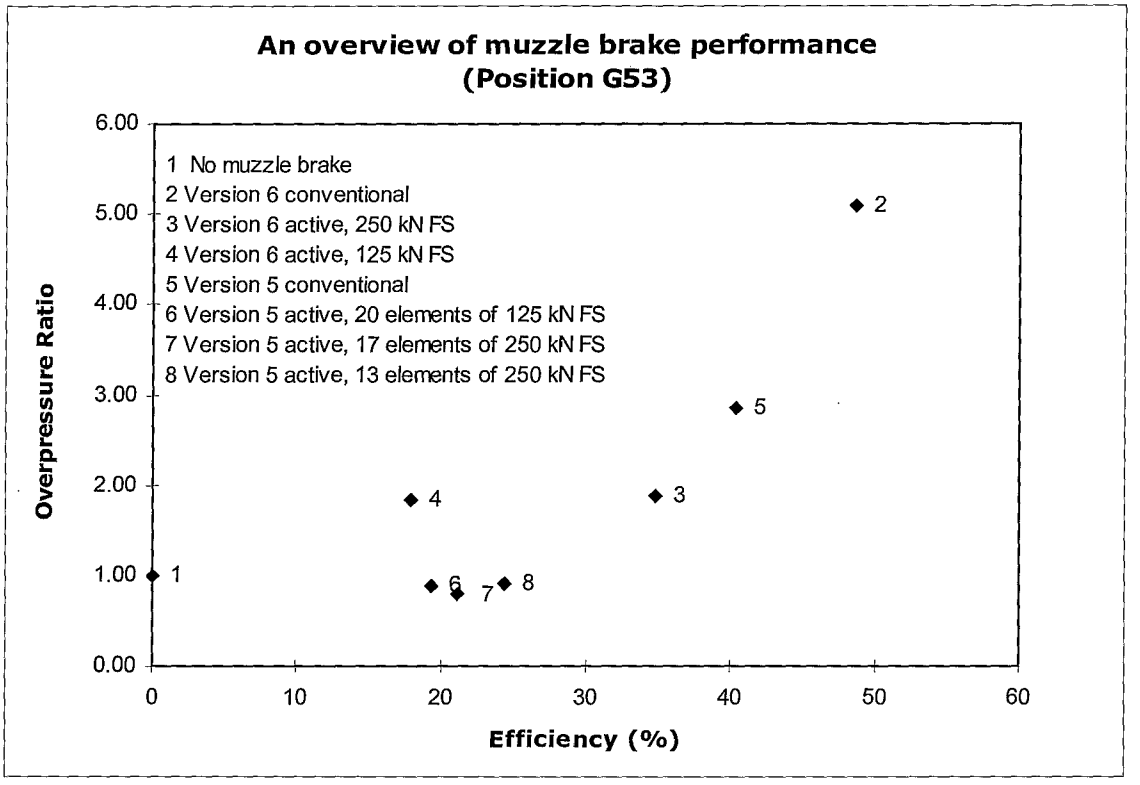

Figure 36. Graph depicting overpressure ratio – Position G53 (Phase 3)

It is evident from figures 35 and 36 that the active muzzle brakes have a positive contribution when a line is drawn from point 1 to 5. All the points that lay beyond that line gave positive results.

It is also evident from figures 35 and 36 in comparison to figure 30 that the increased volume of the main brake chamber of version 5 in comparison to version 4 resulted in a higher efficiency muzzle brake when compared as conventional, but no improvement when utilized as active. The free travel of the dynamic body improved the efficiency considerably.

Version 6 on the contrary yielded a lower efficiency when the friction spring rating was lowered from 250 kN to 125 kN. Again the overpressure stayed very much constant in spite of the modification. A possible reason for this phenomenon is that the forward impulse of version 6 is highly affected by the velocity of the ejecting gas through the aperture after the dynamic body has started to move. The small gap initiates a higher gas velocity in comparison to the larger initial gap when using the lower rating of friction spring and thus gives rise to a higher efficiency.

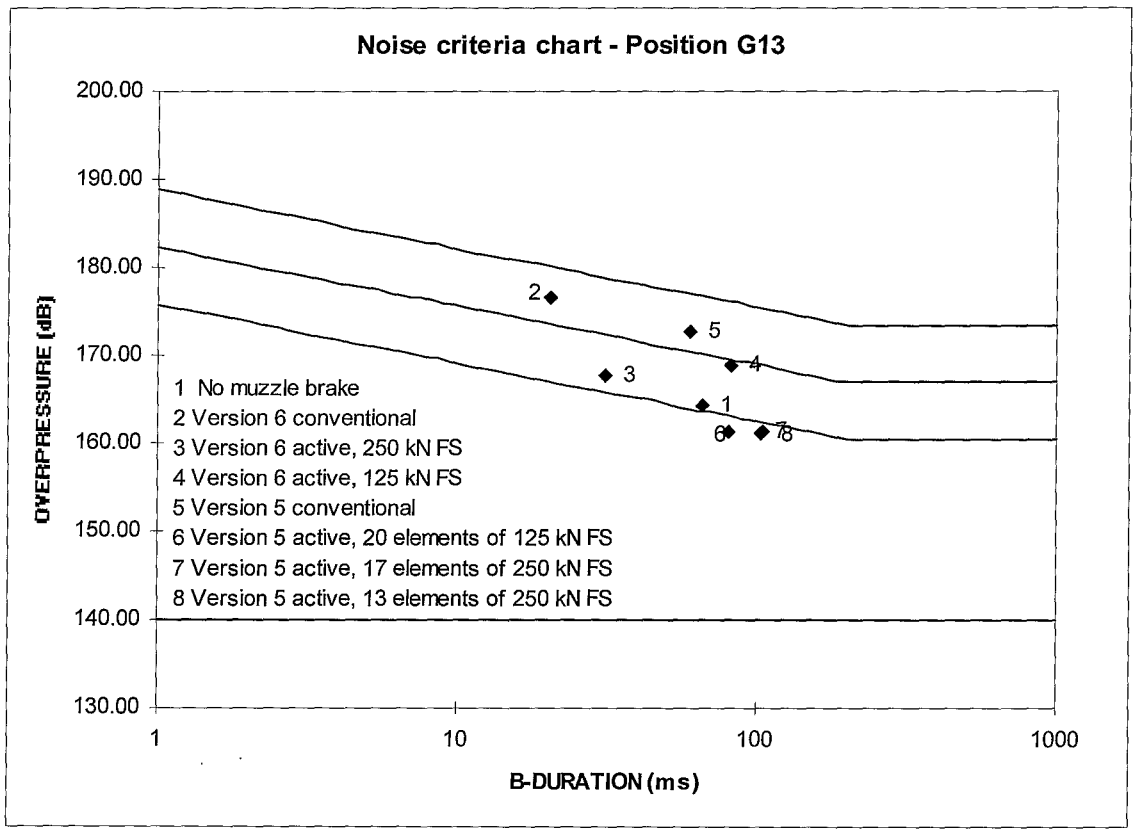

Figure 37. Noise criteria chart – Position G13 (Phase 3)

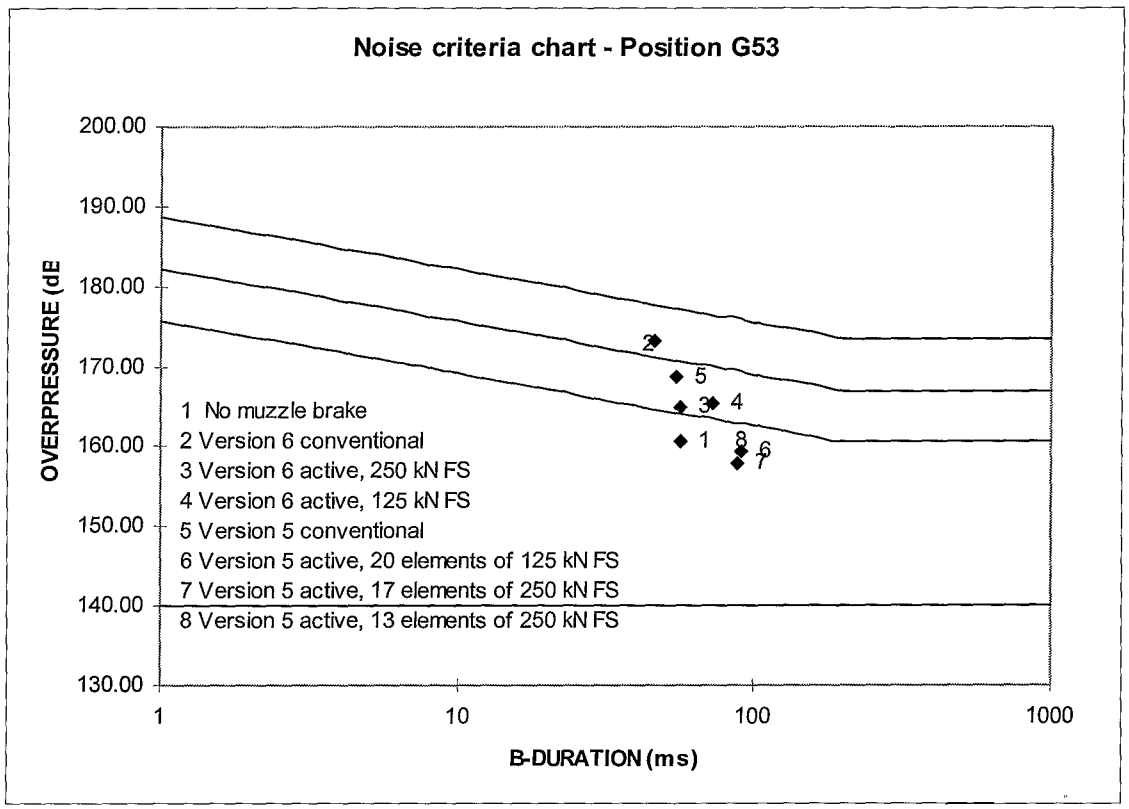

Figure 38. Noise criteria chart – Position G53 (Phase 3)

4.5 *Overall evaluation review*

Muzzle brake configuration	Overpressure G13 (ΔP)		Overpressure ratio	Efficiency (%)
	(kPa)	(dB)		
G5 scale down muzzle brake	8.23	172.3	6.75	32.1
No muzzle brake - Phase 1	1.28	156.1	1	0
Version 4 conventional	8.37	172.4	3.27	31.9
No muzzle brake - Phase 2	2.66	162.5	1	0
Version 6 active with 20 elements of 250 kN rating friction springs	4.86	167.7	1.67	34.8
Version 5 active with 13 elements of 250 kN rating FS - 94 mm travel	2.12	161.1	0.71	24.4
No muzzle brake - Phase 3	3.31	164.4	1	0

Table 16. Overall evaluation review data.

Several conclusions can be made from the data in table 16.

- Version 4 conventional and the G5 scale down version give similar results for the efficiency and overpressure as measured during the trials of phases 1 and 2.

- The value of the overpressure parameter measurement on the no brake situation however is less when tested during phase 1 in comparison to phase 2. The chamber pressure of the shots recorded when measuring the no brake situation during phase 1 was less with a considerable amount to the norm and may be the reason for the lower value. The overpressure value of the no brake situation of phase 2 is therefore taken as the norm.
- The change in overpressure on a decibel scale when comparing version 6 in the active mode with the G5 scaled down version amounts to 4.6 dB (172.3-167.7). This value must be adjusted with the increase in overpressure due to the removal of the blast shield during the trial of phase 3.
- The adjusted change in overpressure amounts to a value of 6.5 dB when comparing version 6 in the active mode to the G5 scaled down version. (4.6 + 164.4-162.5). This compares favorable when using the overpressure ratio as reference. The overall overpressure ratio amounts to 1.96 (3.27/1.67). An increase of 6 dB in the PPL value is equivalent to double the previous PPL value when evaluated as kPa.

Chapter 5

Conclusion & Recommendation for future work.

The conclusion of the study is presented. Of the six prototypes developed, two are of value to be scaled to the 155mm G5. Recommendations for further work based on the final two prototypes that were developed are proposed. These include modifications on the desired prototypes before development and evaluation on the full scale 155 mm are commenced.

5. CONCLUSION & RECOMMENDATION FOR FUTURE WORK

5.1 Conclusion

Of the six prototypes developed, the first two were unsuccessful in demonstrating the novel technique. The one being unable to survive the muzzle exit conditions and the control mechanism on the other one opened before the projectile emerged from the muzzle exit due to the recoil acceleration and respective inertia. This resulted in similar results as the conventional muzzle brakes.

The decrease in overpressure, of muzzle brake versions 3 and 4 in the active mode, was proportional to the decrease in efficiency. A linear presentation of overpressure ratio versus efficiency was obtained that had no positive contribution.

The last two types (versions 5 and 6) that were developed proved to be of value to be scaled to the 155 mm G5. Muzzle brake version 6 when fitted with 250 kN friction springs and utilized in the active mode achieved an efficiency of 34.8% that is very close to the constraint set of 35%. The overpressure constraint that the protection of the crew has to be alleviated with one level when utilizing the novel muzzle brake in relationship to the conventional muzzle brake was also met with this definition of version 6. The overpressure value of *version 6 active* at position G13 lies in the Y limit while the overpressure limit of the conventional reference (Scaled down G5 type on 88 mm) lies in the Z limit.

Version 5 when utilized in the active mode performed better regarding efficiency when the dynamic body had free movement before being restrained by the friction springs. The larger free movement resulted in an increase in efficiency. The overpressure stayed constant in spite of the modifications at a level lower than when firing without a muzzle brake. This is a very positive result and must be investigated for future work. Version 6 on the contrary yielded a lower efficiency when the friction spring rating was lowered from 250 kN to 125 kN. Again the overpressure stayed very much constant in spite of the modification. A possible reason for this phenomenon is that the forward impulse of version 6 is highly affected by the velocity of the ejecting gas through the aperture after the dynamic body has started to move. The small gap

initiates a higher gas velocity in comparison to the larger initial gap when using the lower rating of friction spring and thus gives rise to a higher efficiency.

General conclusions that can be made of the value of the project are as follows.

- The scaled down G5 type muzzle brake gave adequate results when tested on the G1 to serve as a reference for comparison between the different prototypes. A muzzle brake efficiency value of 32.1 % was obtained on the scaled down version in comparison to a value of 35 % for the 155 mm G5 muzzle brake. It can thus be said that the use of the caliber parameter as the scaling driver was successful.
- The design of a novel active muzzle brake is of such a nature that the structure of the closure and restoring mechanism must be very robust to withstand the harsh environment at the muzzle exit.
- Linear movement of the control surface or dynamic body provides a much better solution to the rotational movement. Not only is the mechanism less complicated, but also more robust.
- On the third trial no structural damage occurred to any of the muzzle brakes. On the first and second trial both the flap type of control surface application and restoring mechanism suffered severe damage.
- The introduction of the friction springs as a restoring mechanism was a mayor breakthrough in achieving a robust design.
- The use of recoil energy to evaluate muzzle brake efficiency is a much better way than using total recoil impulse. Two different muzzle brakes when fitted to the same weapon may impose the same impulse values, but the one muzzle brake may be more efficient due to a change in recoil displacement.
- The trace of the recoil displacement as a function of time is very important in the calculation of the recoil energy. The method of integration of the acceleration trace is quite cumbersome, but gave adequate results.

5.2 *Recommendations for future work*

Several improvements need to be done on version 5 and 6 before the development of the full scale 155 mm prototypes.

- It is necessary to investigate a method to improve the efficiency of version 5. The introduction of free travel of the dynamic body did yield positive results. It will thus be necessary to design a method to return the dynamic body to the baffle.

- It is necessary to investigate a method to prevent the dynamic body of version 6 from rotating during movement.
- Both versions need to be evaluated at different gun elevation angles in respect to the evaluated 0 degrees.

It will be useful to find a different technique to ascertain the dynamic recoil displacement trace. This is important not only for the G1 weapon, but also for other projects where the recoil energy has to be defined. This will save time during data analysis and will give more accurate results.

References

1. van Niekerk J.L., "Literature and Feasibility study into the use of active noise control in reducing impulse noise.", March 1995.

2. Williams A.G., "Basic Ballistics. Version 2.", 7June 2002., www.quarry.nildram.co.uk/ballistics.htm

3. Edwards D.G., " A Computational study of the flow through novel 88 mm muzzle brakes.", September 1998.

4. Phan K.C., "On the use of a shock tube as a blast simulator to study the performance of muzzle brake devices."

5. Phan K.C., "On a novel approach to muzzle brake design." Group working paper 4/93 (W7) – Unclassified

6. Schlenker , "Theoretical study of the blast field of artillery with muzzle brakes.", December 1962.

7. MIL – STD – 1474B, "Military standard – Noise limits for Army material."

8. Rheinmetall , "Handbook on Weaponry.", Rheinmetall GmbH, Dusseldorf, 1982.

9. Corner J., "Theory of the Interior Ballistics of Guns.", John Wiley & Sons, 1950.

10. AMCP 706-251, "Engineering design handbook – Muzzle Devices."

11. Schmidt E., "Measurements of Muzzle Brake Effectiveness.", 19th International Symposium of Ballistics 7-11 May 2001, Interlaken, Switzerland.

12. Salsbury J., "The effects of a muzzle brakes diameter & length on overpressure and efficiency.", October 1966.

13. Zucrow J., Hoffman J.D., "Gas Dynamics – Volume 1.", John Wiley & Sons.

14. Soifer M.T., "Muzzle brake analysis.", Watervliet Arsenal, June 1974.

15. Cohen H., Rogers G.F.C., Saravanamuttoo H.I.H., "Gas Turbine Theory.", Second Edition, 1982.

16. Fenstermacher C., "Introduction to friction springs and their use.", www.ringfeder-usa.com/PDF/Friction%.20springs.pdf

Appendix A

Illustration of G5 muzzle brake

The G5 muzzle brake is illustrated with the important scaling dimensions given as a reference to the caliber. The scaled down version of this type served as conventional baseline for the evaluation.

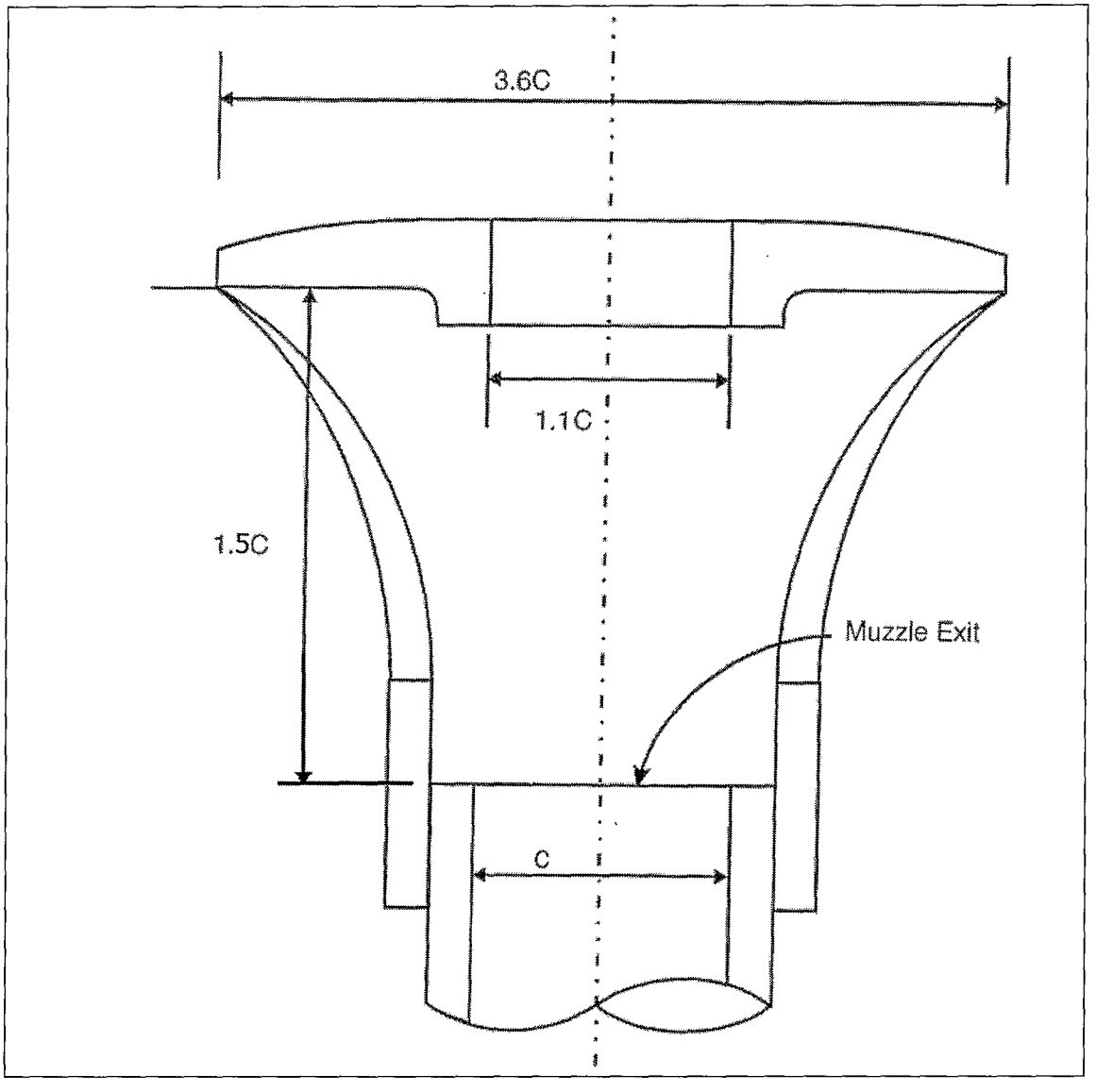

Figure A1. Illustration of G5 muzzle brake dimensioned in calibers.

Appendix B

Internal Ballistic Simulation of the G1

The internal ballistic data of the charge 3 configuration of the G1 weapon is presented. The simulation represent the movement of the projectile from shot starts until it uncorks from the muzzle end.

Weapon: 88mm kanon Charge: 88mm

Details about the empirical parameters

The empirical parameters are based on the following shot data:

Weapon:	88mm kanon
Charge:	88mm
Muzzle velocity:	470.0 m/s
Maximum pressure:	247.0 MPa

Details of weapon and projectile

Projektile mass:	11.0400	kg
Chamber volume:	2.3820	dm**3
Groove length:	1.883	m
Land diameter:	0.088000	m
Groove diameter:	0.088000	m
Groove:land ratio:	1.0000	
Barrel diameter:	0.0880	mm
Barrel crossection area:	0.00608212	m**2

Shot start pressure:	0.0000	MPa
Bullet pull:	0.0000	kN

Resistance pressures due to friction in barrel:

Position in barrel	Pressure
0.0000 m	0.00 MPa
0.0100 m	28.15 MPa
0.0200 m	14.52 MPa
1.8830 m	14.52 MPa

Details of charge

Parasite volume:	0.0000	dm**3
Number of propellants:	2	

Details of ignitor

Type of igniter:	SWARTPOEIER	
Specific energy:	249.0000	J/g
Mass of igniter:	0.0400	kg
Flame temperature:	2126.0000	K
Covolume:	0.3900	cm**3/g
Specific heat ratio:	1.2766	

Weapon: 88mm kanon Charge: 88mm

Details of the propellants

Propellant number 1

Name of propellant:	FNH	
Number of compositions:	1	
Propellant mass:	0.7910	kg
Time of ignition:	0.0000	ms
Name of grain:	FNH023	
Grain configuration:	7-perf. cylindrical	
Diameter of grain:	3.3910	mm
Length of grain:	8.1050	mm
Diameter of central perforation:	0.2350	mm
Diameter of outer perforations:	0.2500	mm
Inner web:	0.6770	mm
Outer web:	0.6510	mm
Specific surface:	0.001329	m**2/kg
Total surface area:	0.001051	m**2
Propellant composition:	FNH	
Specific energy:	971.7000	J/g
Flame temperature:	2629.8000	K
Covolume:	1.1410	cm**3/g
Specific heat ratio:	1.2590	
Density:	1.5800	g/cm**3
Lin. burn rate constant (Beta):	1.4500	mm/s/MPa**0.8189
Burn rate exponent (Alfa):	0.8189	

Weapon: 88mm kanon Charge: 88mm

Propellant number 2

Name of propellant:	NH
Number of compositions:	1
Propellant mass:	0.2130 kg
Time of ignition:	0.0000 ms
Name of grain:	NH012
Grain configuration:	Single perforated cord
Diameter of grain:	0.8250 mm
Length of grain:	4.3880 mm
Diameter of perforation:	0.2490 mm
Web:	0.2880 mm
Specific surface:	0.004714 m**2/kg
Total surface area:	0.001004 m**2
Propellant composition:	NH
Specific energy:	997.7000 J/g
Flame temperature:	2746.9000 K
Covolume:	1.1260 cm**3/g
Specific heat ratio:	1.2544
Density:	1.5700 g/cm**3
Lin. burn rate constant (Beta):	2.0756 mm/s/MPa**0.7930
Burn rate exponent (Alfa):	0.7930

Weapon: 88mm kanon Charge: 88mm

Time (ms)	Displ. (mm)	Vel. (m/s)	Gas-Temp. (K)	Breech pres. (MPa)	Aver. pres. (MPa)	Base pres. (MPa)	Mass fraction burnt	
0.00	0.	0.0	2127.	5.8	5.8	5.8	0.000	0.000
0.58	1.	3.4	2499.	18.9	18.9	18.9	0.013	0.060
1.07	4.	9.8	2601.	43.3	43.2	43.1	0.037	0.169
1.54	11.	20.8	2633.	85.1	84.9	84.4	0.081	0.353
2.02	26.	46.7	2630.	153.9	153.2	151.8	0.160	0.658
2.53	62.	96.8	2582.	232.1	230.4	227.1	0.294	1.000
3.02	124.	156.4	2483.	246.8	244.5	240.1	0.458	1.000
3.52	219.	218.8	2376.	240.0	237.4	232.1	0.642	1.000
4.05	350.	279.1	2273.	219.3	216.4	210.7	0.834	1.000
4.51	490.	325.2	2178.	186.7	184.1	178.7	0.942	1.000
5.01	662.	364.9	2070.	147.5	145.3	141.0	0.982	1.000
5.51	854.	395.6	1971.	116.4	114.7	111.2	0.997	1.000
6.00	1054.	418.7	1886.	93.9	92.5	89.7	1.000	1.000
6.55	1286.	438.4	1805.	75.8	74.7	72.4	1.000	1.000
7.03	1500.	452.1	1743.	64.0	63.1	61.1	1.000	1.000
7.56	1743.	464.3	1684.	54.1	53.3	51.7	1.000	1.000
7.86	1883.	470.1	1651.	49.6	48.8	47.4	1.000	1.000

Weapon: 88mm kanon Charge: 88mm

Maximum breech pressure:	247.0	MPa
Displacement at max. pressure:	0.140	m
Time at maximum pressure:	3.1167	ms
Maximum acceleration:	124281.	m/s**2
Muzzle velocity:	470.1	m/s
Base pressure at muzzle exit:	47.4	MPa
Time at muzzle exit:	7.8550	ms
Kinetic energy at muzzle:	1219.82	kJ
All propellants are burnt out at		
Time:	5.99	ms
Displacement:	1.050	m
Piezometric efficiency:	0.4312	
Ballistic efficiency:	0.3184	

Appendix C

Barrel Discharge Simulation of the G1

The discharge of the barrel after the projectile has left the muzzle of the G1 for the charge 3 configuration is simulated. The data of the muzzle end conditions for the discharge period that served as input to the CFD simulations is presented.

{Listing of BD88.PAS}

Breech Pressure at Muzzle exit (kPa)	49600
Muzzle exit pressure (kPa)	47400
Time of Muzzle exit (s)	0.007850
Breech Area (m^2)	0.0061277
Velocity of projectile at muzzle exit(m/s)	470.1
Average Spesific Energy of Propellant(J/kg)	971000
Flame temperature of propellant (K)	2629
Gas temperature at muzzle exit (K)	1652
Ratio of specific heats of gas	1.2587
CoVolume (m^3/kg)	1.1410e-3
Mass of projectile (kg)	11.04
Mass of propellant (kg)	1.044
Total volume of bore and chamber (m^3)	0.01406

Input Filename = C:\Program Files\Borland\Delphi6\Projects\Mydir\Afblaas\BD88.PAS
Output Filename = C:\Program Files\Borland\Delphi6\Projects\Mydir\Afblaas\output.dat

BLOWDOWN ANALYSIS
****

TIME (sec)	MASSFLOW (kg/s)	MUZZLE EXIT PRESSURE (kPa)	MUZZLE EXIT TEMPERATURE (K)	DENSITY (kg/m^3)	GAS VELOCITY (m/s)
0.0079	237.78	47400.00	1652.00	71.36	543.78
0.0089	185.11	34585.21	1569.13	55.87	540.67
0.0099	145.11	25457.72	1492.55	43.87	539.82
0.0109	114.51	18895.49	1421.64	34.57	540.62
0.0119	90.93	14135.66	1355.84	27.35	542.63
0.0129	72.64	10654.11	1294.66	21.73	545.54
0.0139	58.35	8087.21	1237.68	17.34	549.11
0.0149	47.13	6180.30	1184.51	13.90	553.17
0.0159	38.25	4753.47	1134.81	11.20	557.59
0.0169	31.21	3678.50	1088.29	9.06	562.27
0.0179	25.57	2863.32	1044.67	7.36	567.14
0.0189	21.05	2241.26	1003.71	6.00	572.15
0.0199	17.40	1763.75	965.20	4.92	577.25
0.0209	14.44	1395.08	928.94	4.05	582.41
0.0219	12.04	1108.90	894.76	3.34	587.61
0.0229	10.07	885.57	862.50	2.77	592.84
0.0239	8.45	710.41	832.01	2.31	598.06
0.0249	7.12	572.38	803.17	1.93	603.28
0.0259	6.01	463.09	775.86	1.61	608.49
0.0269	5.10	376.17	749.97	1.36	613.68
0.0279	4.34	306.75	725.40	1.14	618.84
0.0289	3.70	251.07	702.06	0.97	623.97
0.0299	3.16	206.24	679.86	0.82	629.07
0.0309	2.71	170.00	658.74	0.70	634.14
0.0319	2.33	140.59	638.63	0.60	639.17
0.0329	2.01	116.65	619.46	0.51	644.17
0.0339	1.74	97.09	601.16	0.44	649.13
0.0349	1.51	81.05	583.70	0.38	654.05
0.0359	1.31	67.86	567.01	0.32	658.94
0.0369	1.14	56.98	551.06	0.28	663.79
0.0379	0.99	47.97	535.79	0.24	668.60

Velocity of sound = 876.36 m/s
Spesific Energy at muzzle exit = 971.00 J/g
Impuls on Muzzle (Modified Hugeniot Method) = 145.12 kPa.s

Appendix D

CFD Simulation data of Versions 5 and 6.

The pressure contour plots showing the flowfield for a run time of 3 ms of versions 5 and 6 with and without the dynamic body are presented.

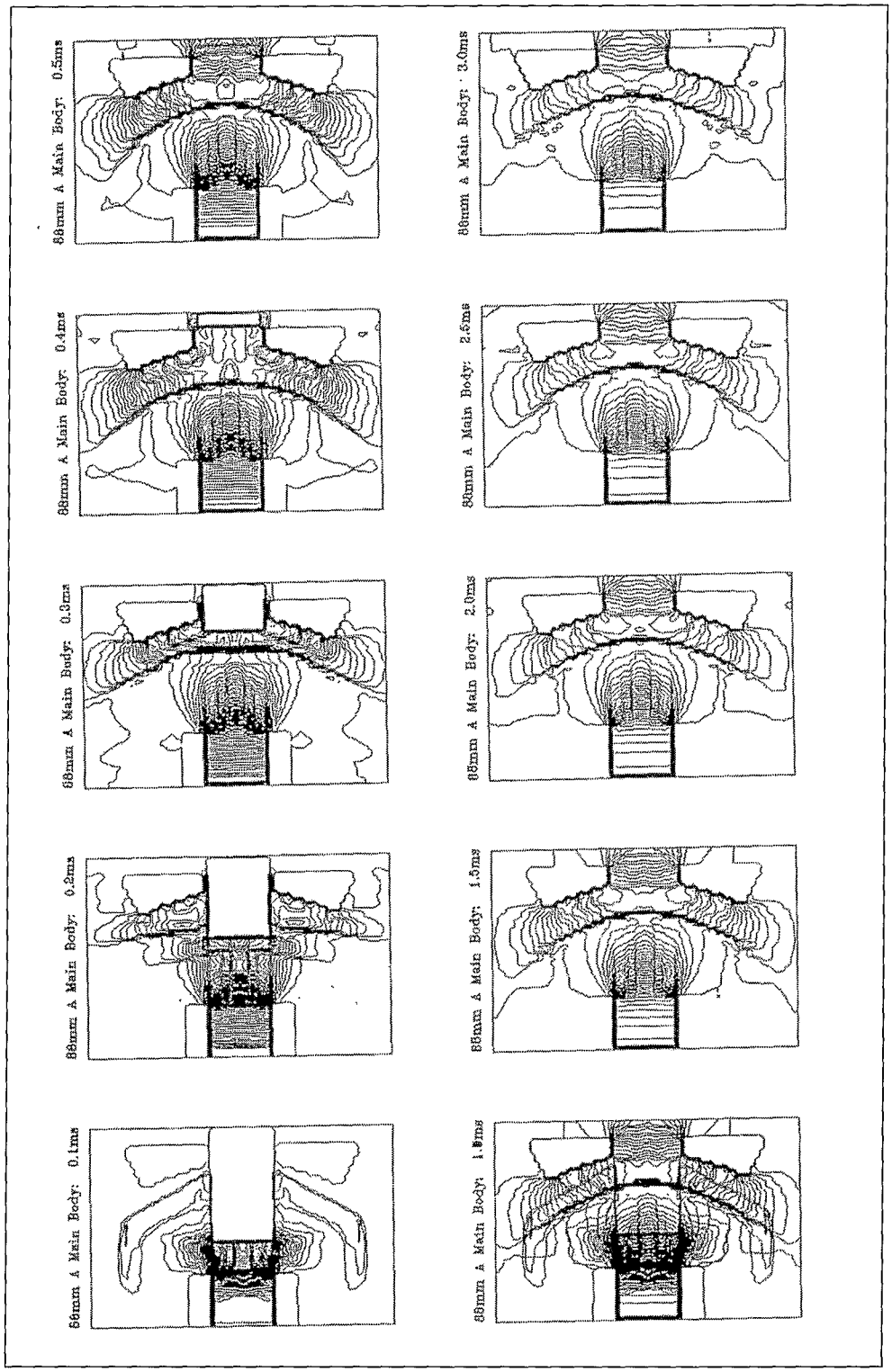

Figure D1. CFD simulation of Version 5 as conventional muzzle brake. Pressure contour plots showing flowfield.

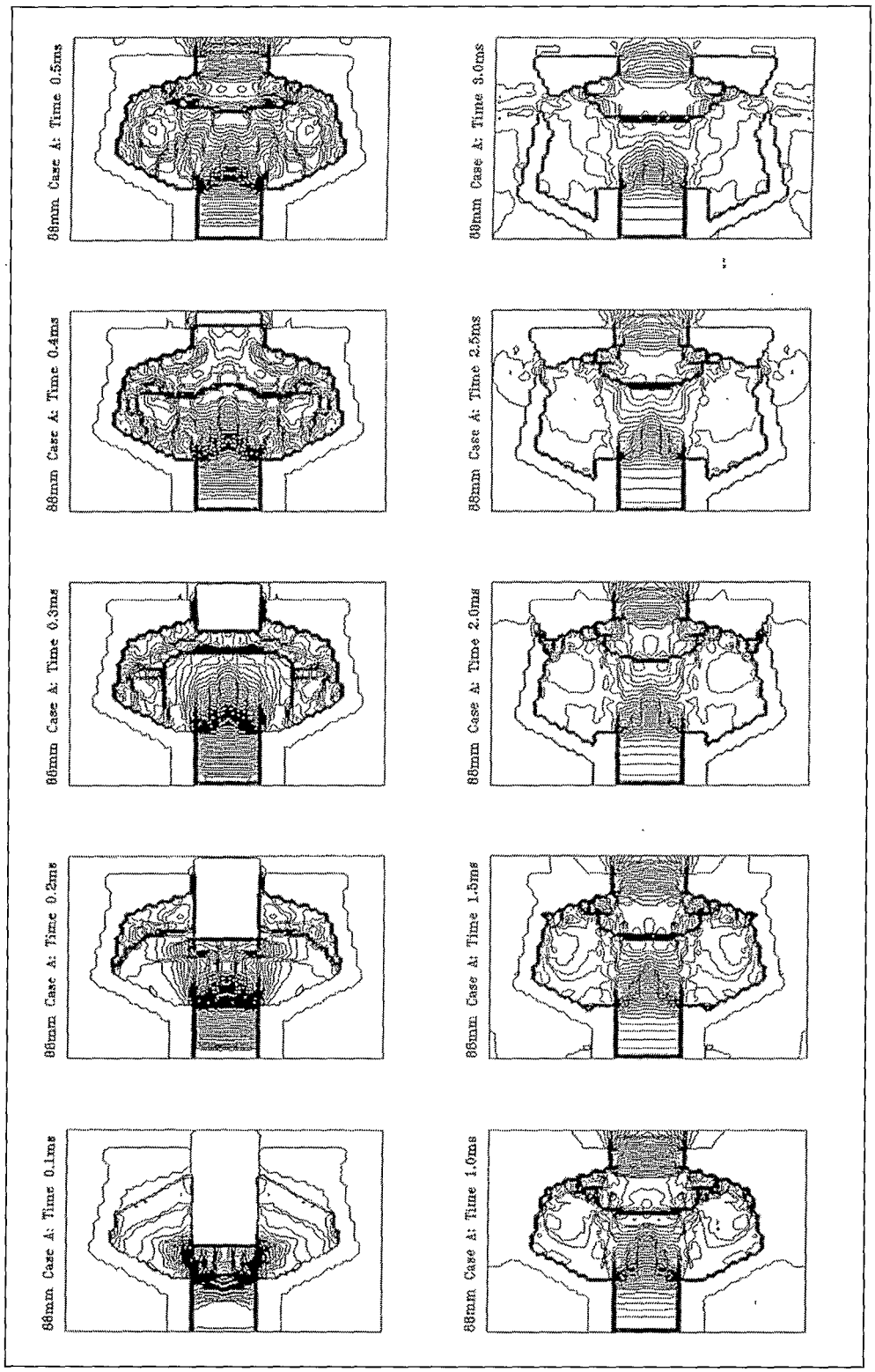

Figure D2. CFD simulation of Version 5 with dynamic body.Pressure contour plots showing flowfield.

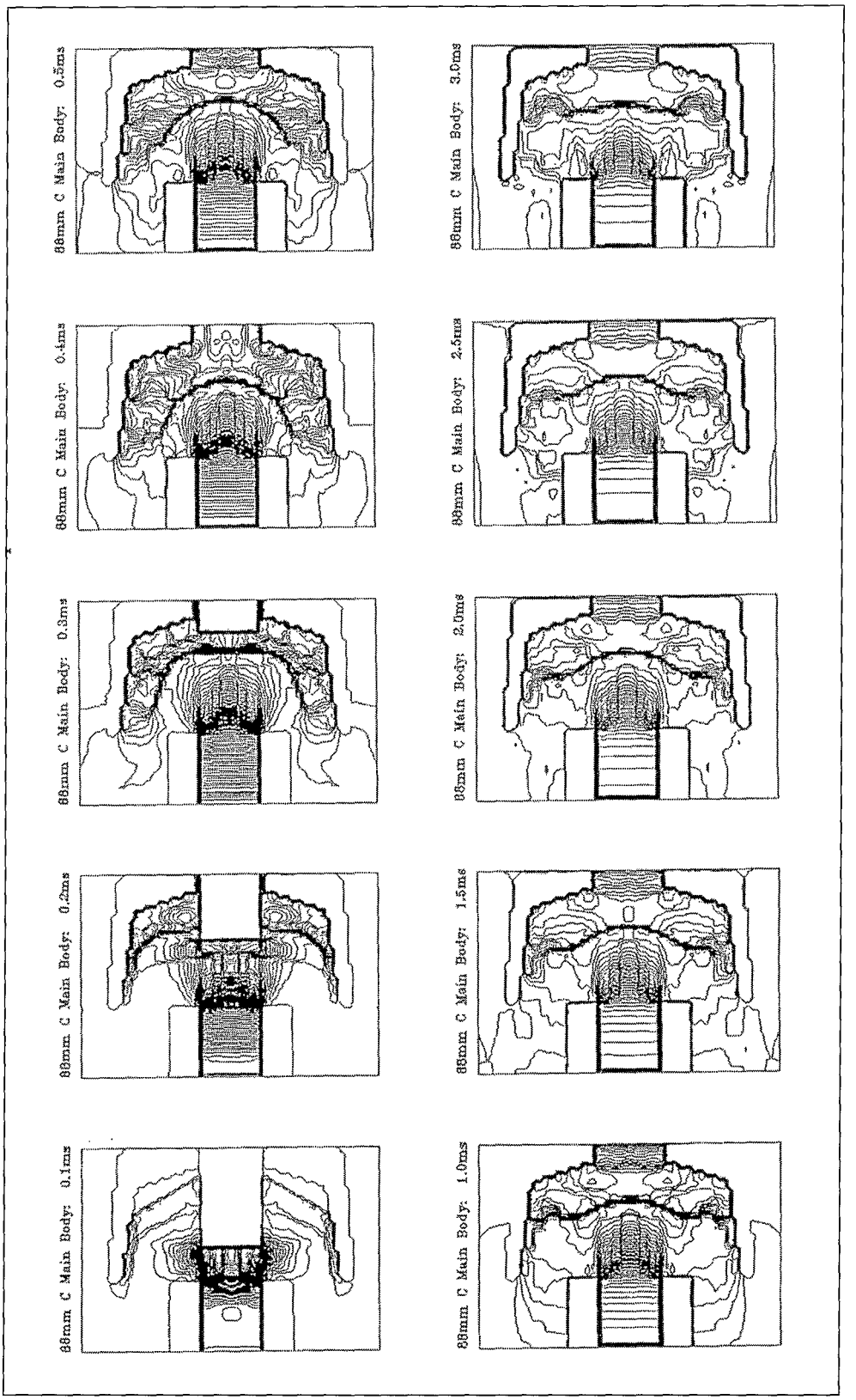

Figure D3. CFD simulation of Version 6 as conventional muzzle brake. Pressure contour plots showing flowfield.

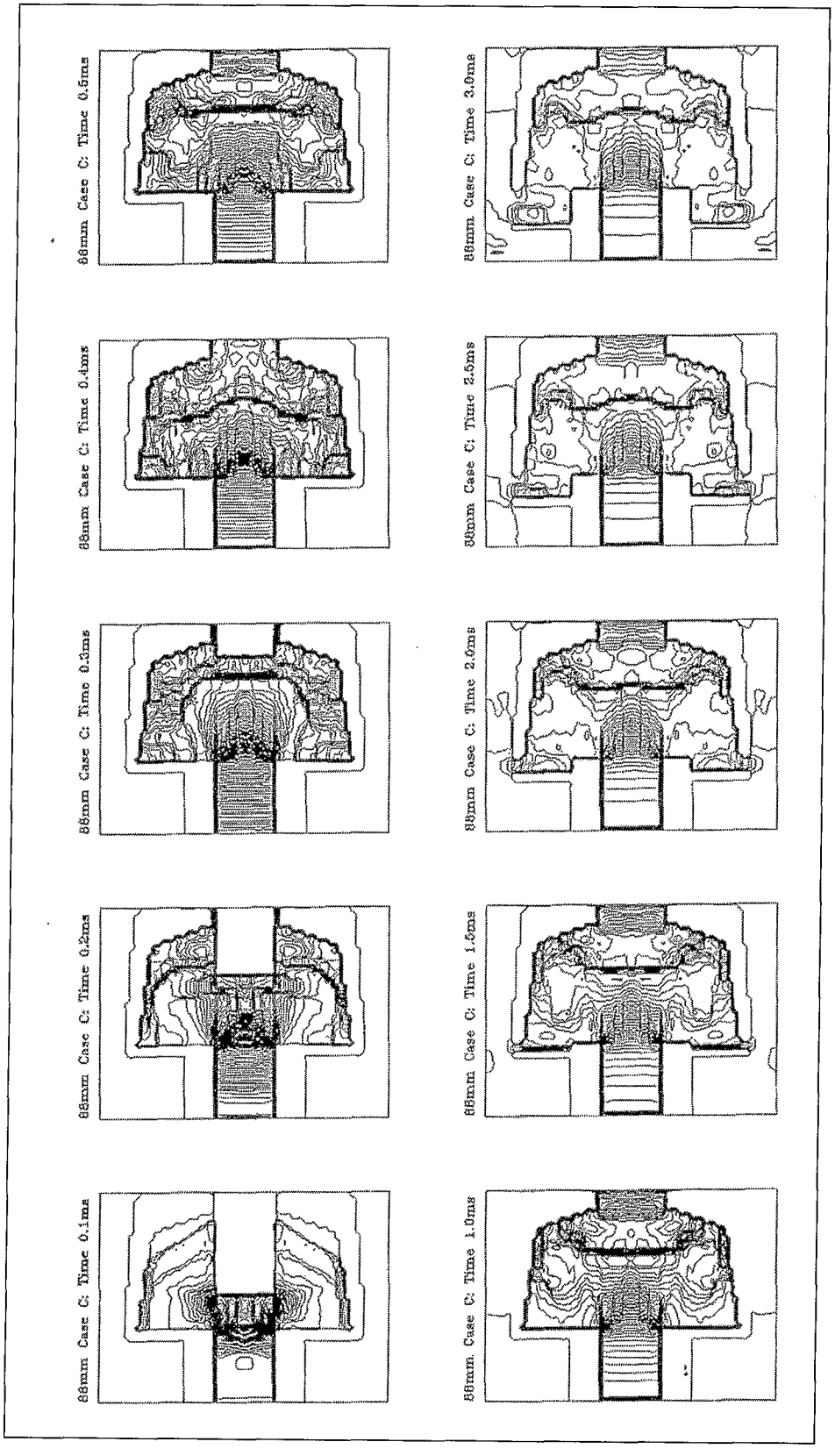

Figure D4. CFD simulation of Version 6 with dynamic body.Pressure contour plots showing flowfield.

Appendix E

Detail evaluation data of phases 1, 2 and 3.

The detail data per round fired of the evaluation trials of phases 1, 2 and 3 in tabular format is presented. The condensed data forms part of the main body of the dissertation.

Muzzle brake configuration	Shot No	Chamber pressure Mpa	Recoil length (mm)	Recoil Impulse kN.s	Counter Impulse kN.s	Total Impulse kN.s	Recoil Energy kJ
No muzzle brake	Mbb01	218	855	3.34	3.55	6.89	25.8
	Mbb02	222	850	3.35	3.65	7.00	26.2
	Mbb03	213	845	3.20	3.91	7.11	25.7
	Mbb04	219	845	3.20	3.85	7.05	25.6
	Mbb05	221	845	3.15	3.75	6.90	26.1
	Mbb06	223	850	3.2	3.65	6.85	26.1
	Mbb07	226	850	3.22	3.64	6.86	26.2
	Mbb08	215	850	3.08	3.63	6.71	25.8
G5 scale down muzzle brake	Maz01	230	750	1.97	3.8	5.77	18.2
	Maz02	235	760	1.96	3.85	5.81	18.5
	Maz03	236	755	1.99	3.85	5.84	18.7
	Maz04	235	760	2.00	3.89	5.89	19.1
	Maz05	236	760	2.03	3.52	5.55	16.8
	Maz06	234	755	2.00	3.62	5.62	17.3
	Maz07	235	760	2.00	3.62	5.62	17.3
	Maz08	236	765	2.05	3.72	5.77	18.2
G5 scale down muzzle brake 70 degree to rear Version 1 with flap fixed in open position	May01	228	740	1.92	3.75	5.67	17.6
	May02	246	745	1.98	3.77	5.75	18.1
	May03	230	740	1.95	3.65	5.6	17.2
	May04	235	740	1.97	3.65	5.62	17.3
	May05	225	735	2.20	3.20	5.4	15.9
	May06	225	735	1.92	3.4	5.32	15.5
	May07	244	740	1.90	3.65	5.55	16.9
	May08	248	740	1.97	3.80	5.77	18.2
Slotted sleeve Version 2 with sleeve fixed in open position	Max01	239	815	2.67	3.26	5.91	19.2
	Max02	235	810	2.71	3.20	5.91	19.3
	Max03	230	810	2.61	3.23	5.84	18.9
	Max04	234	800	2.65	3.20	5.85	18.8
	Max05	235	810	2.69	3.22	5.91	19.3

Table E1. Impulse data – Phase 1

Muzzle brake configuration	Shot No	Chamber pressure (MPa)	Overpressure (ΔP) in kPa and B-duration (τ_B) in ms					
			G11		G12		G13	
			ΔP	τ_B	ΔP	τ_B	ΔP	τ_B
No muzzle brake	Mbb01	218	3.15	17.95	4.16	10.35	1.33	18.95
	Mbb02	222	3.15	17.72	3.90	11.30	1.39	18.95
	Mbb03	213	2.64	18.65	4.04	10.35	0.95	19.45
	Mbb04	219	2.76	18.95	3.77	11.65	1.10	18.70
	Mbb05	221	-	-	-	-	-	-
	Mbb06	223	2.84	18.59	3.85	11.48	1.28	19.00
	Mbb07	226	2.83	18.59	3.89	11.45	1.22	19.10
	Mbb08	210	3.09	17.98	4.17	10.30	1.39	18.95
G5 scale down muzzle brake	Maz01	230	18.67	8.05	19.24	12.12	10.33	13.86
	Maz02	235	18.21	7.95	18.49	12.30	9.01	14.15
	Maz03	236	19.71	7.68	19.42	12.10	9.27	14.15
	Maz04	235	19.02	7.75	20.23	12.05	10.15	14.18
	Maz05	236	20.67	7.95	19.48	12.10	10.54	13.98
	Maz06	234	18.31	7.98	17.04	12.74	8.70	14.20
	Maz07	235	17.79	8.31	18.43	12.28	8.23	14.53
	Maz08	236	17.95	8.26	18.90	12.25	10.13	13.95
G5 scale down muzzle brake. Baffle 70° to rear. Version 1 with flap fixed in open position	May01	228	21.68	8.42	17.02	11.76	9.75	11.84
	May02	246	22.02	8.35	14.85	12.16	9.12	11.87
	May03	230	22.56	8.23	17.81	11.85	10.26	11.82
	May04	235	23.17	8.18	14.66	12.29	10.22	11.80
	May05	225	23.74	8.13	15.65	12.13	10.29	11.86
	May06	225	22.02	8.31	14.18	12.35	10.08	11.76
	May07	244	22.83	8.25	16.41	11.75	10.61	10.98
	May08	248	22.36	8.25	14.43	12.24	10.78	10.87
Slotted sleeve version 2 with sleeve fixed in open position	Max01	239	12.50	14.03	11.75	13.67	7.58	9.89
	Max02	235	11.35	14.08	12.78	13.15	6.88	10.62
	Max03	230	11.06	14.11	11.87	13.65	6.95	10.67
	Max04	234	13.62	13.97	12.22	13.12	7.75	10.15
	Max05	235	12.84	13.95	-	-	8.18	9.76

Table E2. Overpressure data – Phase 1

	Shot No	Charge	Chamber pressure (Mpa)	Recoil length (mm)	Wind (m/s)	Temp (ºC)
No muzzle brake	A5	2	158	580	3.4	38.4
	A6	2	160	570	5.5	38.3
	A7	2	162	570	3.6	39.1
	A8	2	-	570	6.1	39.3
Version 3 Double baffle open (Conventional)	A9	2	163	460	3.4	37.6
	A10	2	163	455	4.9	35.8
	A11	2	162	455	5.9	36.5
	A12	2	162	455	3.9	36.9
Version 3 Double baffle active	A17	2	162	515	5.2	38.3
	A18	2	158	510	3.9	38.9
	A19	2	164	515	5.3	39.7
	A20	2	159	512	4.6	40.4
Version 4 Single baffle open (Conventional)	A29	2	164	500	0.5	28.3
	A30	2	153	485	0.4	28.5
	A31	2	149	480	2.2	28.5
	A32	2	161	498	1.8	29.5
Version 4 Single baffle active	A37	2	153	522	2.7	30.9
	A38	2	154	522	2.4	30.6
	A39	2	150	522	3.5	31
	A40	2	150	524	2.3	33
No muzzle brake	A25	3	261	737	2.1	26.8
	A26	3	261	742	3	27.5
	A27	3	267	740	2.8	26.7
	A28	3	275	745	3.3	27.1
Version 3 Double baffle open (Conventional)	A13	3	246	590	5.1	36.4
	A14	3	248	595	5	37.3
	A15	3	248	593	4	38.2
	A16	3	257	600	5.8	38.5
Version 3 Double baffle active	A21	3	257	676	7.7	40.9
	A22	3	268	670	10.3	40.8
	A23	3	259	670	8.9	39.9
	A24	3	252	670	11.1	40.5
Version 4 Single baffle open (Conventional)	A33	3	235	639	1.7	30.1
	A34	3	238	636	1.7	31.1
	A35	3	242	639	2	30.3
	A36	3	240	638	1	30.9
Version 4 Single baffle active	A41	3	236	685	2.2	33.2
	A42	3	232	685	2.5	33.1

Table E3. Summary of general data on all shot fired during the evaluation of phase 2.

Muzzle brake configuration	Shot No	Charge	Chamber pressure Mpa	Chamber Impulse kN.s	Recoil Impulse kN.s	Counter Impulse kN.s	Total Impulse kN.s
No muzzle brake	A5	2	158	5.44	1.64	2.25	3.89
	A6	2	160	5.49	1.66	3.15	4.81
	A7	2	162	5.44	-	1.64	-
	A8	2	-	-	-	3.2	-
Version 3 conventional	A9	2	163	5.31	1.32	1.37	2.69
	A10	2	163	5.43	1.28	2.09	3.37
	A11	2	162	5.42	1.34	2.18	3.52
	A12	2	162	5.43	1.28	2.35	3.63
Version 3 active	A17	2	162	5.44	1.66	2.37	4.03
	A18	2	158	5.23	1.58	2.38	3.96
	A19	2	164	-	1.66	2.56	4.22
	A20	2	159	5.21	1.58	2.56	4.14
Version 4 conventional	A29	2	164	5.58	1.52	2.13	3.65
	A30	2	153	5.44	1.42	2.24	3.66
	A31	2	149	5.44	1.42	2.17	3.59
	A32	2	161	5.54	1.54	2.25	3.79
Version 4 active	A37	2	153	5.25	1.66	2.27	3.93
	A38	2	154	5.27	1.66	2.28	3.94
	A39	2	150	5.27	1.64	2.25	3.89
	A40	2	150	5.31	1.74	2.32	4.06
No muzzle brake	A25	3	261	6.56	4.04	3.25	7.29
	A26	3	261	6.60	4	3.6	7.6
	A27	3	267	6.64	3.84	3.58	7.42
	A28	3	275	6.60	3.96	3.68	7.64
Version 3 conventional	A13	3	246	6.77	2.12	3.11	5.23
	A14	3	248	6.60	2.12	3.15	5.27
	A15	3	248	6.79	2.06	-	-
	A16	3	257	6.60	2.1	3.17	5.27
Version 3 active	A21	3	257	6.56	3.3	3.5	6.8
	A22	3	268	6.64	2.98	3.46	6.44
	A23	3	259	6.82	3.06	2.98	6.04
	A24	3	252	6.77	2.96	-	-
Version 4 conventional	A33	3	235	6.52	2.6	2.93	5.53
	A34	3	238	6.38	2.6	2.96	5.56
	A35	3	242	6.66	2.66	3	5.66
	A36	3	240	6.42	2.63	3.02	5.65
Version 4 active	A41	3	236	6.42	3.36	3.19	6.55
	A42	3	232	6.31	3.3	3.17	6.47

Table E4. Impulse data per round fired – Phase 2.

Muzzle brake configuration	Shot No	Charge	Chamber pressure (MPa)	Overpressure (ΔP) in kPa and B-duration (τ_B) in ms							
				G11		G12		G13		G53	
				ΔP	τ_B	ΔP	τ_B	ΔP	τ_B	ΔP	τ_B
No muzzle brake	A5	2	158	3.22	25.44	1.97	19.1	2.1	21.89	1.45	21.78
	A6	2	160	3.39	25.45	2.03	19.1	1.71	21.60	1.28	22.30
	A7	2	162	9.48	28.68	6.12	26.43	6.91	25.48	4.07	22.11
	A8	2	-	7.04	30.28	6.87	25.10	6.47	23.90	5.01	22.31
Version 3 Conventional	A9	2	163	16.51	16.24	5.59	14.43	7.83	16.83	5.75	12.21
	A10	2	163	15.88	16.85	6.07	14.54	8.89	16.73	5.57	12.34
	A11	2	162	15.85	17.32	7.68	14.21	7.46	16.21	5.63	11.85
	A12	2	162	16.52	17.21	5.69	15.11	7.87	17.20	5.09	11.87
Version 3 active	A17	2	162	4.09	17.11	2.87	13.89	3.37	16.43	2.52	12.11
	A18	2	158	4.64	16.54	2.88	14.21	3.06	16.12	2.45	11.98
	A19	2	164	5	17.23	2.91	14.45	3.46	16.32	2.59	11.76
	A20	2	159	4.56	16.85	3.27	14.12	3.52	16.23	2.59	11.32
Version 4 Conventional	A29	2	164	13.1	20.11	5.09	12.56	6.37	17.65	4.67	15.67
	A30	2	153	14	22.57	5.16	13.03	5.47	17.32	4.44	15.23
	A31	2	149	13.91	23.11	5.04	14.97	5.72	17.06	4.63	15.86
	A32	2	161	13.7	22.21	5.08	13.88	6.13	18.11	4.46	15.17
Version 4 active	A37	2	153	3.81	23.12	2.68	12.10	2.31	20.16	1.32	19.66
	A38	2	154	3.35	25.34	2.41	12.08	1.87	19.55	1.37	19.43
	A39	2	150	3.21	25.12	2.08	13.12	1.87	19.64	1.33	18.74
	A40	2	150	3.51	24.67	2.4	12.77	-	-	1.48	19.04
No muzzle brake	A25	3	261	4.87	18.45	2.13	19.78	2.81	16.45	1.82	20.16
	A26	3	261	4.92	18.59	1.96	20.71	2.66	16.59	1.73	20.32
	A27	3	267	5.03	18.29	2.19	19.56	2.79	16.45	1.93	20.35
	A28	3	275	5.19	18.25	2.34	19.56	2.81	16.78	1.86	20.13
Version 3 Conventional	A13	3	246	20.75	13.94	7.38	13.68	10.59	12.08	7.85	11.28
	A14	3	248	20.19	13.98	7.49	13.76	10.26	13.07	6.84	11.45
	A15	3	248	22.2	11.70	7.38	13.65	10.28	12.12	7.39	11.10
	A16	3	257	22.67	12.67	8.45	12.67	12.25	11.89	7.09	11.28
Version 3 active	A21	3	257	7.17	13.12	4.82	13.67	4.76	12.54	3.36	10.45
	A22	3	268	8.16	12.11	5.29	12.35	5.58	11.69	3.74	10.62
	A23	3	259	7.57	13.38	4.85	13.65	5.49	11.74	4.17	10.34
	A24	3	252	7.67	13.38	4.32	13.45	5.33	11.67	3.88	10.65
Version 4 Conventional	A33	3	235	16.52	14.23	5.75	13.46	8.12	12.34	5.79	14.78
	A34	3	238	17.64	13.90	6.13	13.28	8.37	12.22	5.78	14.78
	A35	3	242	20.36	12.67	6.26	13.25	8.35	12.23	5.41	14.34
	A36	3	240	19.92	12.65	7.14	12.65	8.73	12.56	5.67	14.45
Version 4 active	A41	3	236	3.91	17.67	7.75	12.89	3.2	15.23	1.86	18.79
	A42	3	232	5.08	15.94	5.27	12.61	3.2	15.14	1.98	18.58

Table E5. Overpressure data per round fired – Phase 2.

Muzzle brake configuration	Shot No	Chamber pressure (MPa)	Recoil Length (mm)	Total Impulse (kNs)	Recoil Energy (kJ)
No muzzle brake	2	259.8	776	6.03	27.15
	3	258.1	776	5.89	26.47
	4	261.5	780	6.13	28.21
	5	262.3	782	5.77	28
	6	263.6	782	5.81	26.4
Version 5 Conventional	7	265	686	3.92	15.75
	8	270.3	686	4.24	16.23
	9	261.4	682	4.26	16.28
	10	259.1	676	4.16	14.53
	11	266.5	682	4.35	16.43
Version 5 Active with 20 elements of 125 kN FS	12	260	756	4.44	19.12
	13	259.7	757	-	-
	14	256.5	751	5.05	21.65
	15	264.9	753	5.16	19.75
	16	258.3	750	5.26	21.68
Version 5 Active with 17 elements of 250 kN FS (38 mm free)	17	259.6	747	4.13	16.06
	18	261.3	745	4.90	21.1
	19	262	741	5.18	20.95
	20	259.9	740	5.07	21.3
	21	267.4	743	5.07	21.13
Version 5 Active with 13 elements of 250 kN FS (94 mm free)	22	261.6	726	4.89	19.74
	23	260.6	730	4.56	19.71
	24	256.6	728	3.79	19.08
	25	260.5	735	-	-
	26	263.2	732	4.66	18.83
Version 6 Conventional	27	261.3	647	3.438	13.62
	28	258.5	649	3.15	13.25
	29	259.8	651	3.55	13.28
	30	256.2	646	3.36	13.98
	31	259.4	645	3.18	14.55
Version 6 Active with 20 elements of 125 kN FS	32	264.9	762	4.41	21.35
	33	264	758	4.96	20.96
	34	260	758	4.89	20.09
	35	265.5	760	4.86	22.07
Version 6 Active with 20 elements of 250kN FS	36	263.5	730	3.54	13.71
	37	262.6	722	4.54	17.33
	38	266.7	719	4.02	17.86
	39	267	721	4.76	18.25

Table E6. Impulse data per round fired – Phase 3

Muzzle brake configuration	Shot No	Chamber pressure (MPa)	Overpressure (ΔP) in kPa and B-duration (τ_B) in ms							
			G11		G12		G13		G53	
			ΔP	τ_B	ΔP	τ_B	ΔP	τ_B	ΔP	τ_B
No muzzle brake	2	259.8	4.90	81.4	4.68	75.8	3.31	65.3	2.12	56.7
	3	258.1	4.90	78.65	4.68	72.5	3.35	65.1	1.89	62.3
	4	261.5	4.77	79.6	4.63	73.7	3.18	83	2.07	61.5
	5	262.3	4.5	82.15	4.68	90.7	3.18	68.5	2.07	84.5
	6	263.6	4.5	80.1	4.94	74.7	3.09	83.9	1.99	80.2
Version 5 Conventional	7	265	14.69	39.4	13.46	36.1	9	30.4	5.83	52.6
	8	270.3	17.17	24.4	15.32	34.7	9.67	56.9	6.05	51.1
	9	261.4	16.33	30.8	14.17	-	8.56	59.6	5.43	55.2
	10	259.1	16.59	21.3	14.35	43.5	10.15	21.7	6.36	38.8
	11	266.5	16.15	28.3	-	-	8.87	23	5.34	49.2
Version 5 Active with 20 elements of 125 kN FS	12	260	4.59	78.6	5.16	46.3	2.25	80.8	1.85	90.9
	13	259.7	-	-	5.43	73.8	2.29	96.9	1.81	97.6
	14	256.5	-	-	5.12	73.7	2.25	102.5	1.81	91.3
	15	264.9	4.86	73.7	5.29	65.8	2.38	95.9	1.81	88.9
	16	258.3	4.59	78.6	5.29	66.8	2.38	96.5	1.81	91.7
Version 5 Active with 17 elements of 250 kN FS (38 mm free)	17	259.6	4.33	79.5	4.59	89.8	2.52	94.8	1.72	-
	18	261.3	3.93	77.2	5.16	84.9	2.25	105	1.55	88.1
	19	262	3.88	76.9	4.94	71.4	2.34	107.7	1.37	106.2
	20	259.9	4.33	77.2	5.87	72.5	2.38	104.7	1.63	89
	21	267.4	4.77	75.9	5.25	74.8	2.34	95.2	1.77	90.4
Version 5 Active with 13 elements of 250 kN FS (94 mm free)	22	261.6	4.68	78.9	5.08	46.6	2.34	105	1.81	-
	23	260.6	4.41	77.1	5.69	71.3	2.12	103.1	1.85	90
	24	256.6	4.68	78.7	5.34	73.3	2.12	-	1.89	101.8
	25	260.5	5.12	73.9	5.52	83.1	2.16	103.7	1.81	90.6
	26	263.2	4.86	75.2	5.29	69.6	2.64	111.1	1.89	101.7
Version 6 Conventional	27	261.3	32.26	-	15.23	30.1	13.64	20.4	9	37.9
	28	258.5	35.05	-	16.64	30.5	16.38	22.2	11.2	46.4
	29	259.8	32.97	-	15.67	-	13.55	24.3	10.2	47.1
	30	256.2	33.68	-	14.78	33.4	14.21	23.3	10.4	49.8
	31	259.4	34.96	-	18.1	24.3	16.15	17.7	10.7	48.9
Version 6 Active with 20 elements of 125 kN FS	32	264.9	20.48	58	7.9	69.3	4.76	66.3	3.66	57.6
	33	264	19.86	30.4	7.11	65.4	5.58	67.6	4.11	59.4
	34	260	19.24	43.8	6.97	65.4	5.49	81.2	3.75	73.1
	35	265.5	19.99	43.1	8.39	65.9	5.33	59.7	3.39	92
Version 6 Active with 20 elements of 250kN FS	36	263.5	11.29	21.5	7.64	38.2	5.21	22.6	3.79	58.3
	37	262.6	9.93	26.5	10.33	35.8	4.86	31.3	3.53	56.1
	38	266.7	11.17	37.3	9.93	39.3	5.65	59.4	4.15	57
	39	267	10.55	37.2	9.53	65.4	4.94	64.7	3.75	57.4

Table E7. Overpressure data – Phase 3

Appendix F

Traces of trial data of No brake situation – Phase 2.

Traces of the important parameters verified during the trial of phase 2 for the no muzzle brake situation – shot 26 is presented.

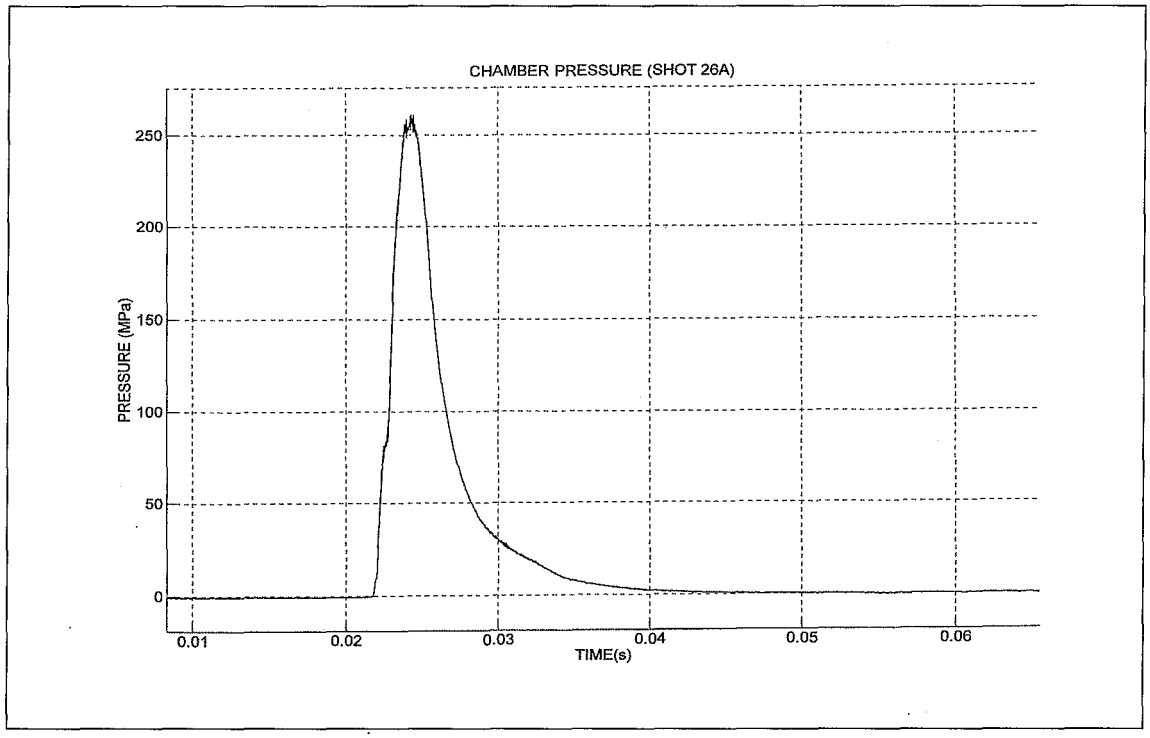

Figure F1. Chamber pressure

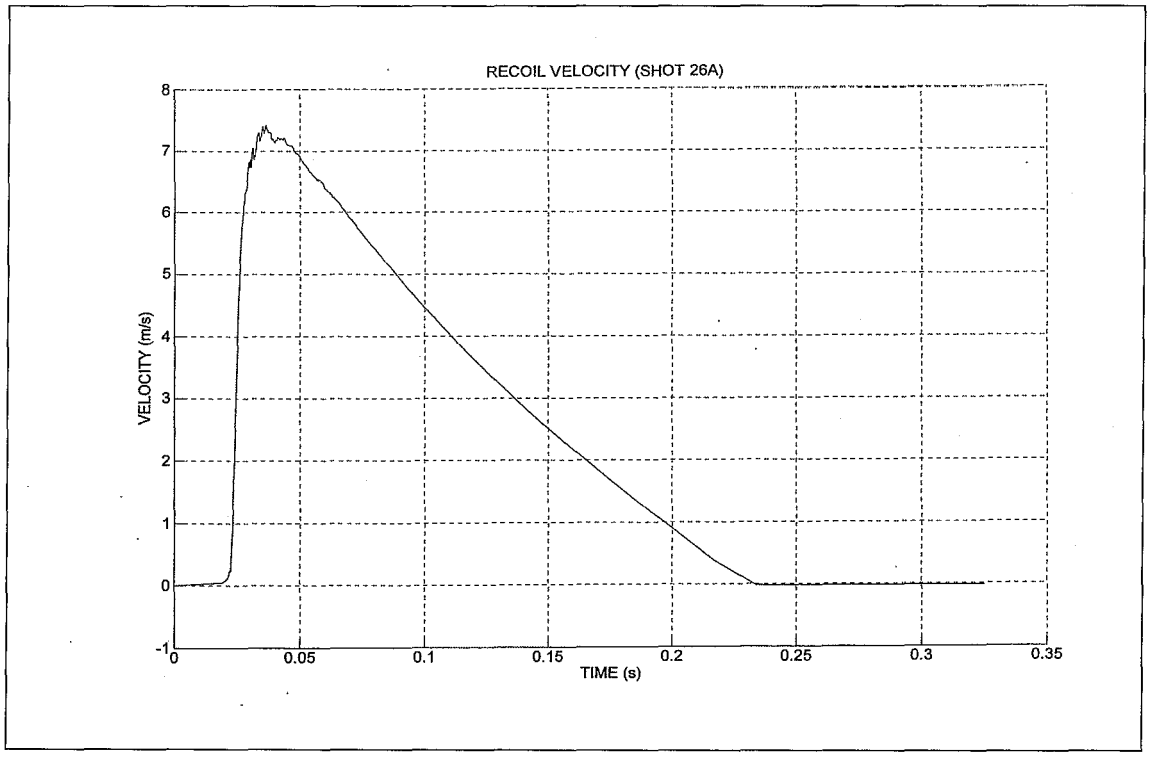

Figure F2. Recoil velocity

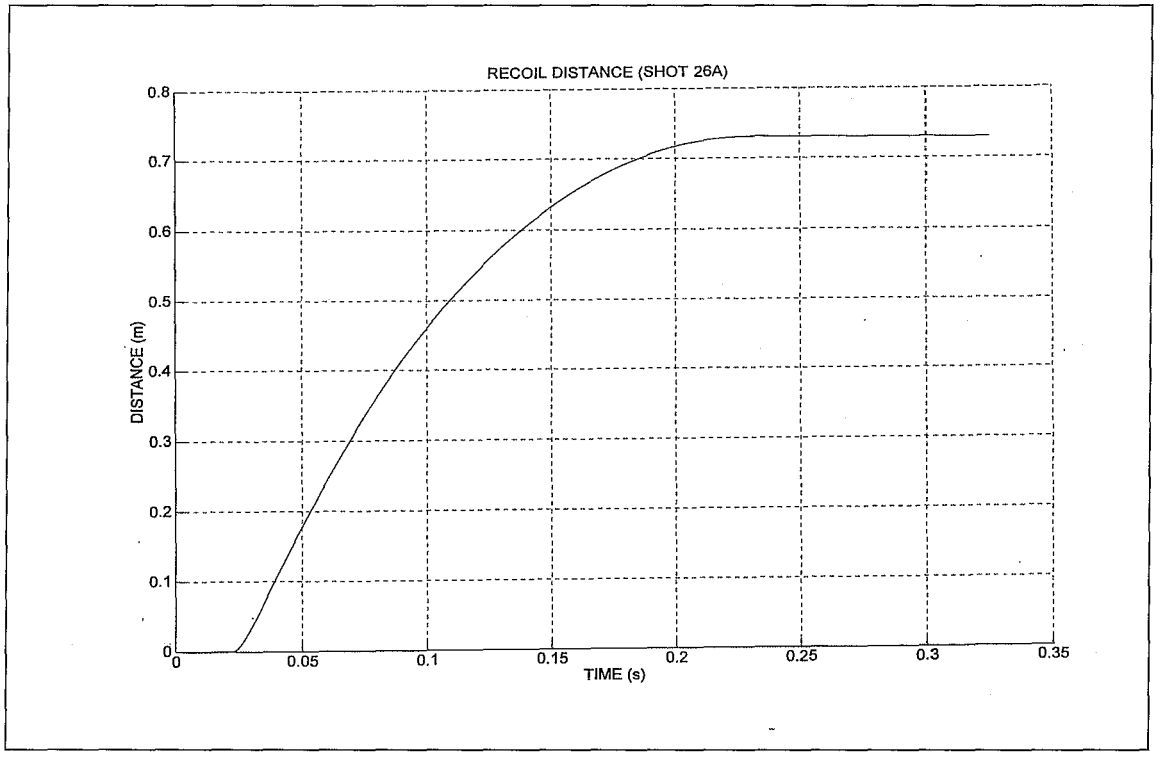

Figure F3. Recoil displacement

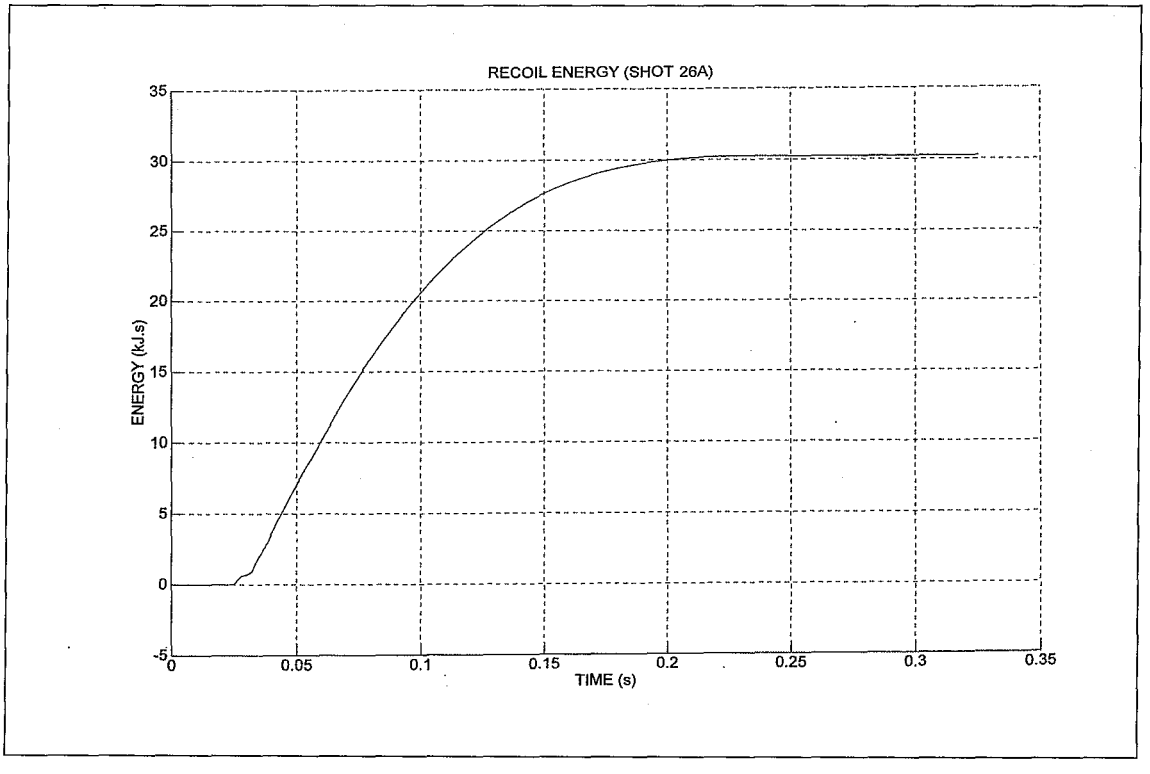

Figure F4. Recoil energy

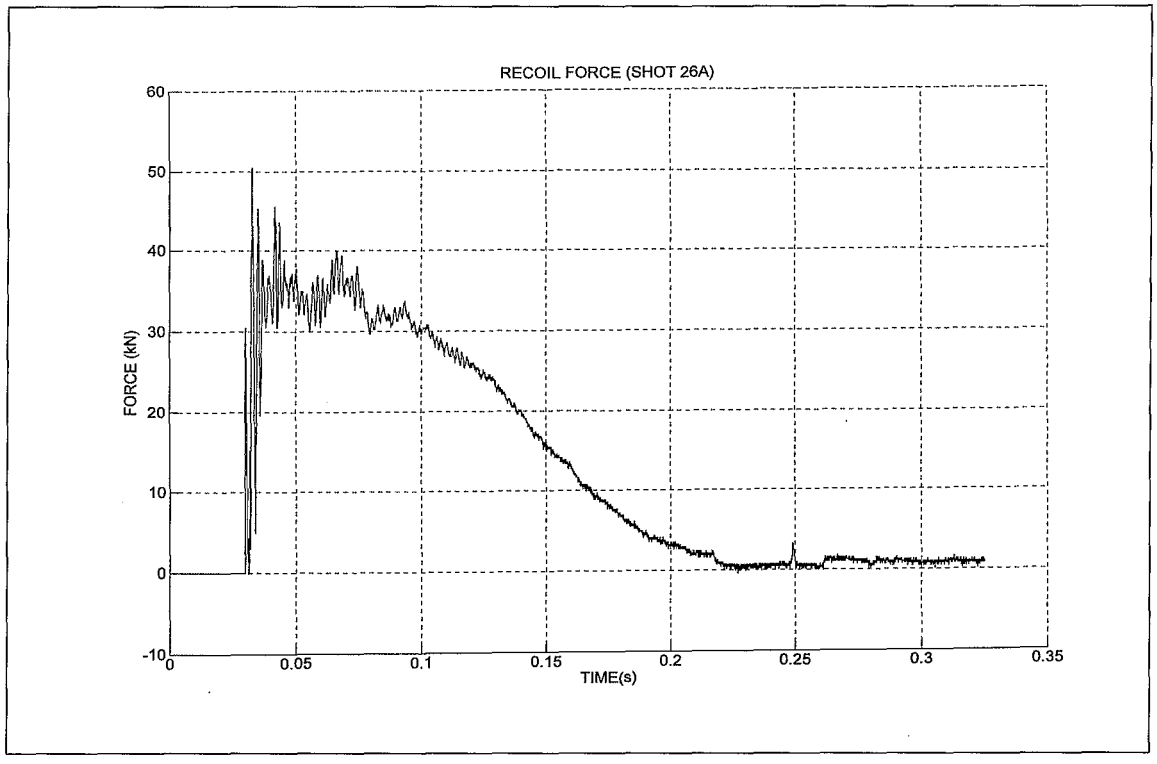

Figure F5. Recoil force

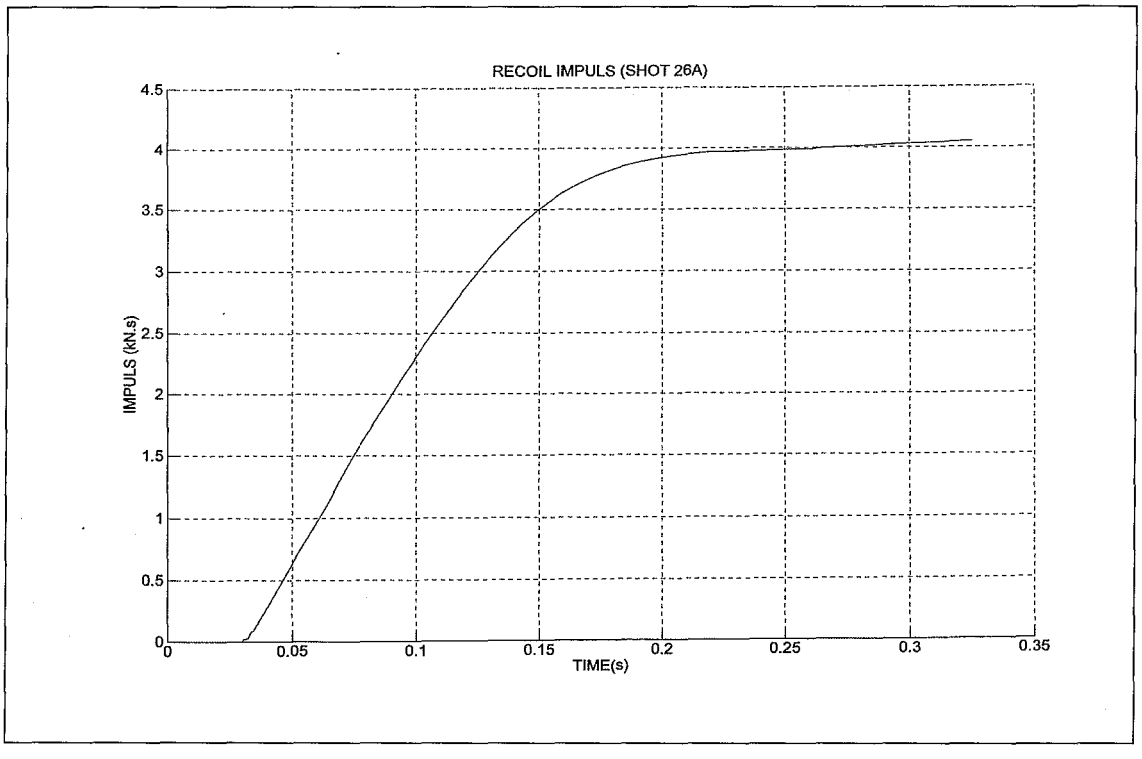

Figure F6. Recoil impulse

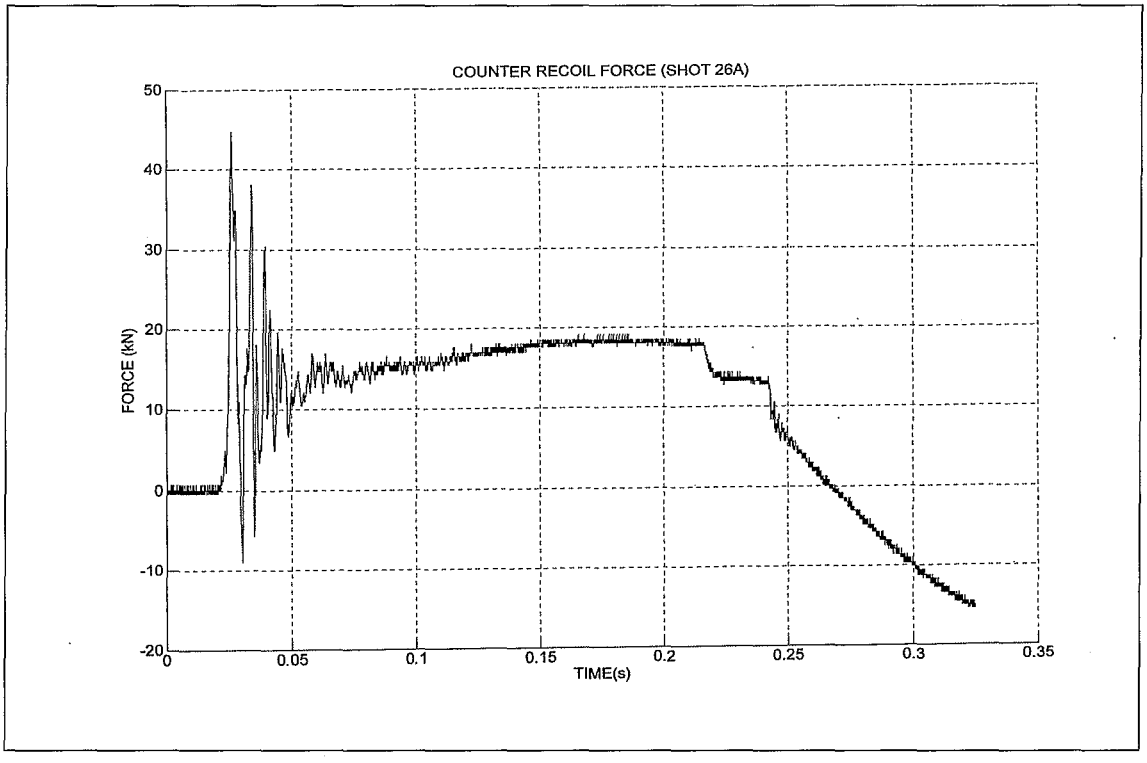

Figure F7. Counter recoil force

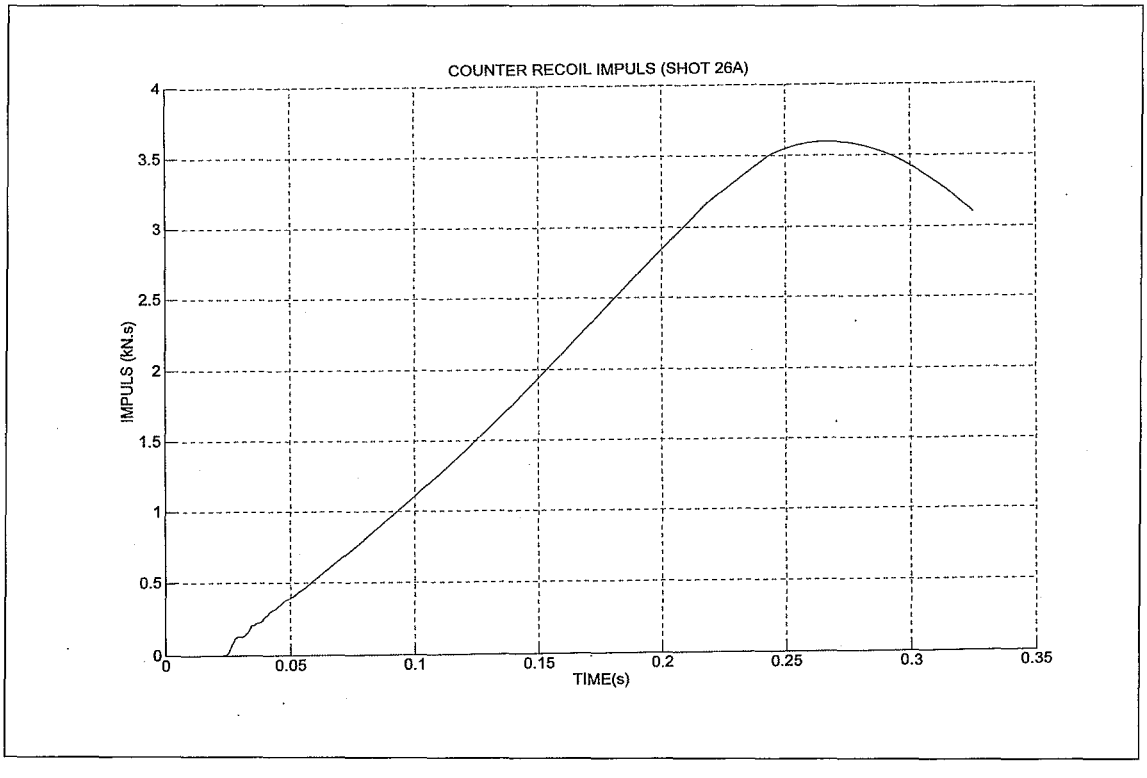

Figure F8. Counter recoil impulse

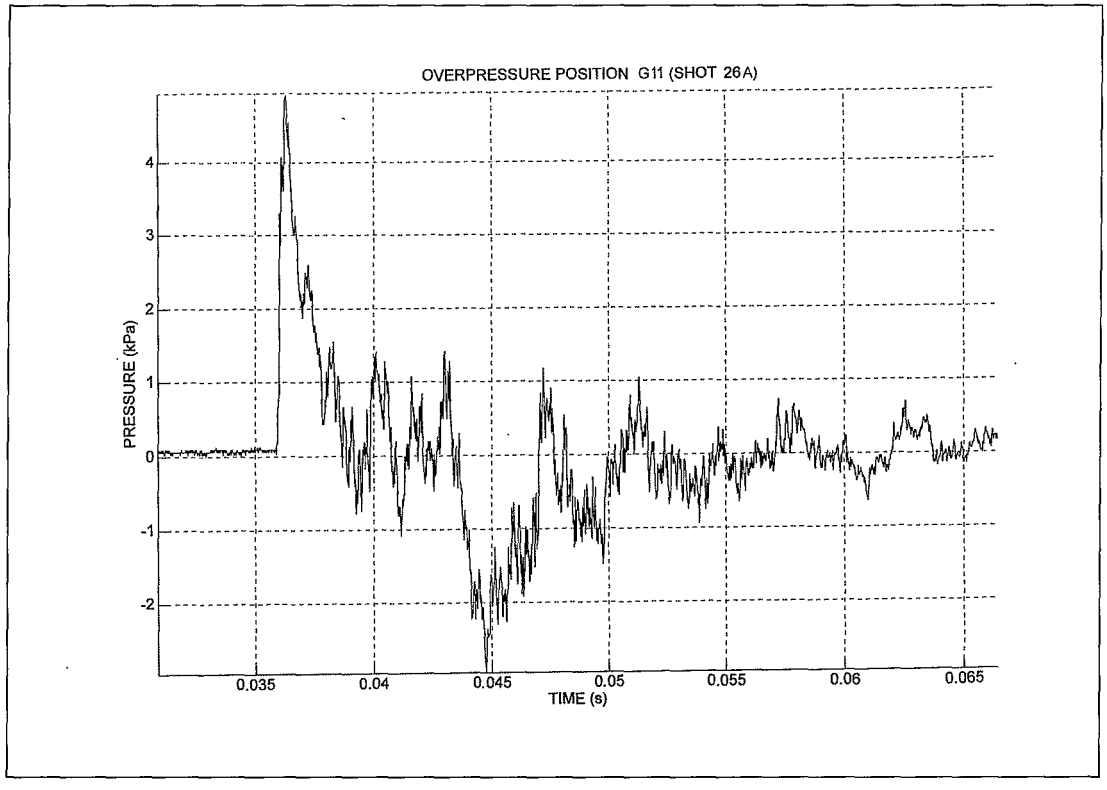

Figure F9. Overpressure position G11

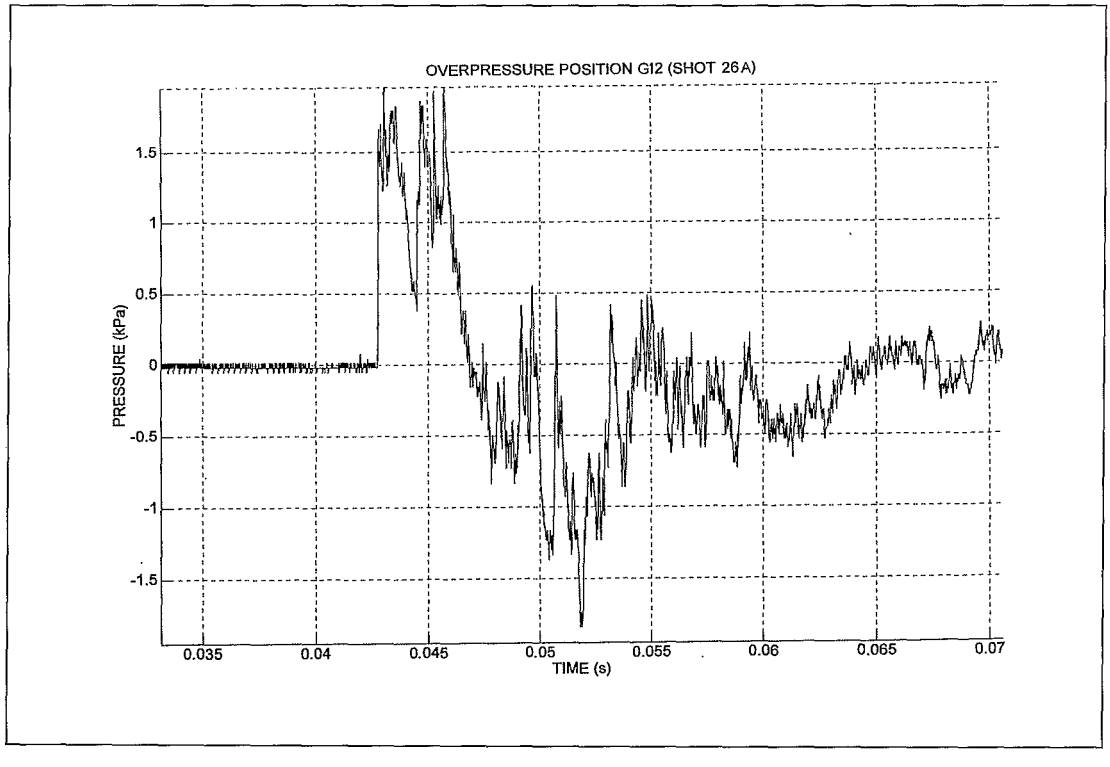

Figure F10. Overpressure position G12.

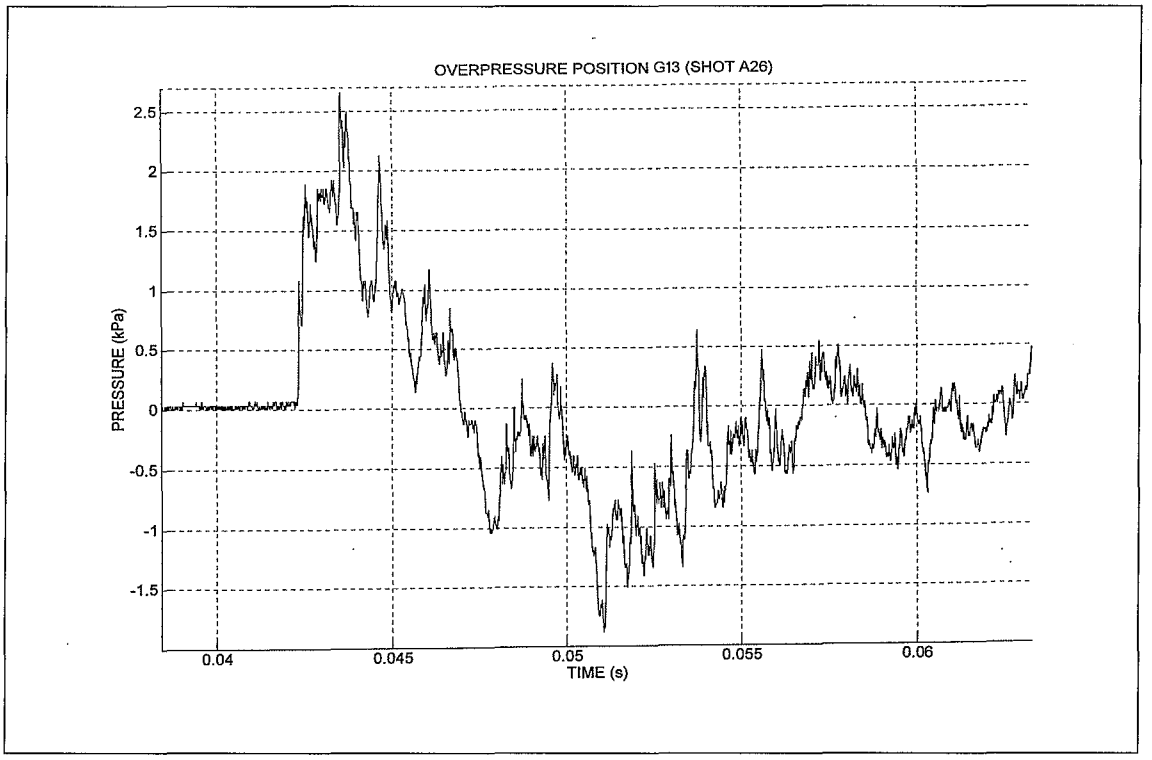

Figure F11. Overpressure position G13.

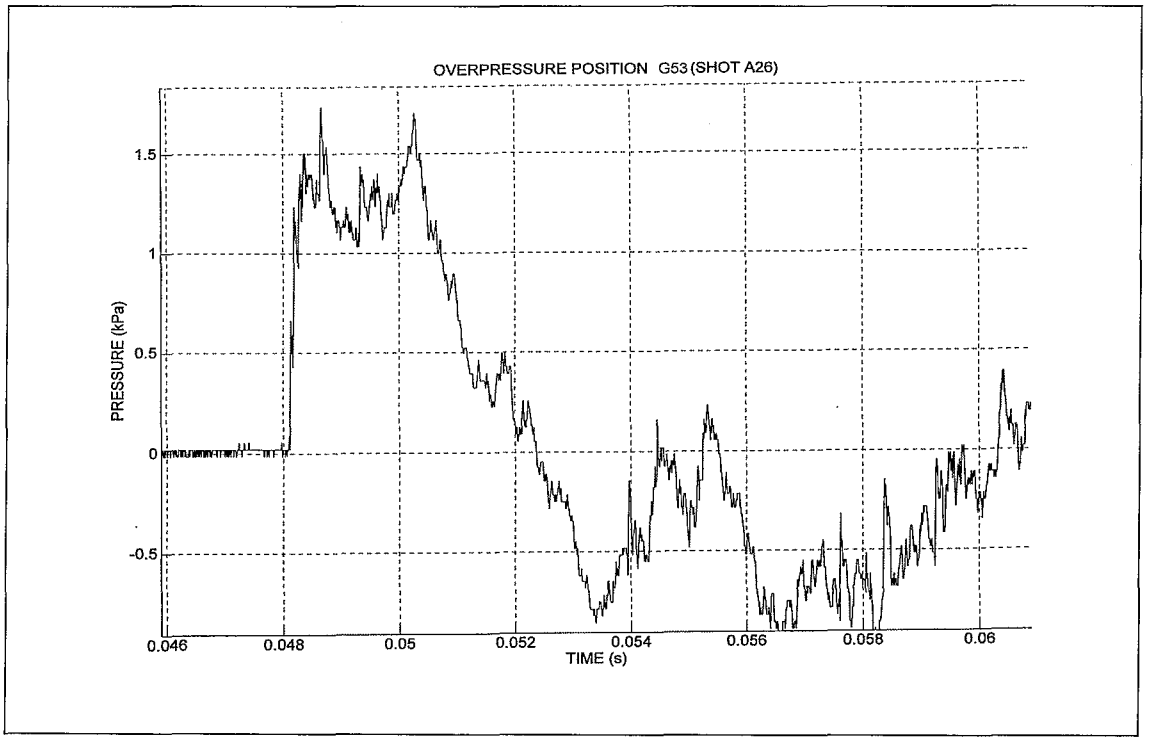

Figure F12. Overpressure position G53.

Appendix G

Traces of trial data of Version 3 conventional – Phase 2.

Traces of the important parameters verified during the trial of phase 2 for version 3 as a conventional muzzle brake – shot 13 is presented.

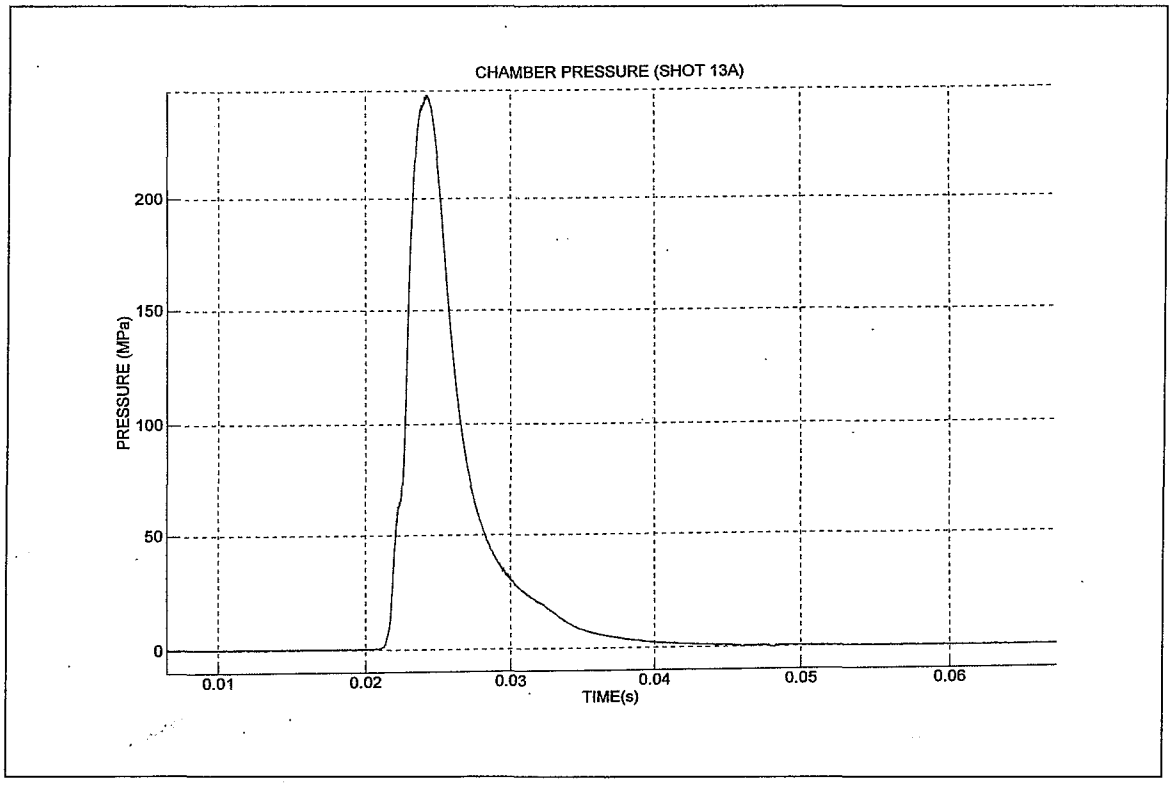

Figure G1. Chamber pressure

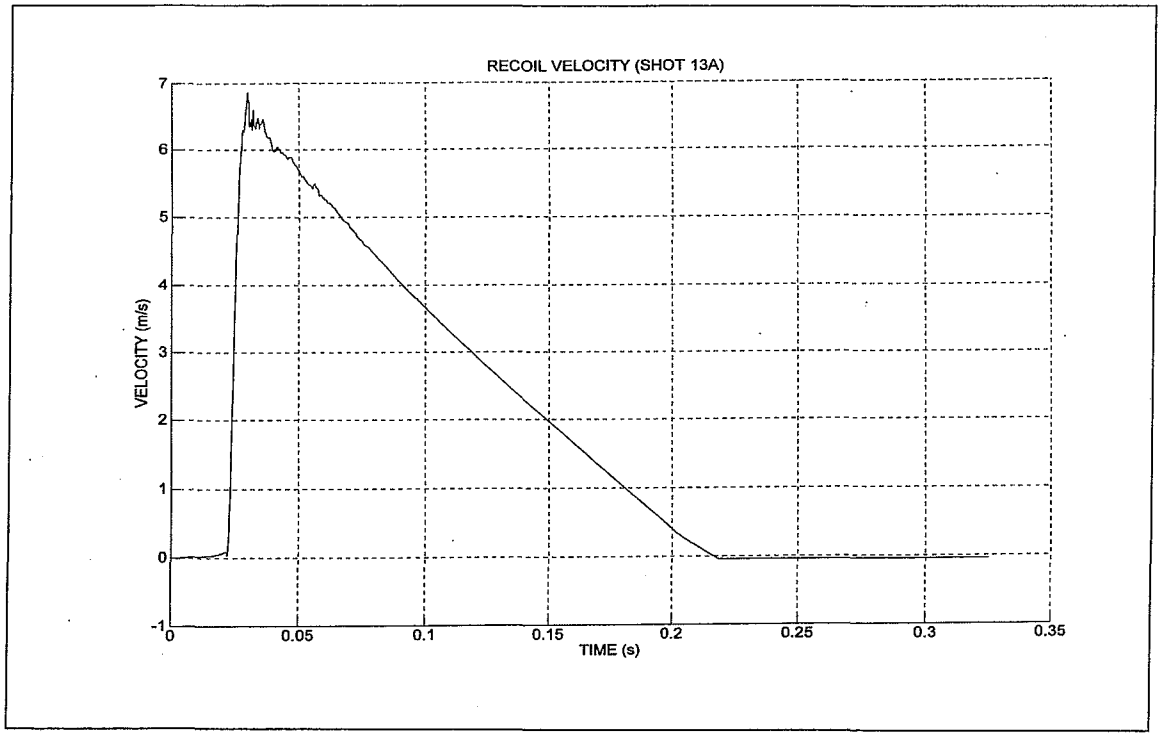

Figure G2. Recoil velocity

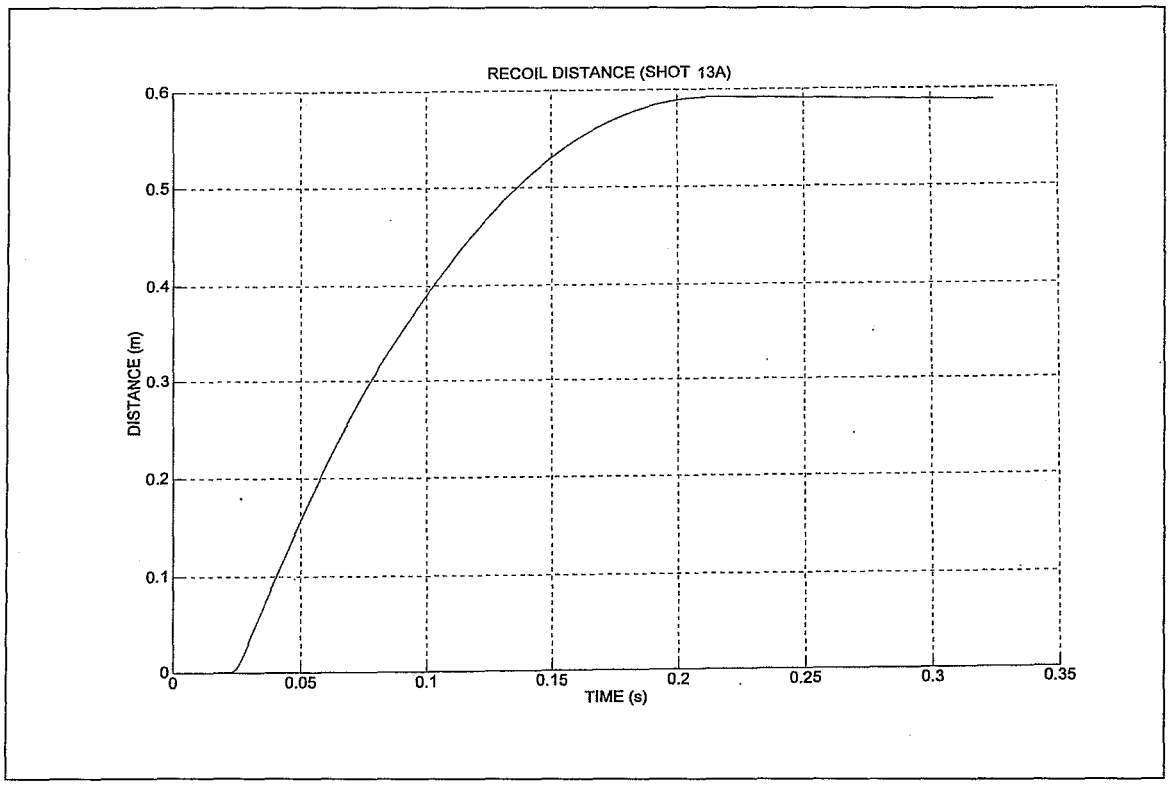

Figure G3. Recoil displacement

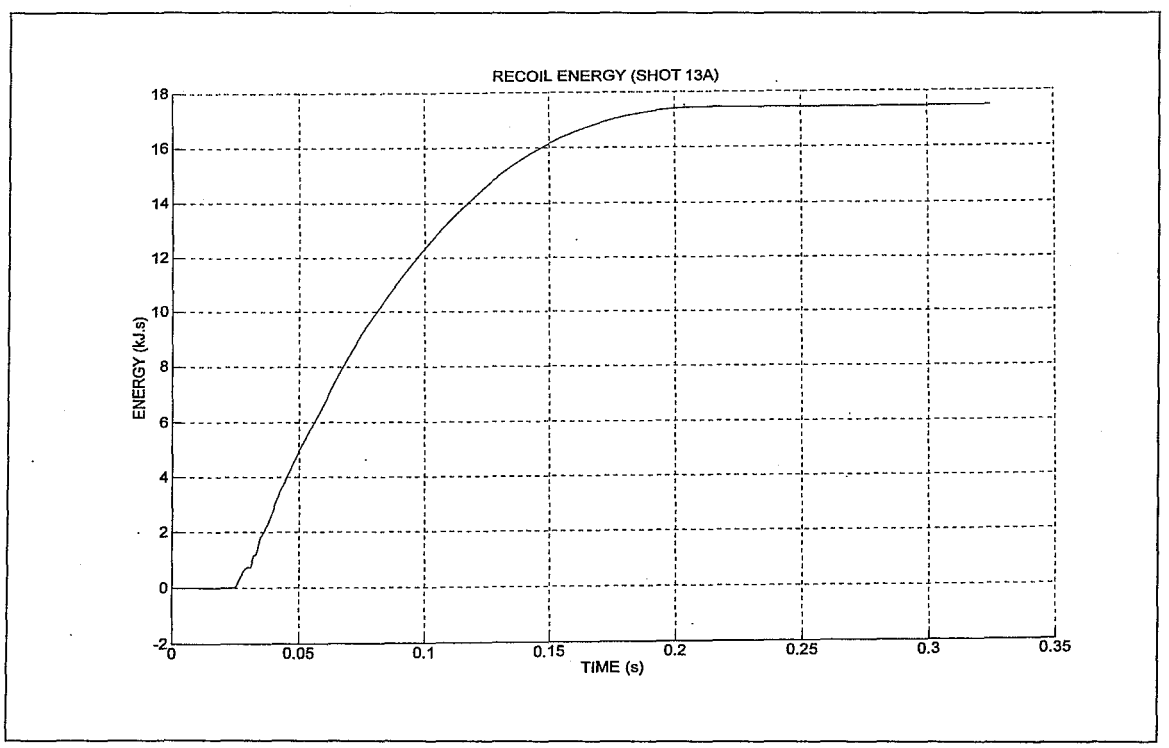

Figure G4. Recoil energy

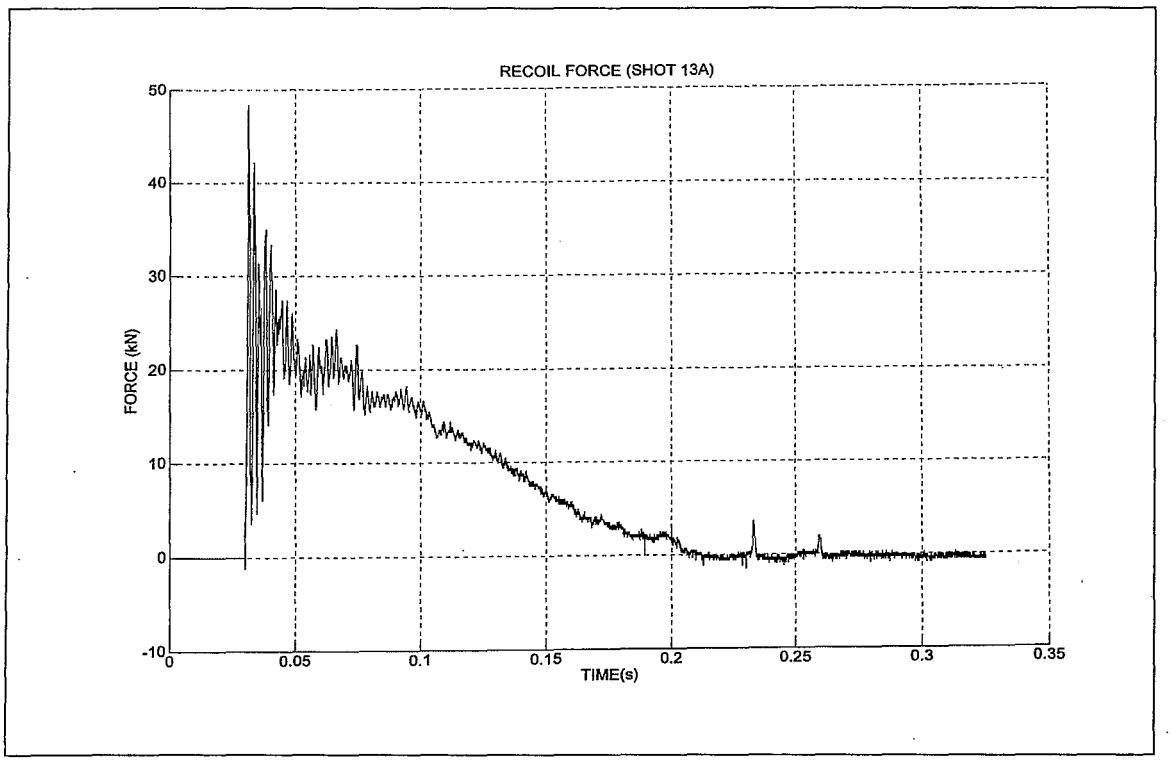

Figure G5. Recoil force

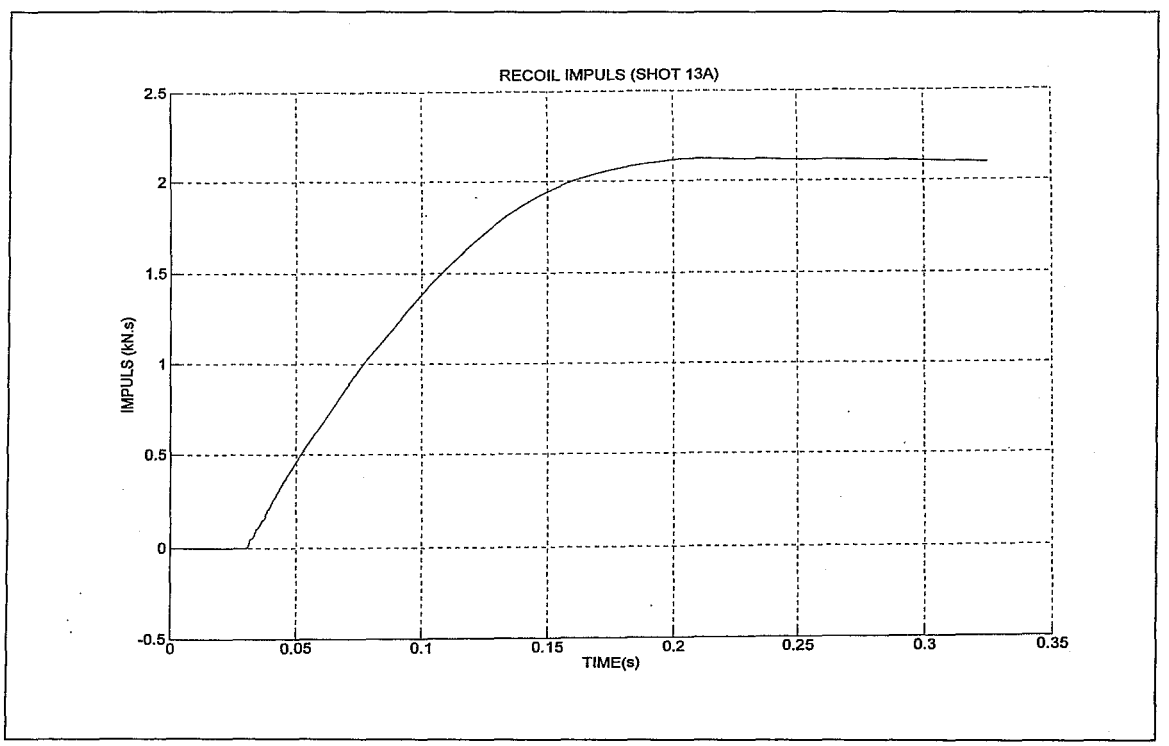

Figure G6. Recoil impulse

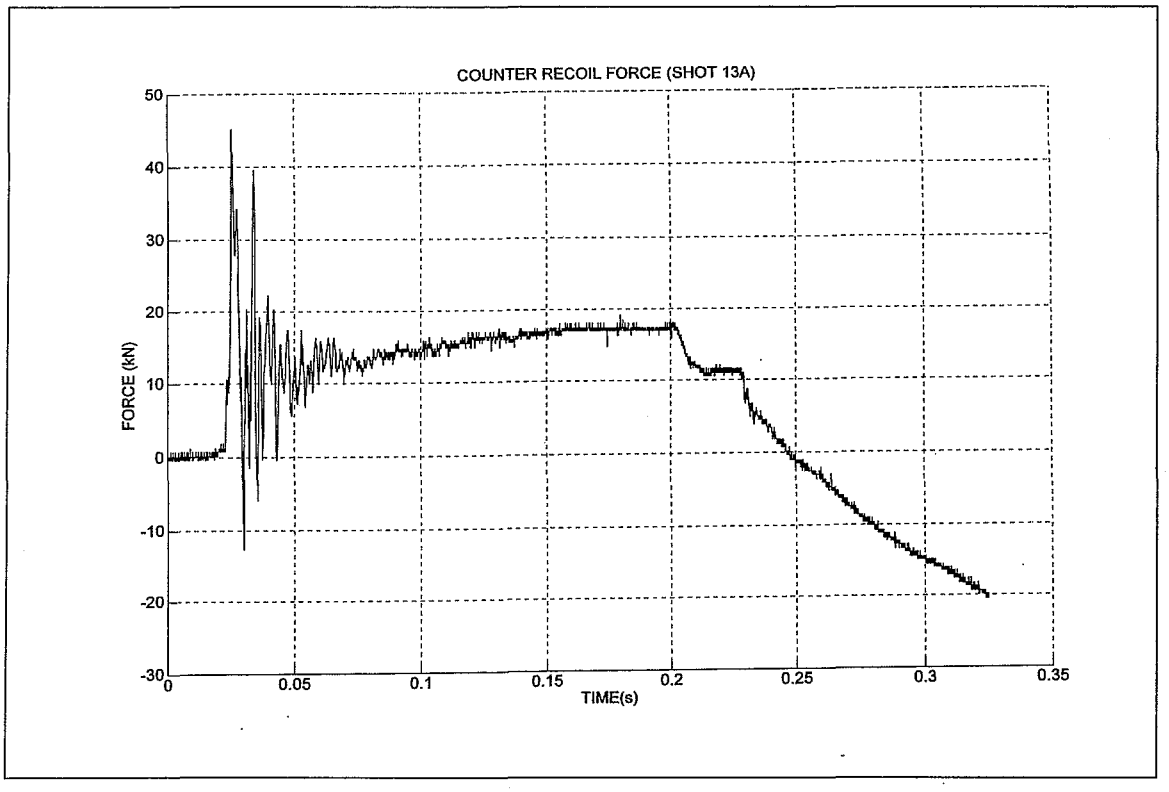

Figure G7. Counter recoil force

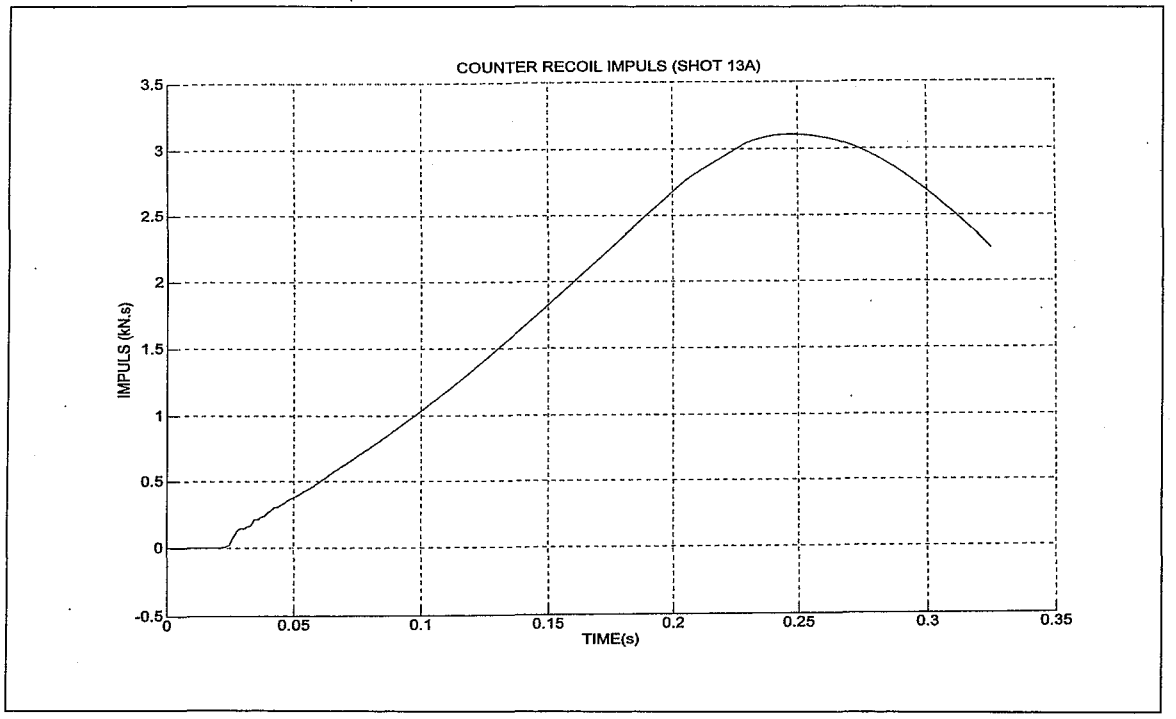

Figure G8. Counter recoil impulse

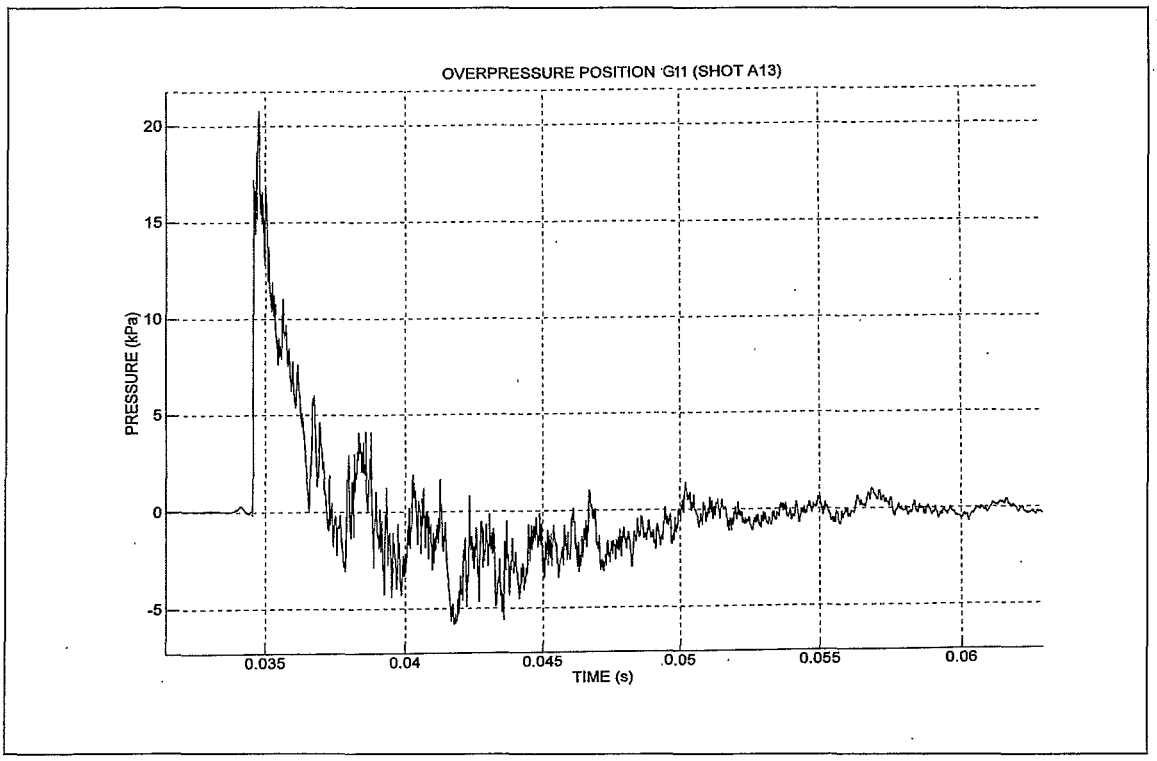

Figure G9. Overpressure position G11

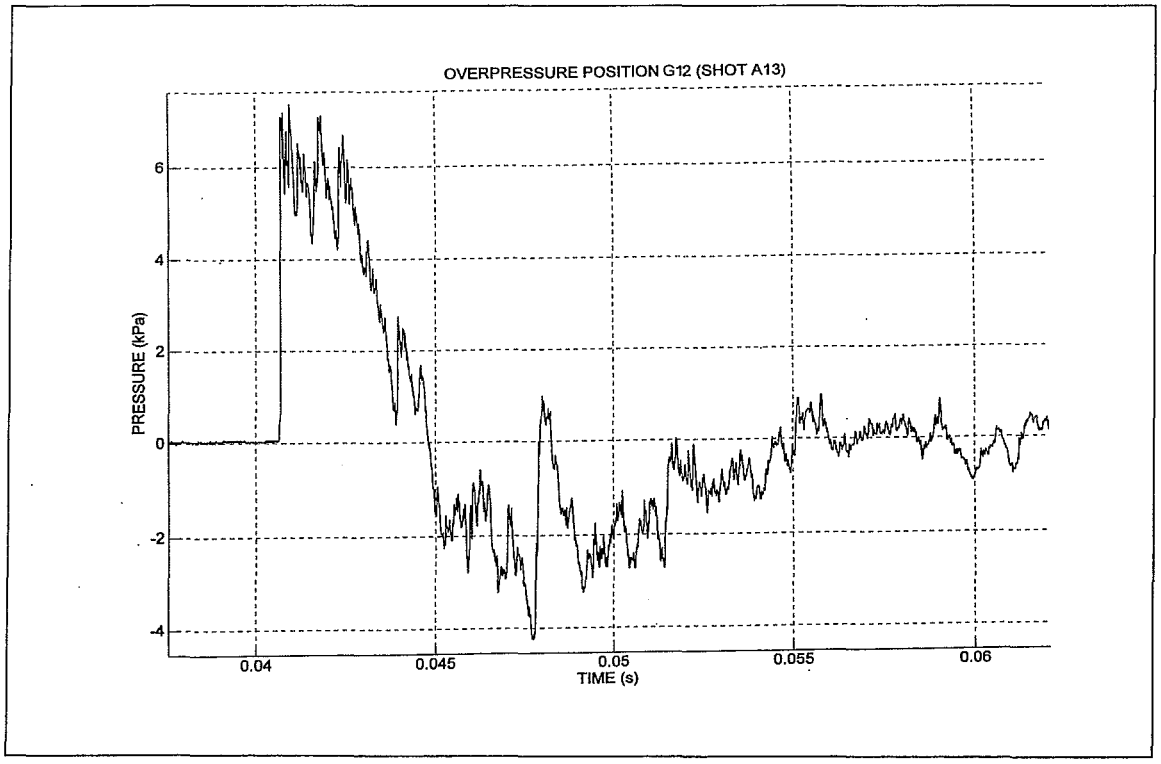

Figure G10. Overpressure position G12

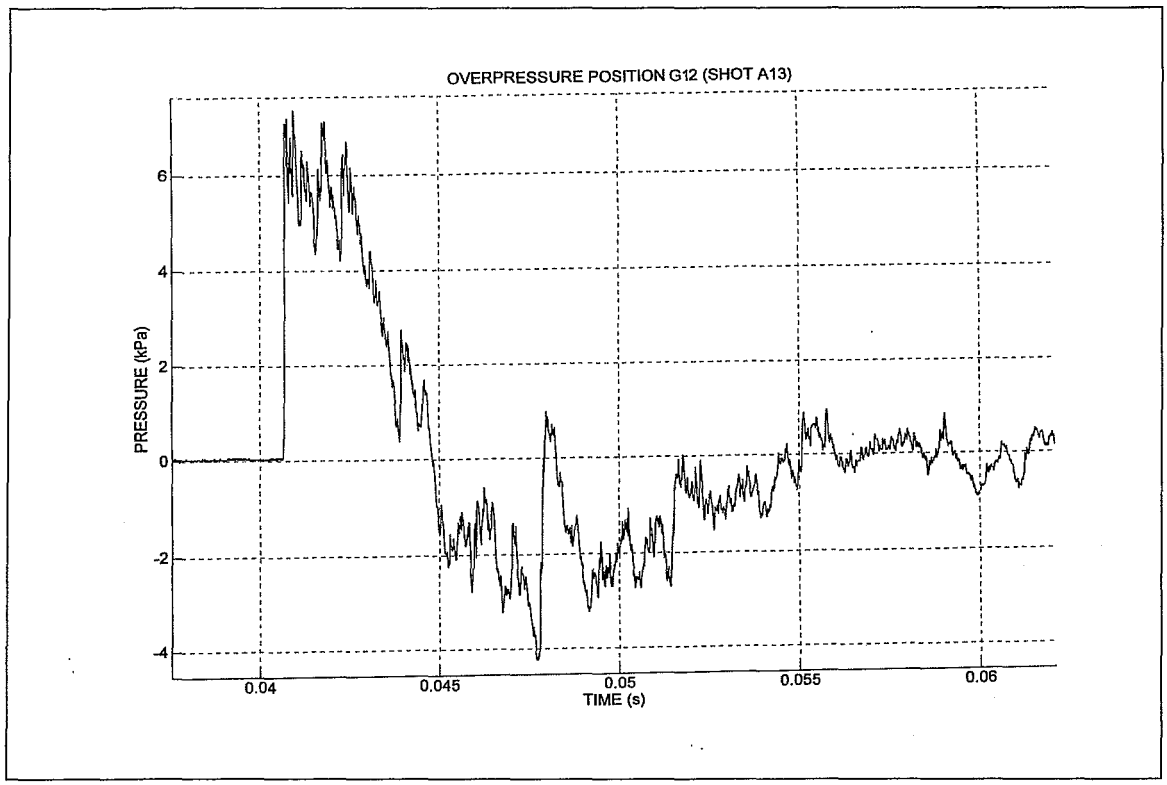

Figure G11. Overpressure position G13

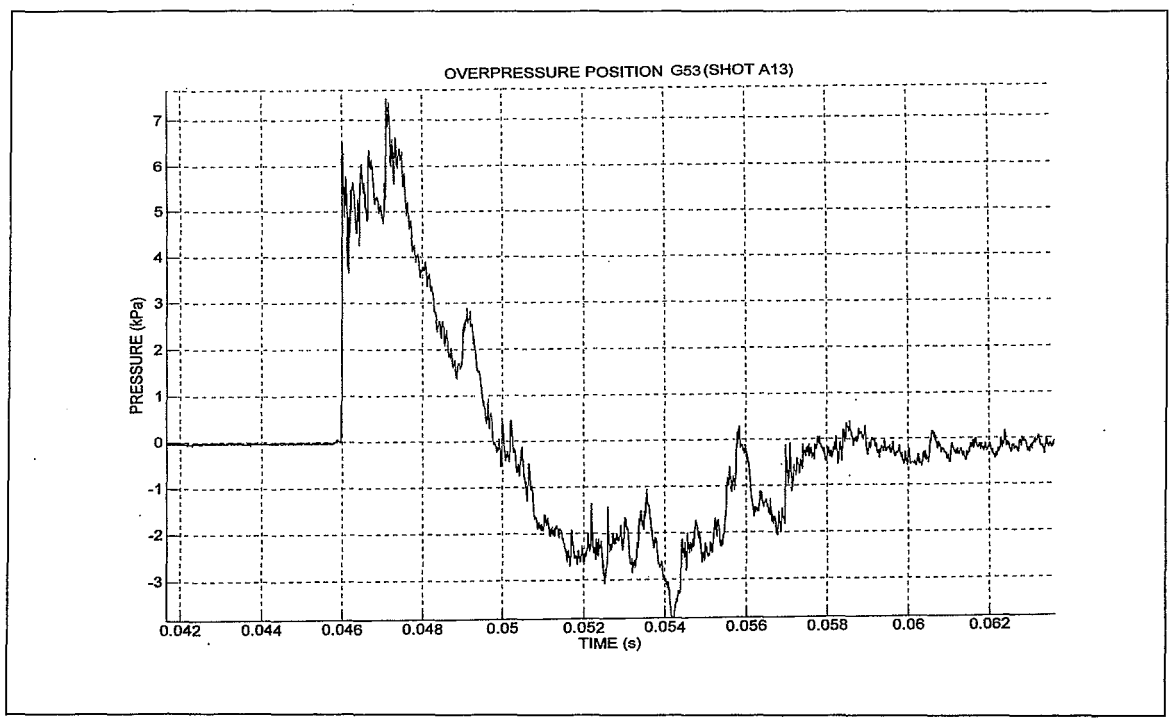

Figure G12. Overpressure position G53

Appendix H

Traces of trial data of Version 3 active – Phase 2.

Traces of the important parameters verified during the trial of phase 2 for version 3 as an active muzzle brake – shot 22 is presented.

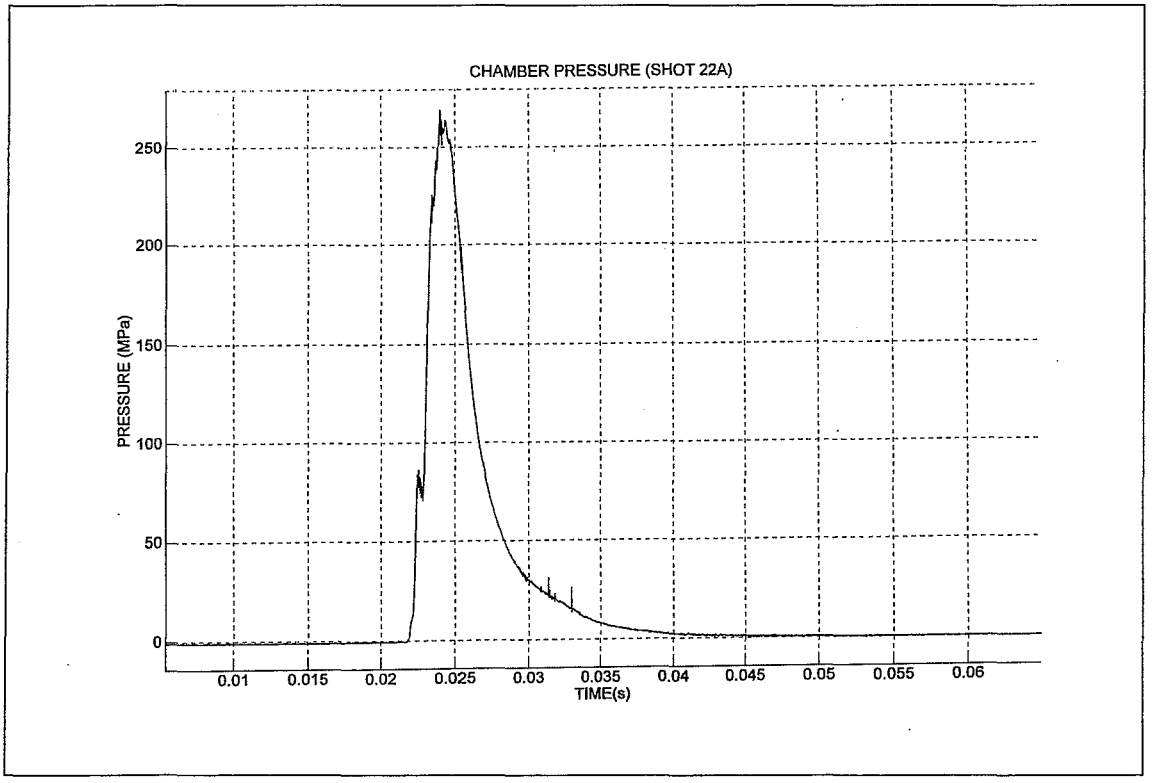

Figure H1. Chamber pressure

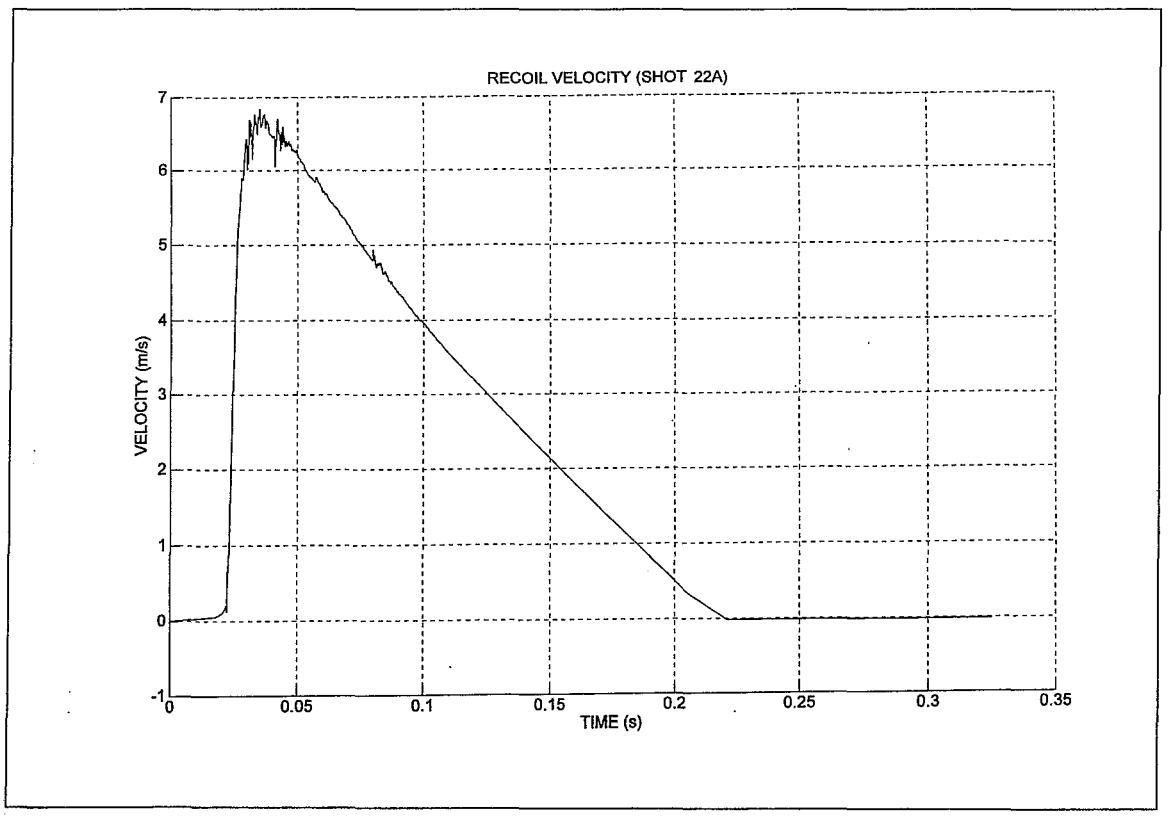

Figure H2. Recoil velocity

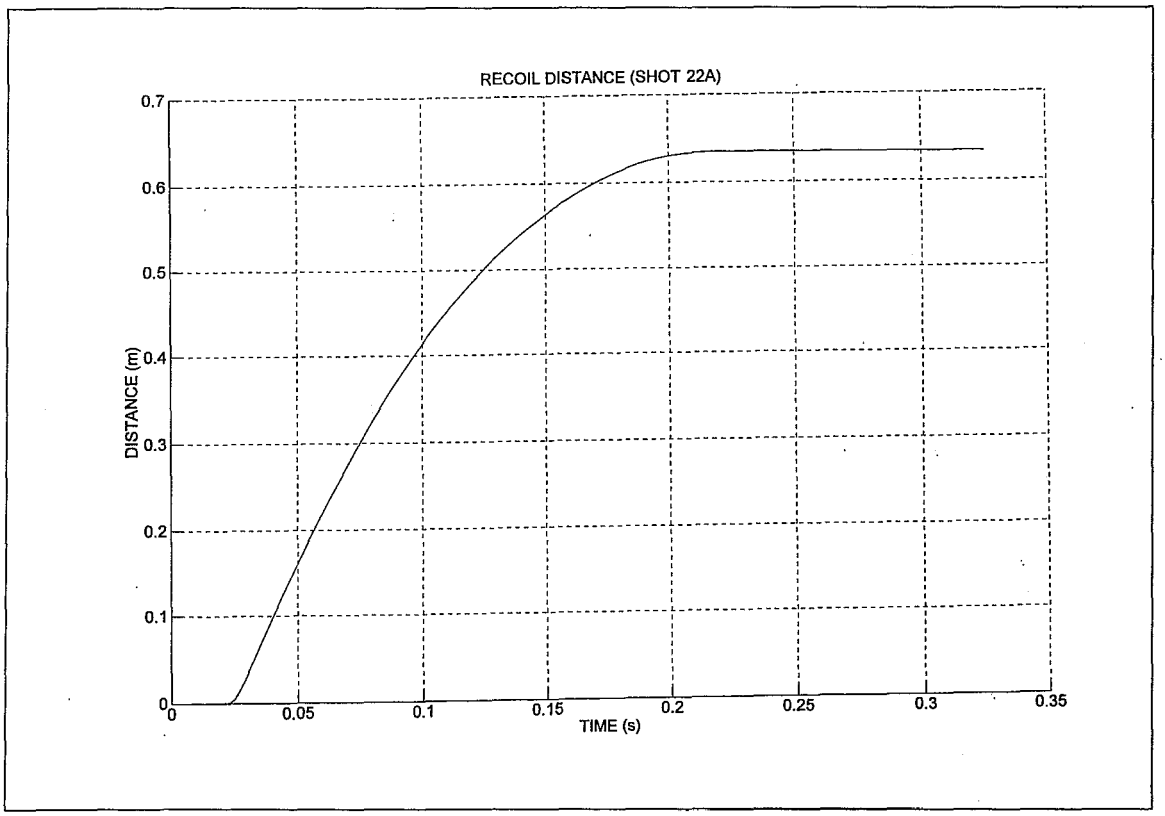

Figure H3. Recoil displacement

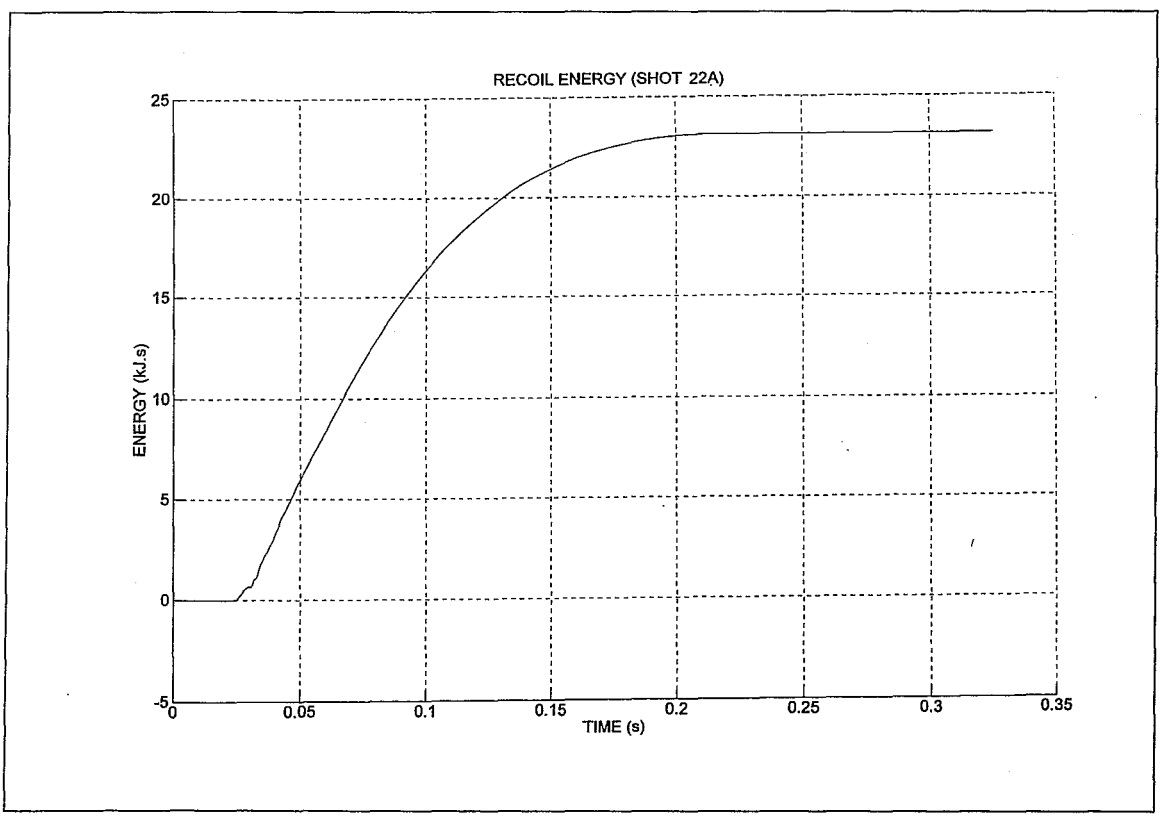

Figure H4. Recoil energy

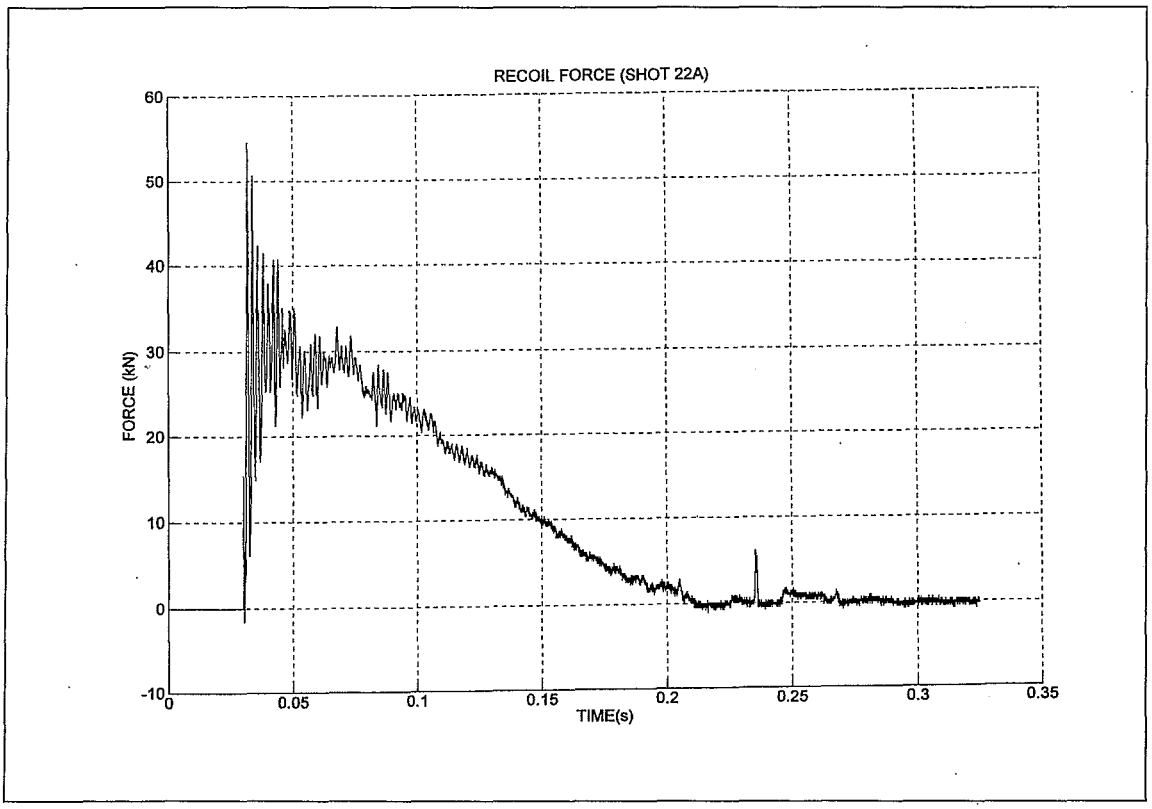

Figure H5. Recoil force

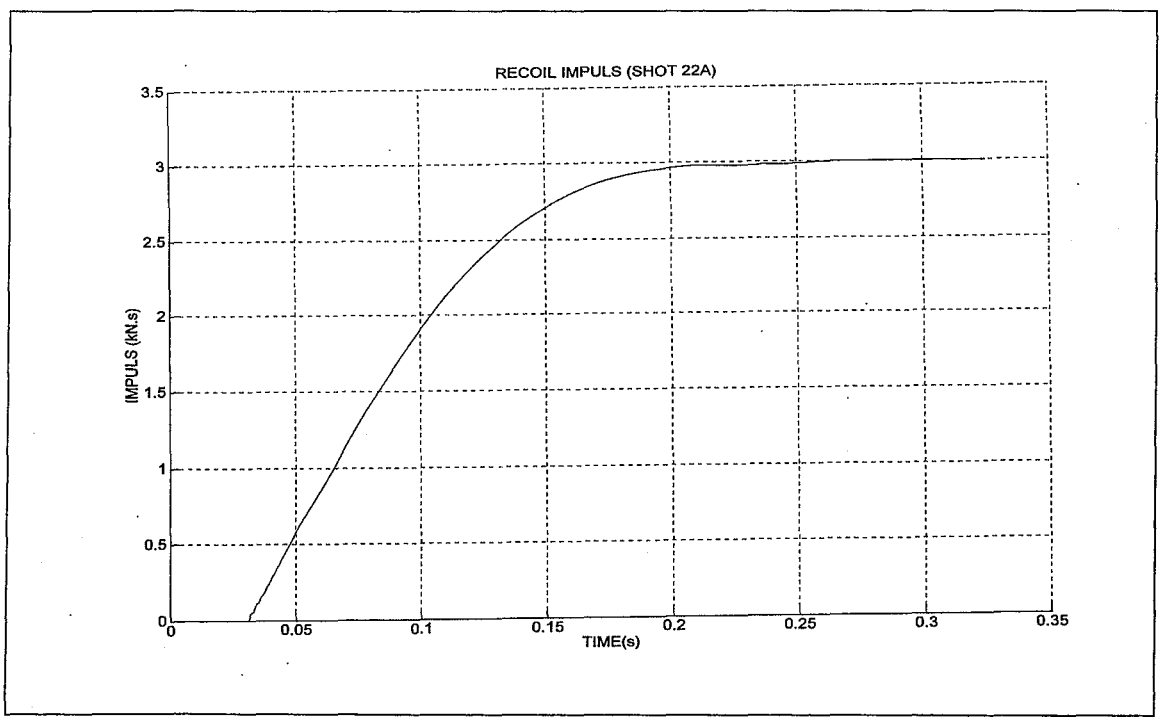

Figure H6. Recoil impulse

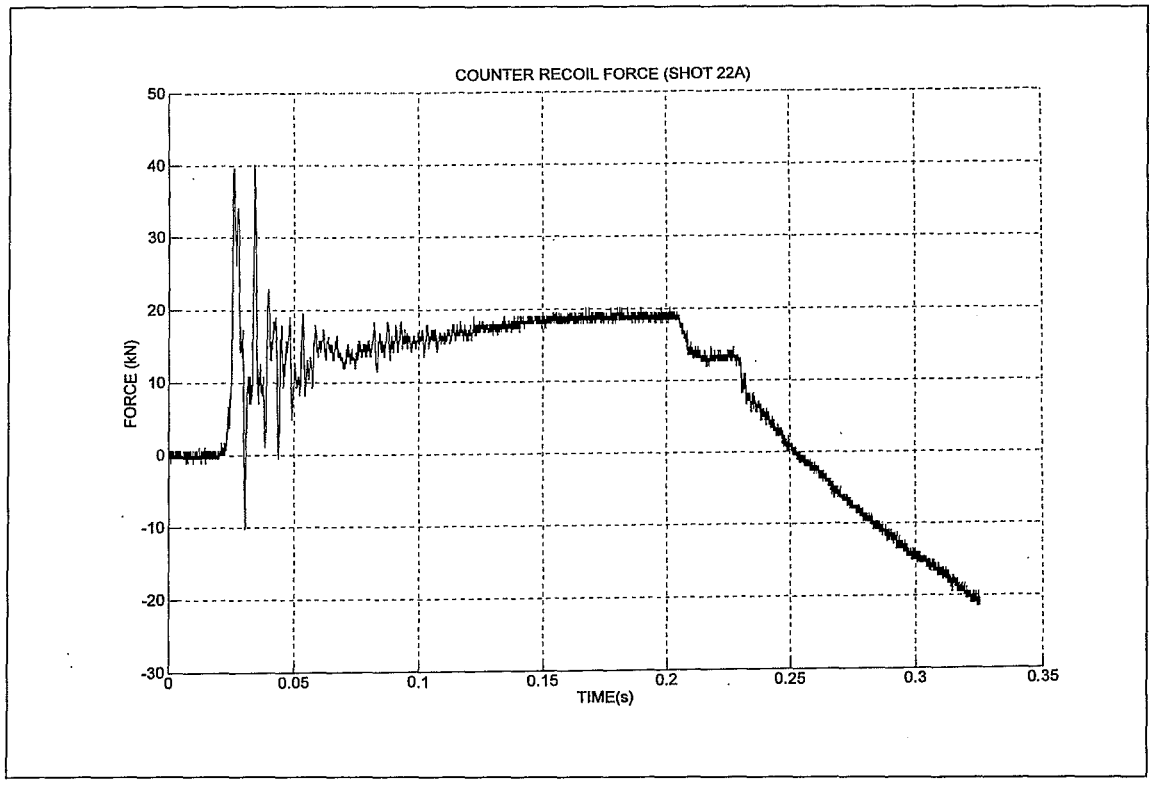

Figure H7. Counter recoil force

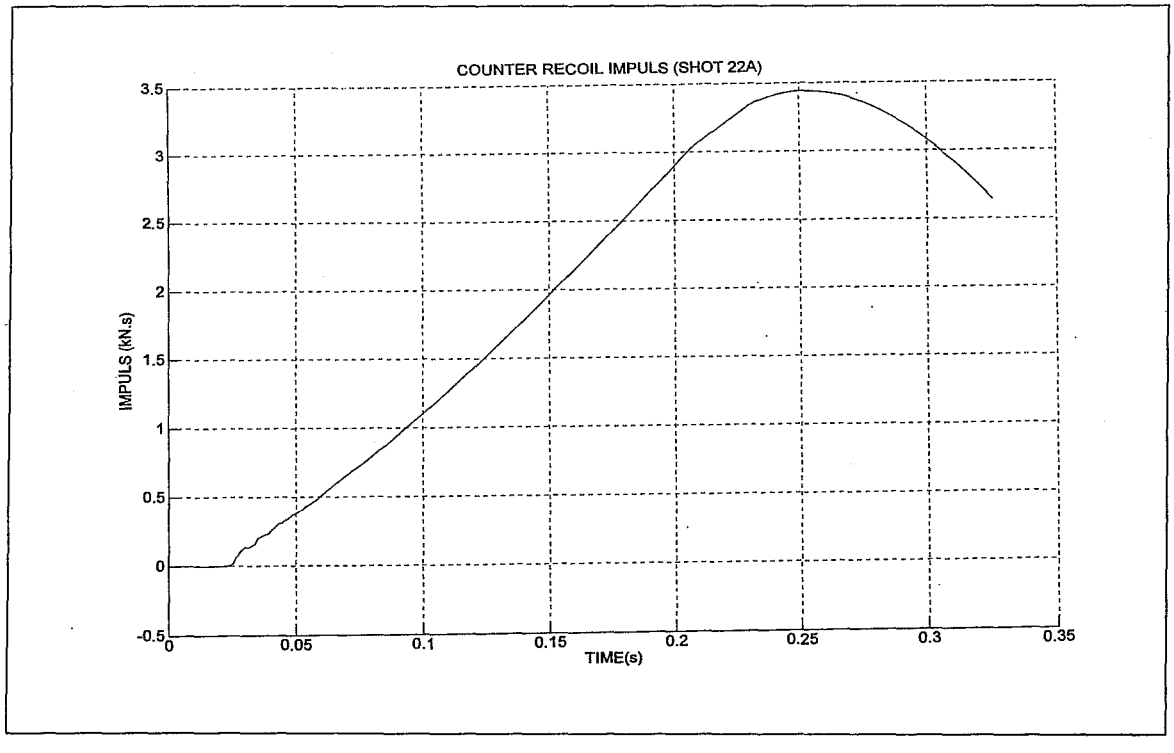

Figure H8. Counter recoil impulse

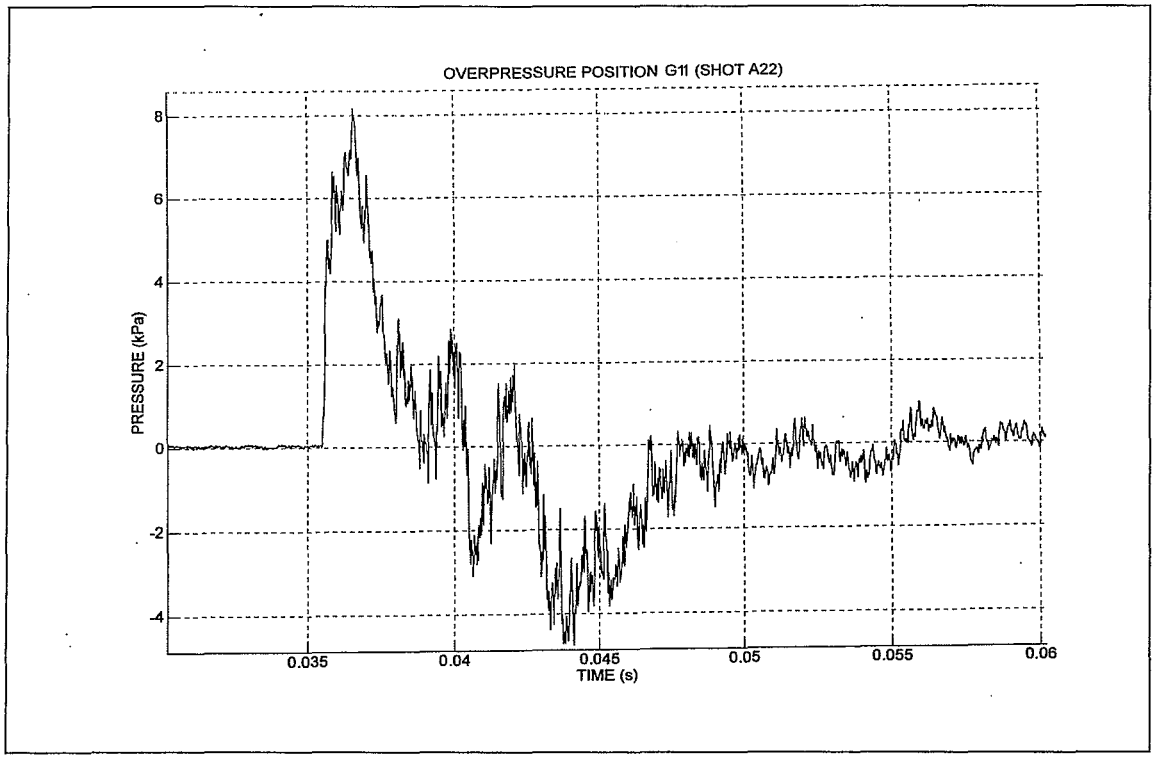

Figure H9. Overpressure position G11

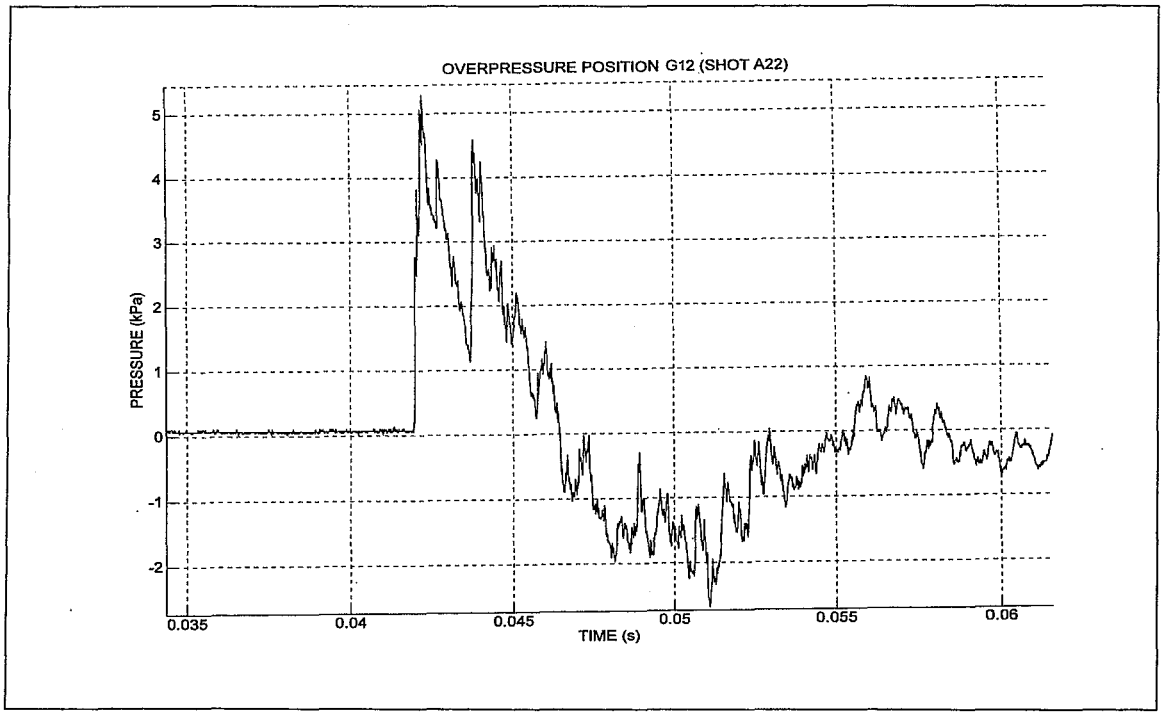

Figure H10. Overpressure position G12

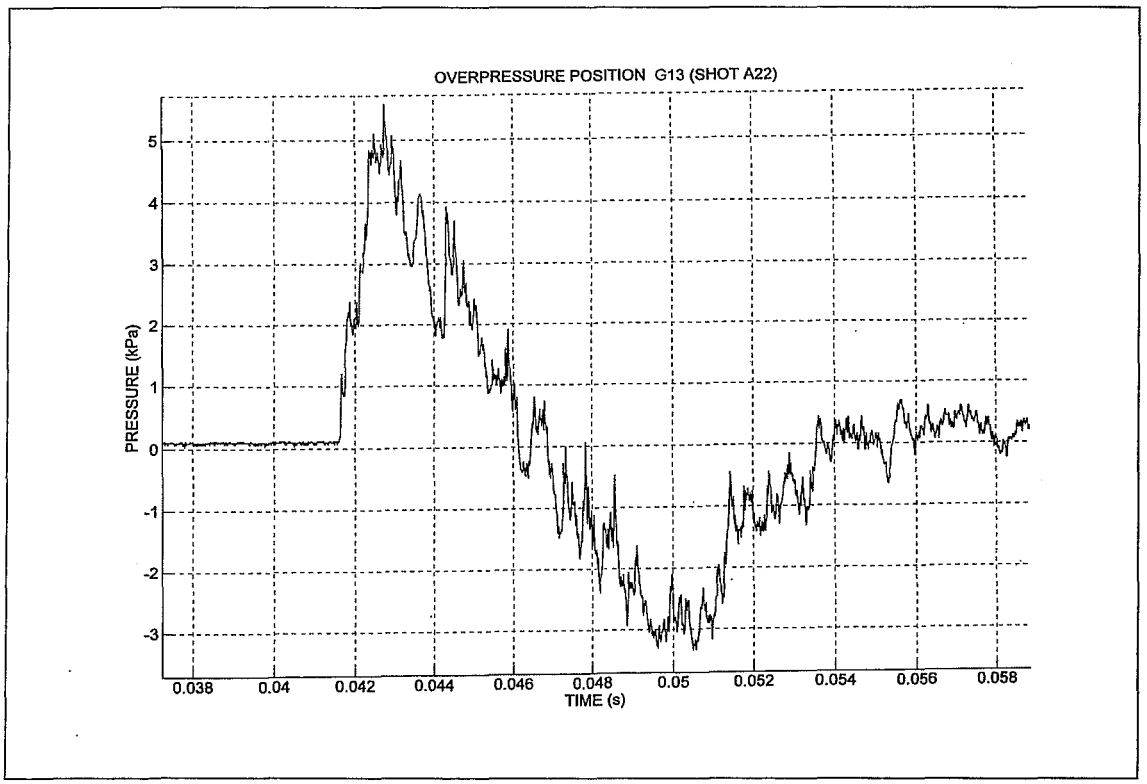

Figure H11. Overpressure position G13

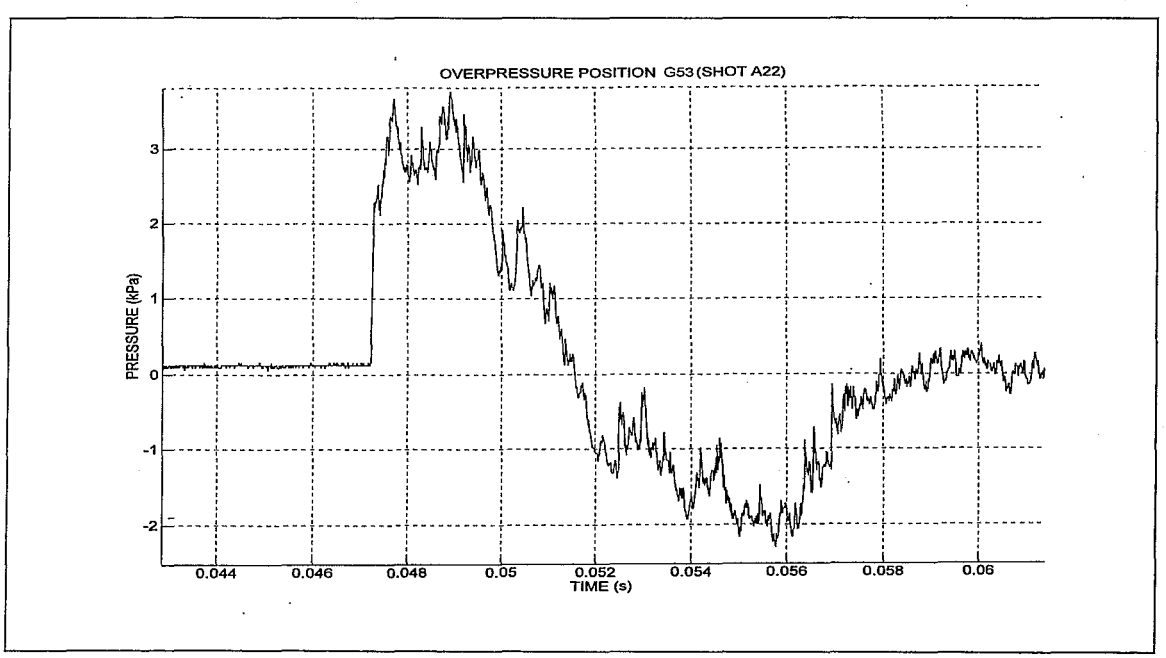

Figure H12. Overpressure position G53

Appendix I

Traces of trial data of Version 4 conventional – Phase 2.

Traces of the important parameters verified during the trial of phase 2 for version 4 as a conventional muzzle brake – shot 34 is presented.

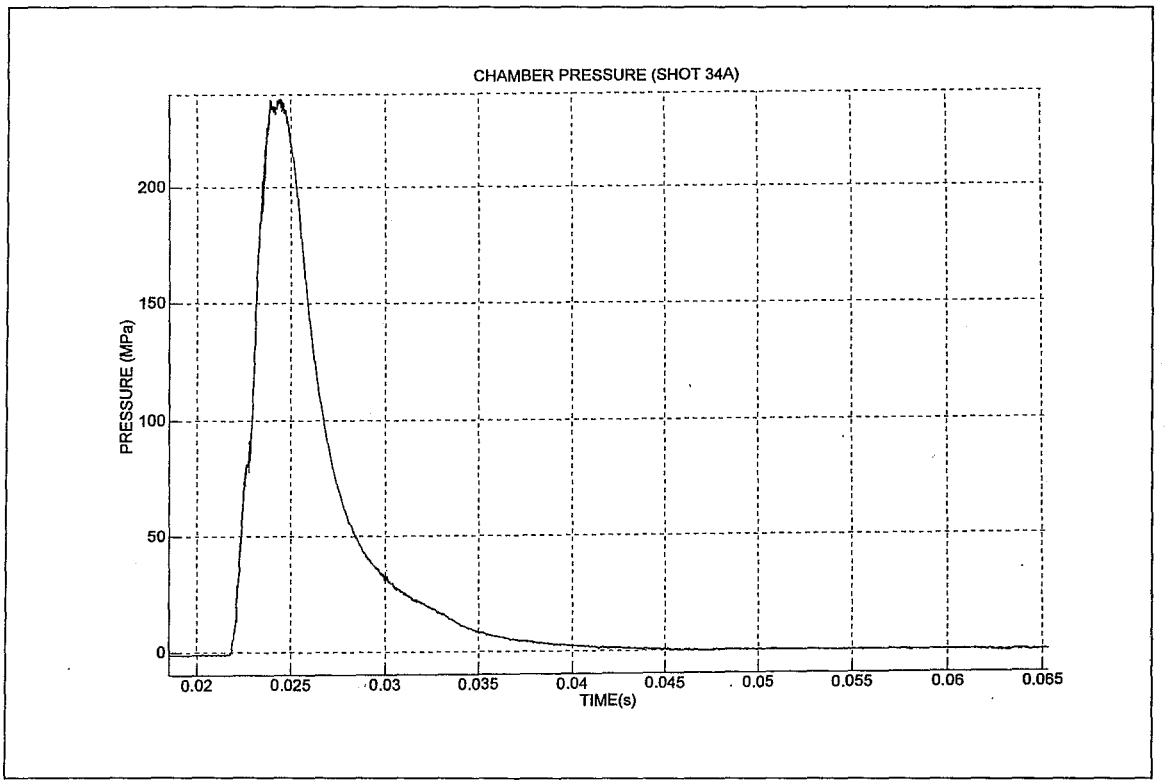

Figure I1. Chamber pressure

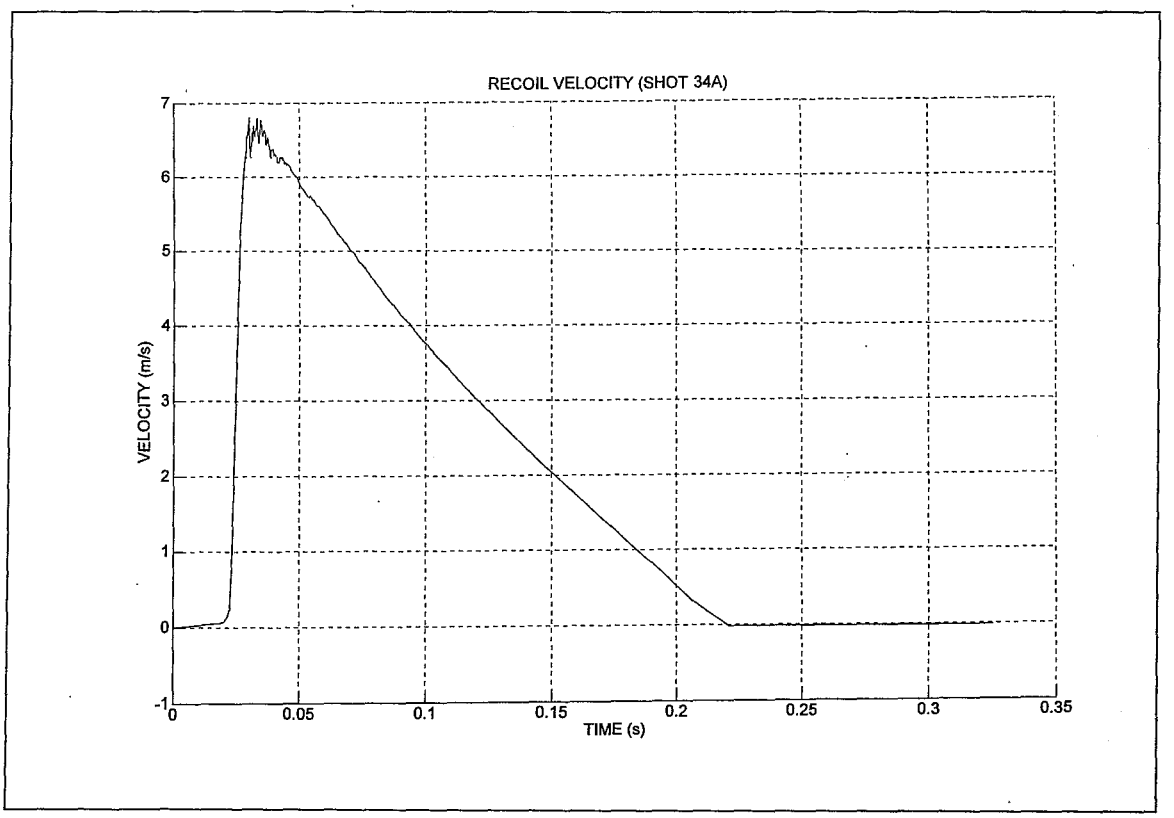

Figure I2. Recoil velocity

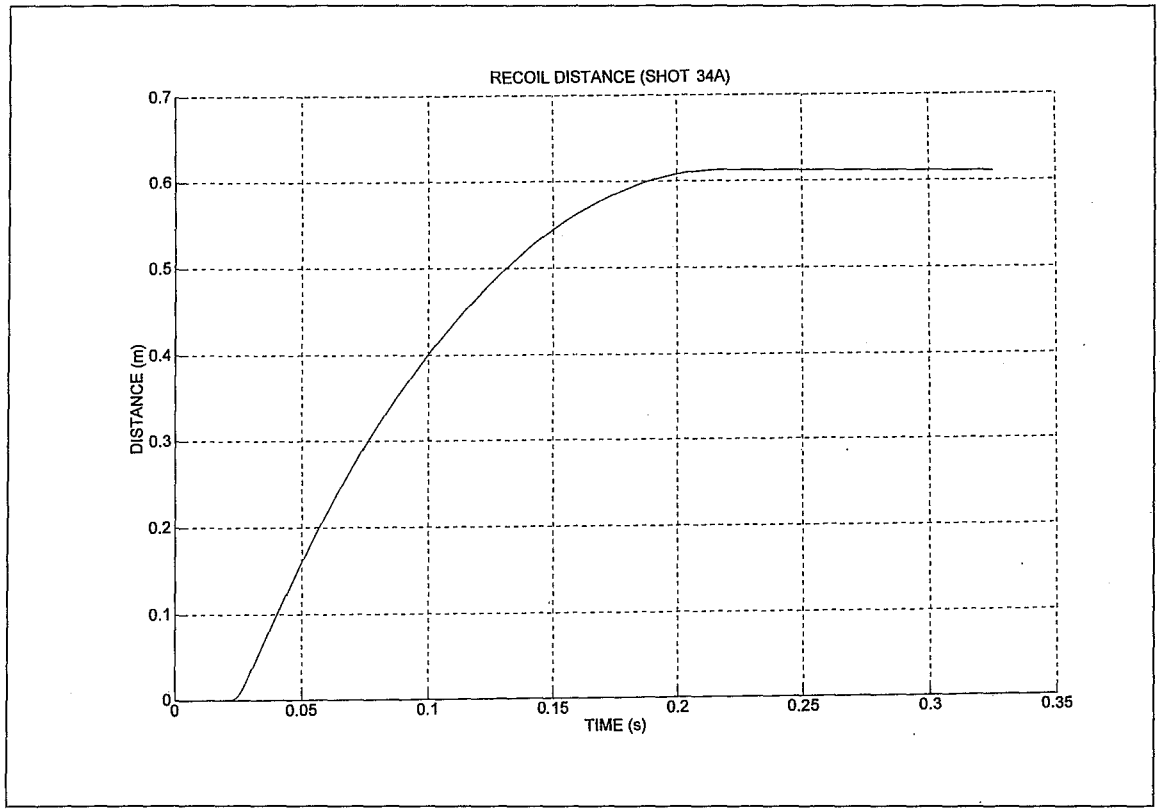

Figure I3. Recoil displacement

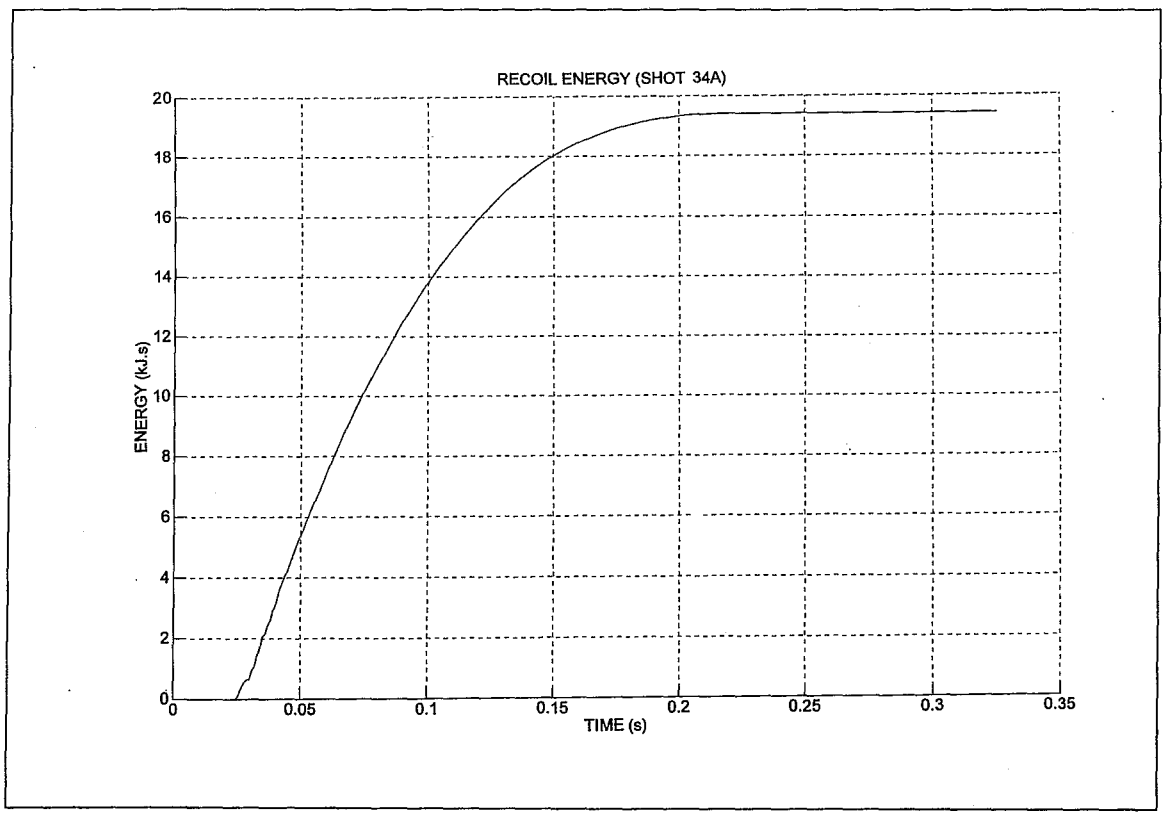

Figure I4. Recoil energy

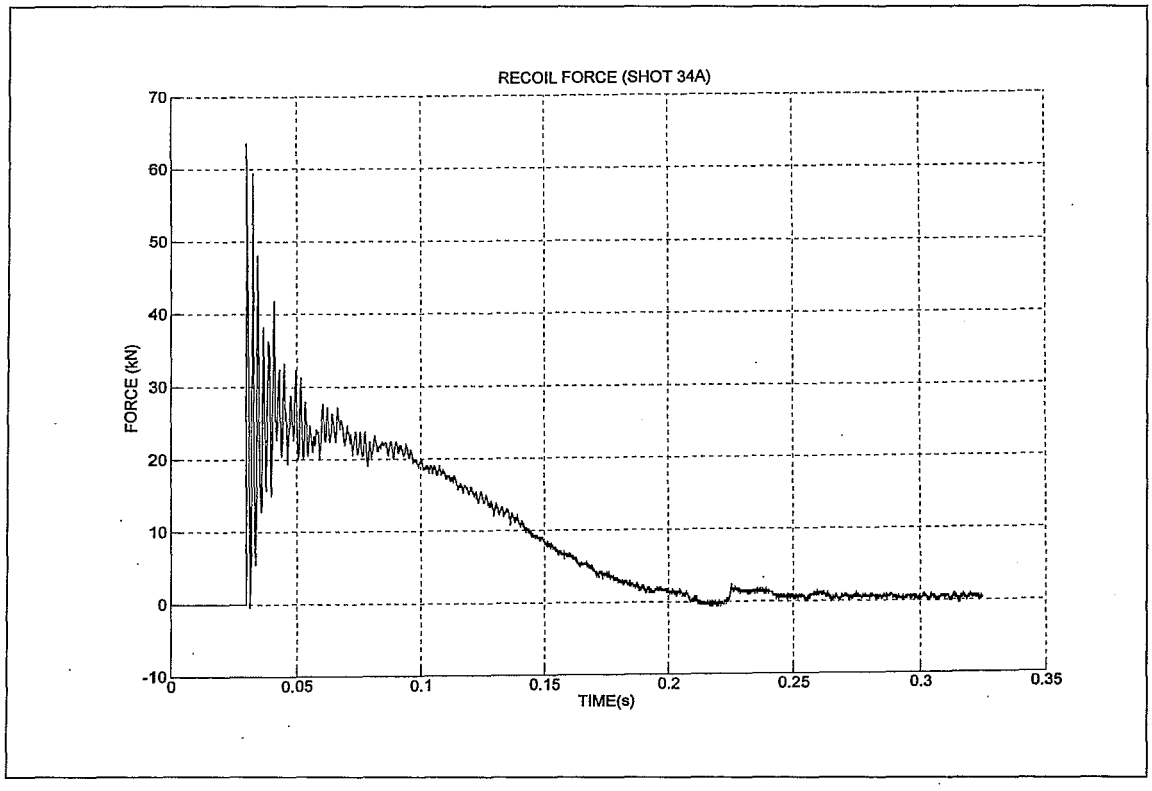

Figure I5. Recoil force

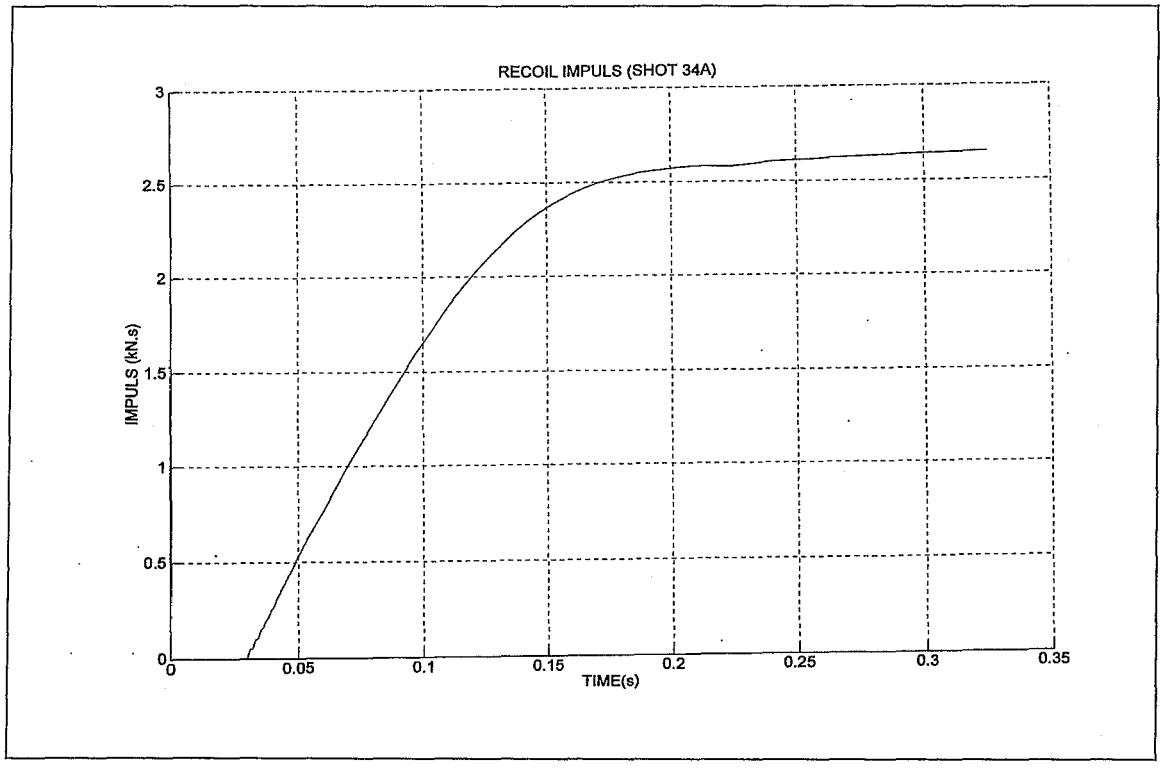

Figure I6. Recoil impulse

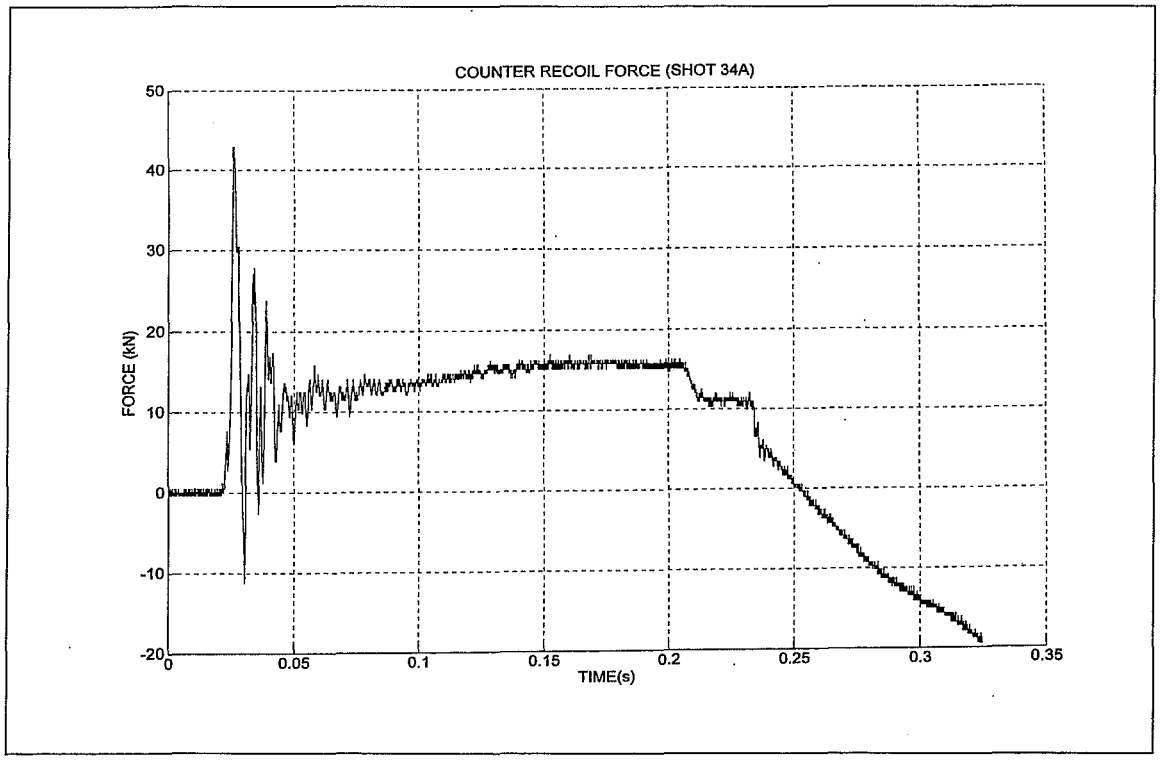

Figure I7. Counter recoil force

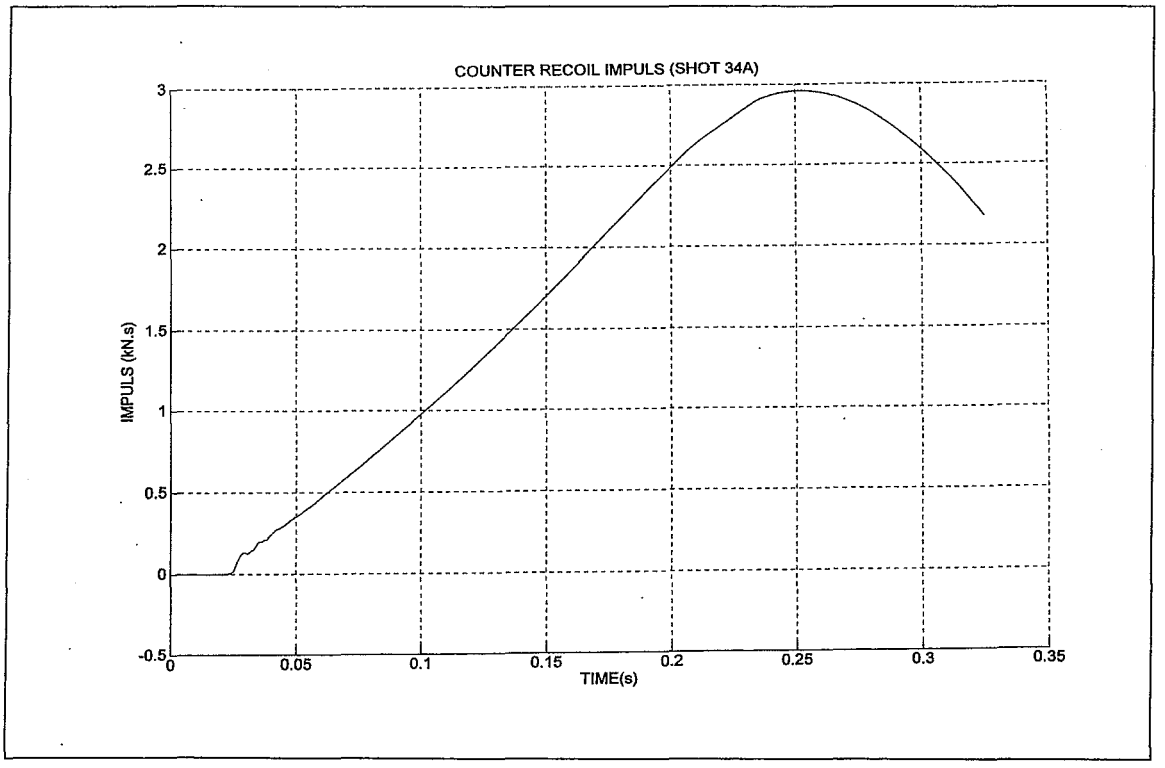

Figure I8. Counter recoil impulse

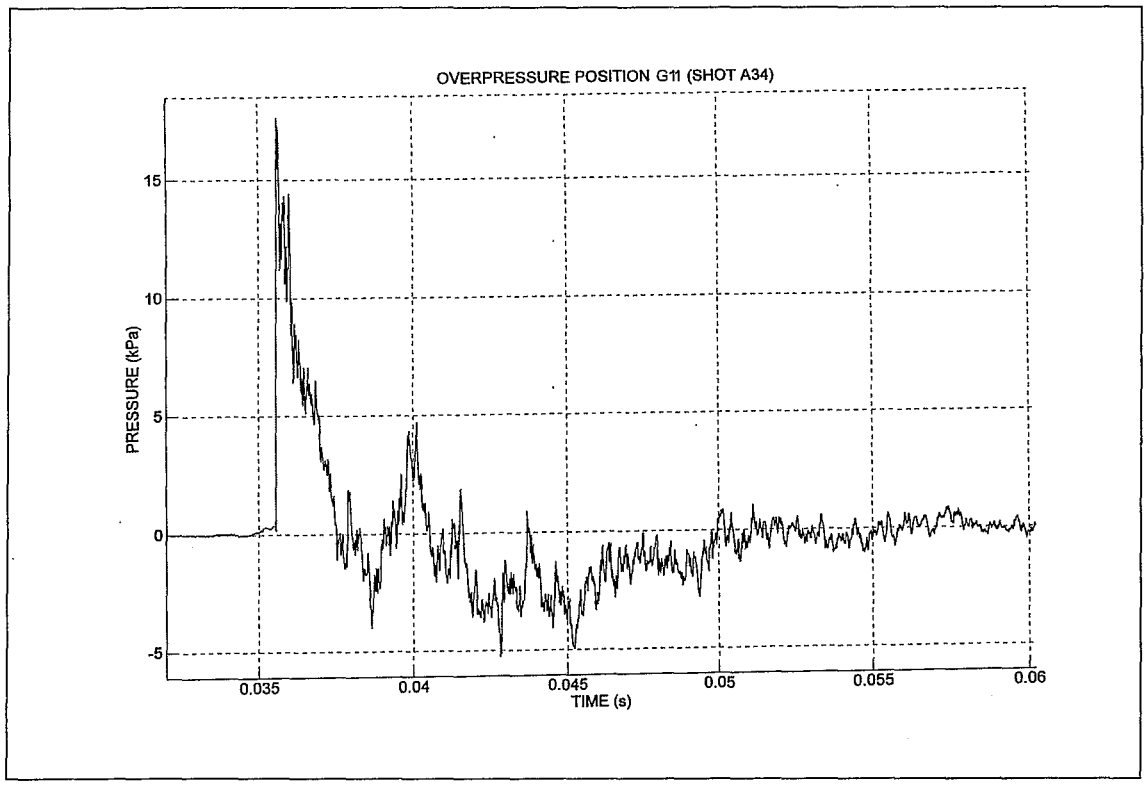

Figure I9. Overpressure position G11

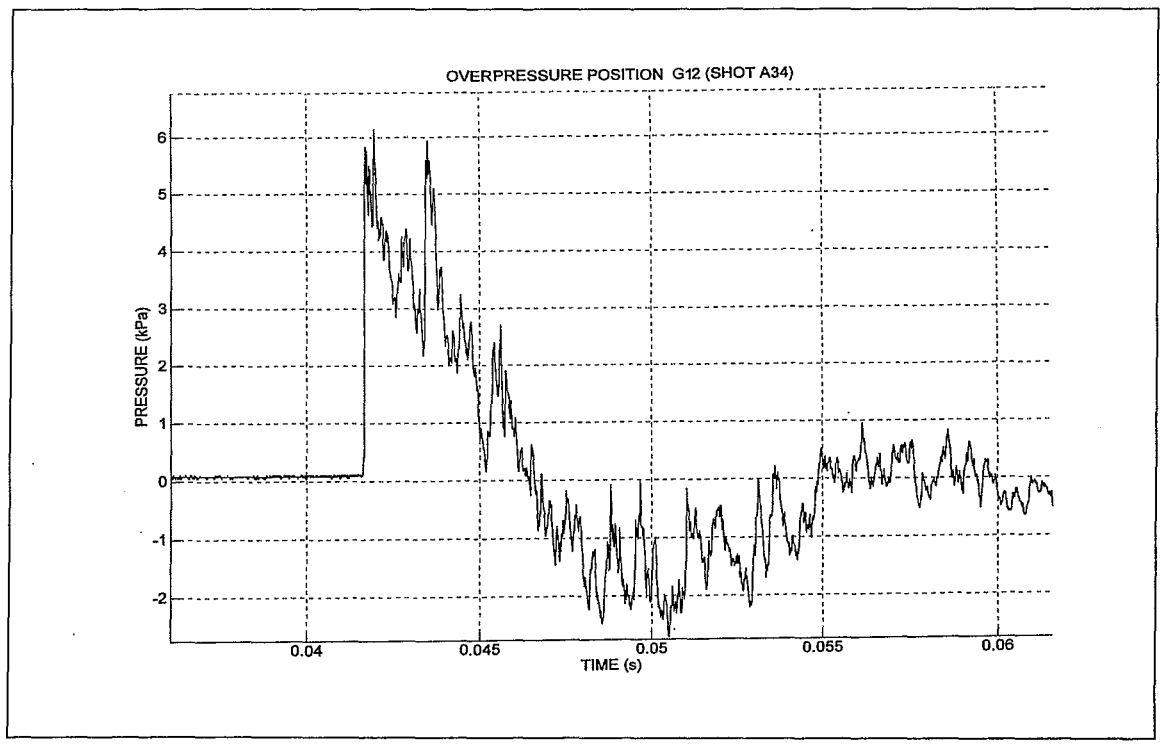

Figure I10. Overpressure position G12

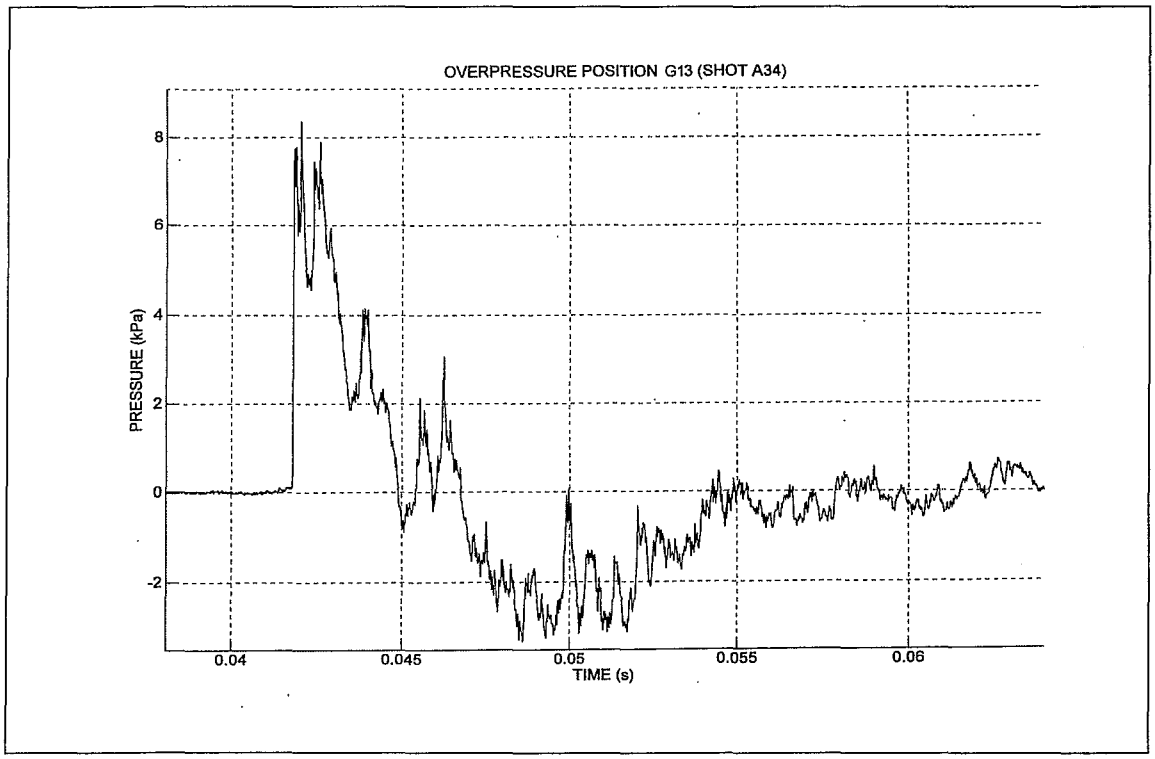

Figure I11. Overpressure position G13

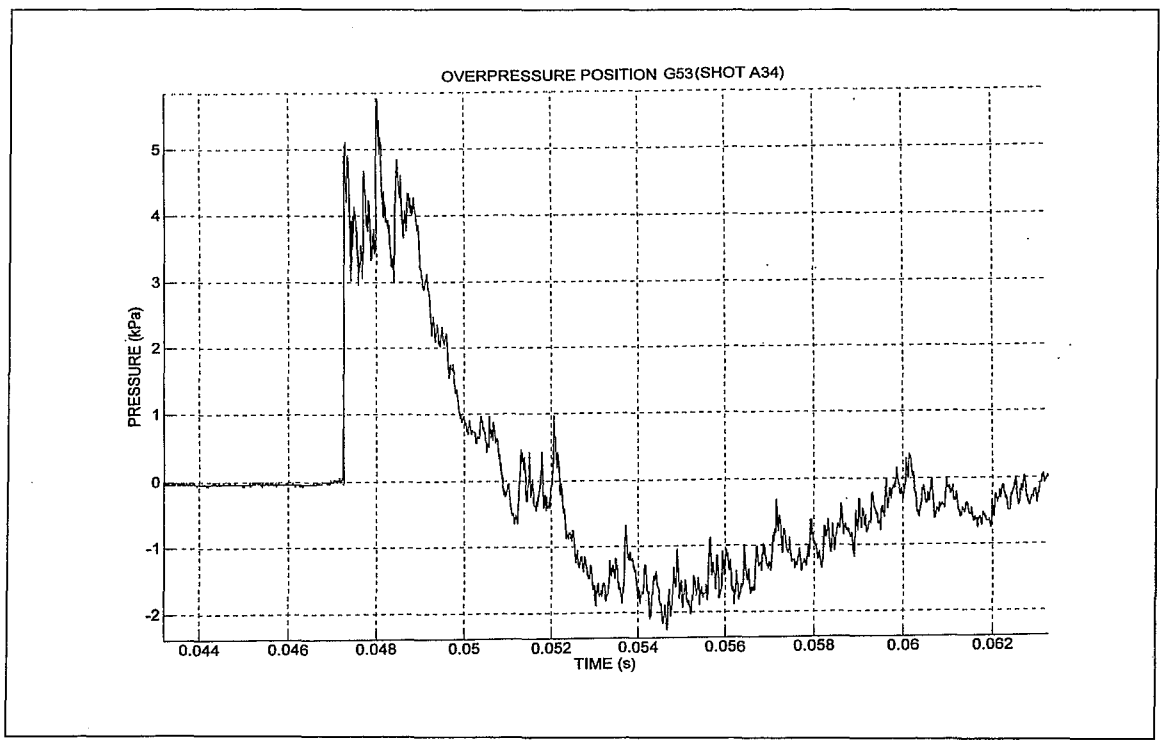

Figure I12. Overpressure position G53

Appendix J

Traces of trial data of Version 4 active – Phase 2.

Traces of the important parameters verified during the trial of phase 2 for version 4 as an active muzzle brake – shot 42 is presented.

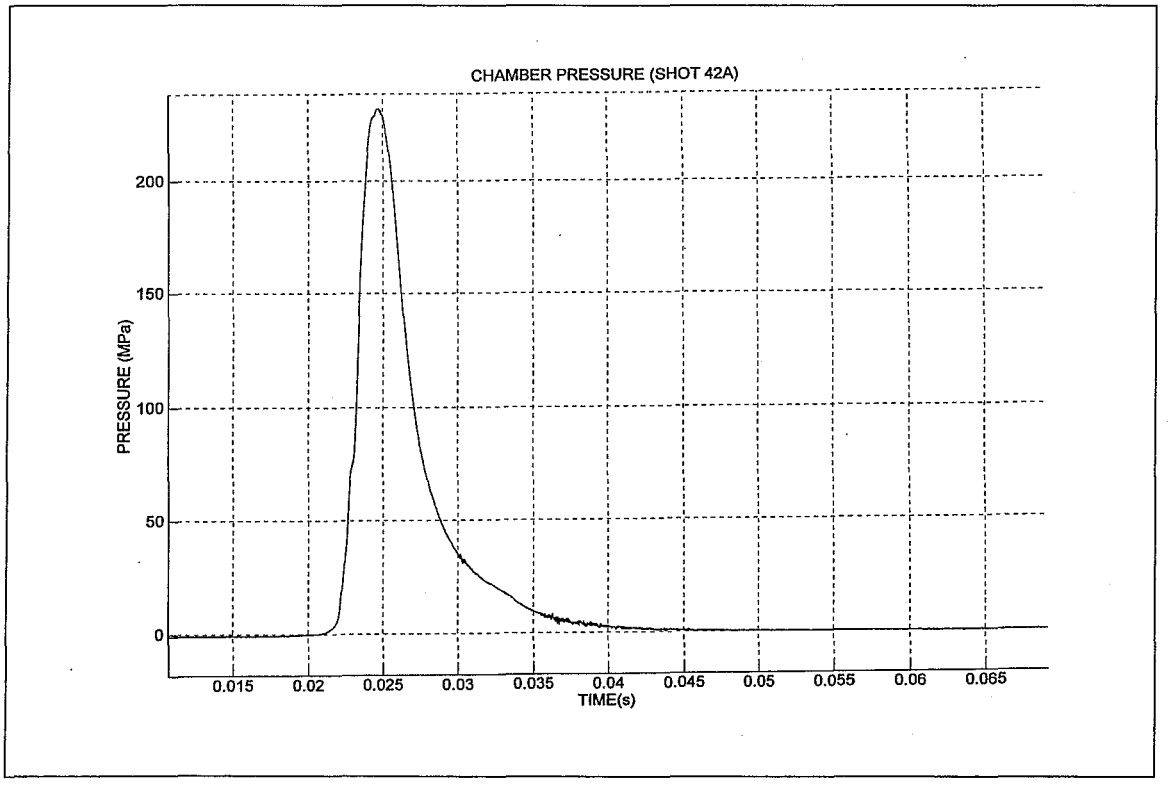

Figure J1. Chamber pressure

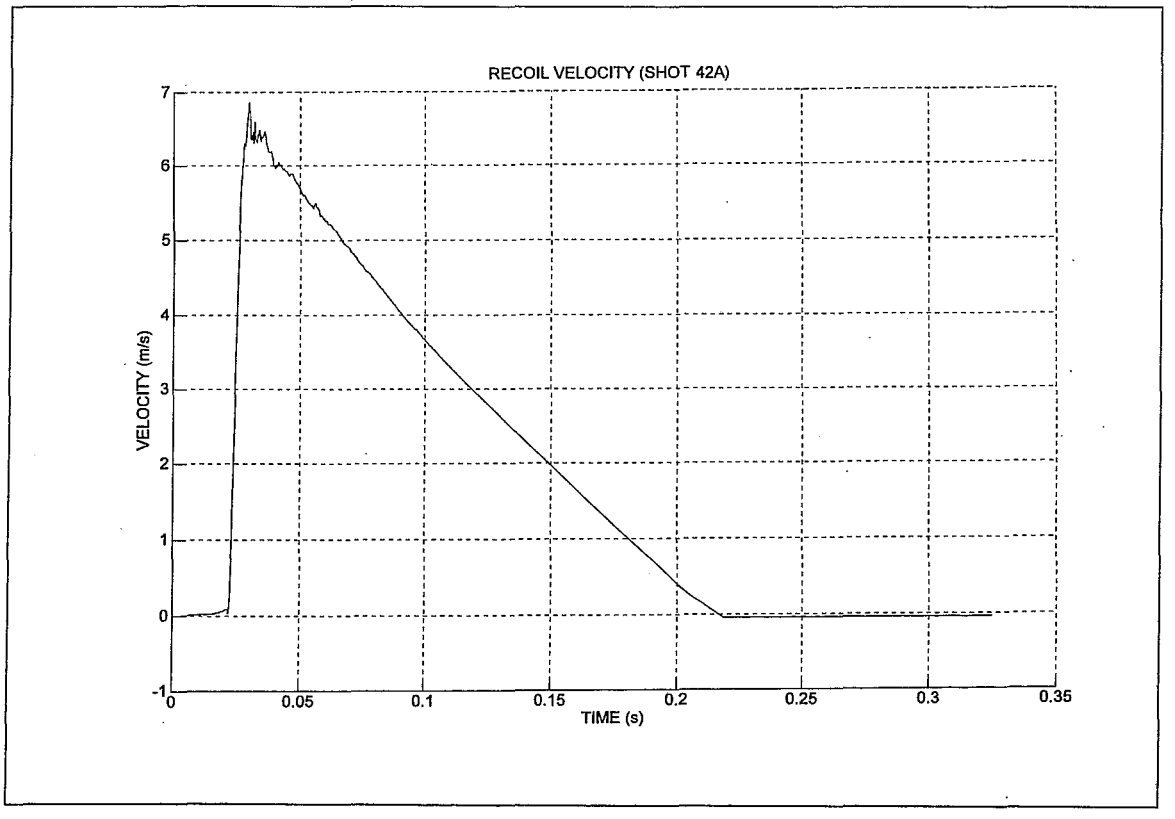

Figure J2. Recoil velocity

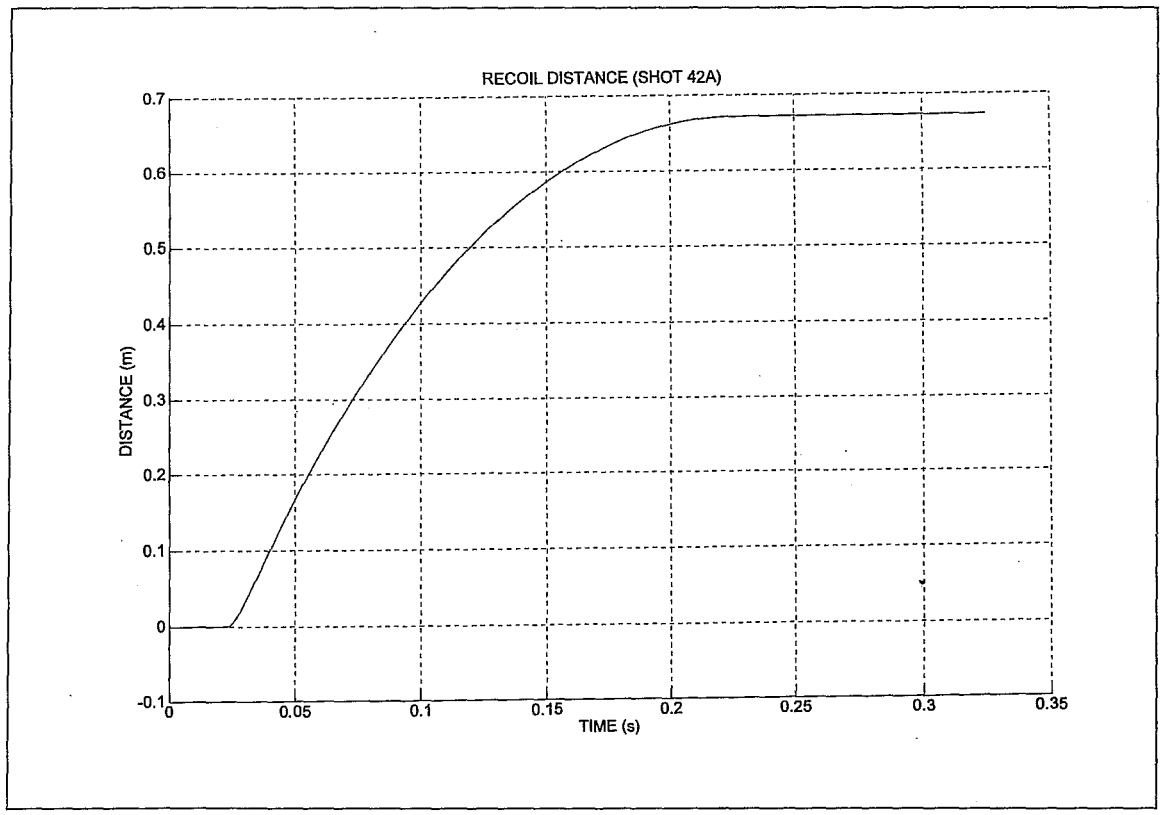

Figure J3. Recoil displacement

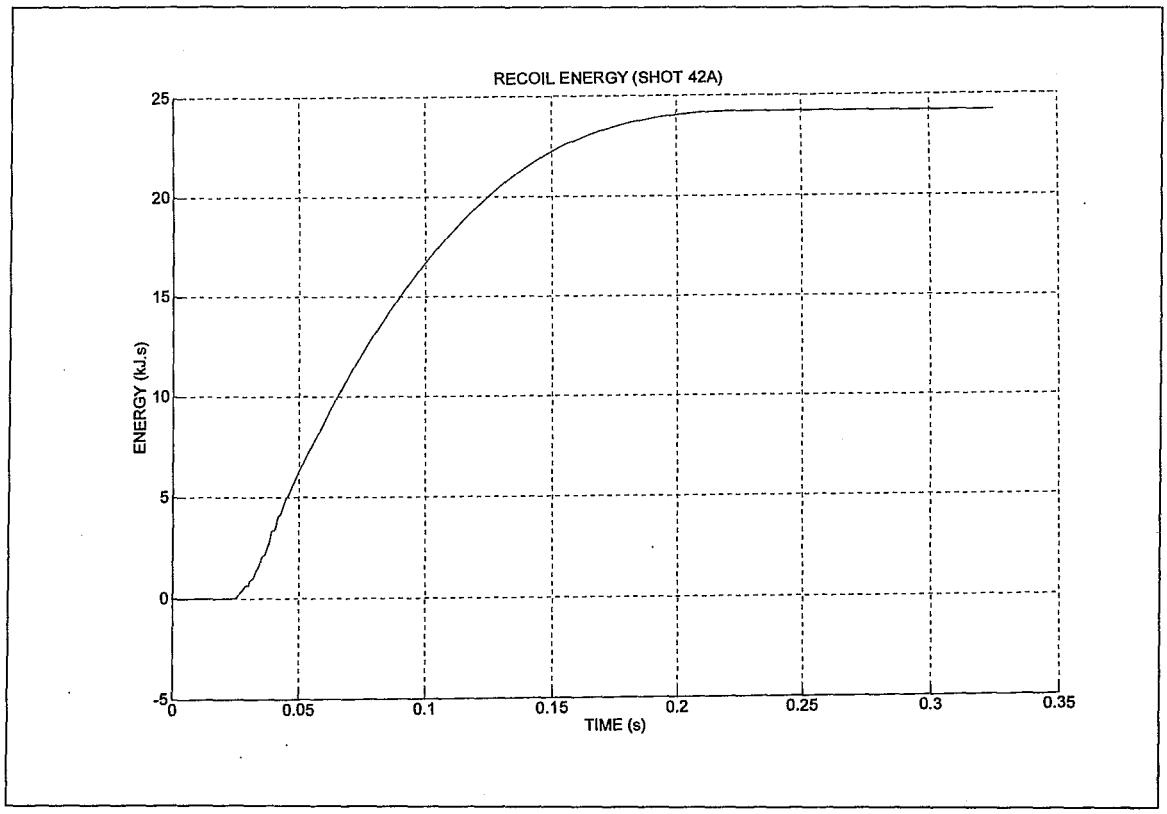

Figure J4. Recoil energy

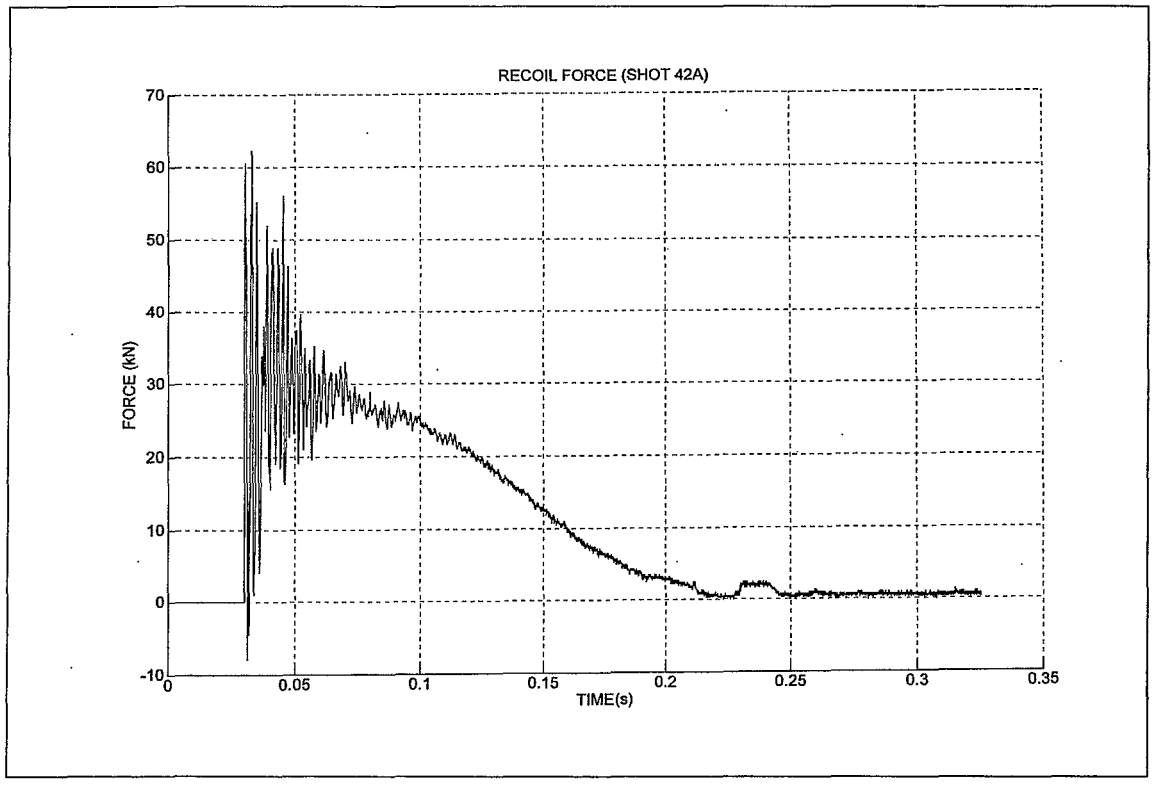

Figure J5. Recoil force

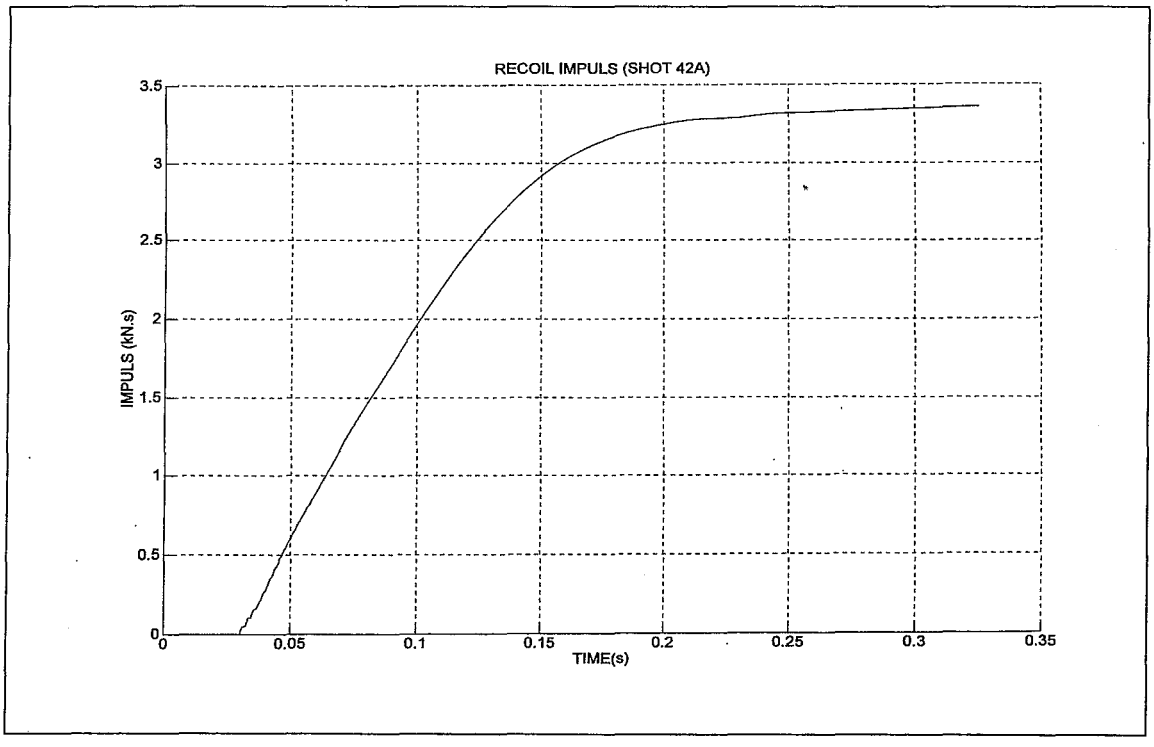

Figure J6. Recoil impulse

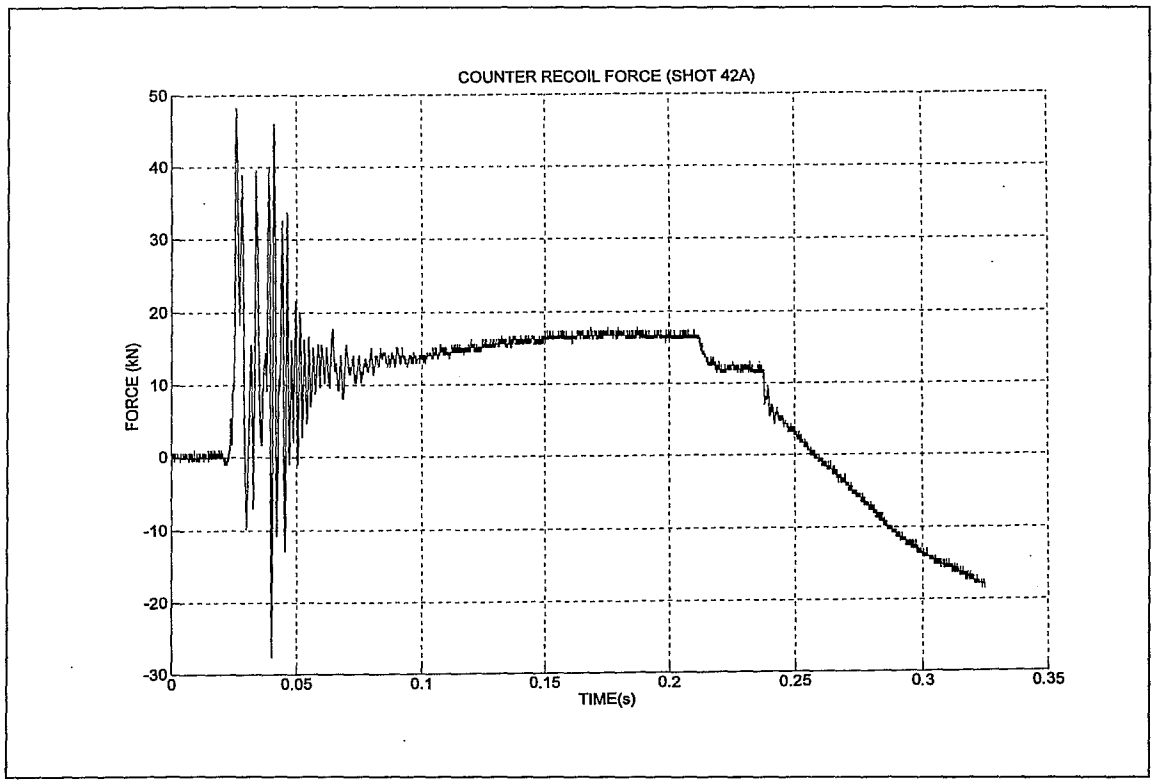

Figure J7. Counter recoil force

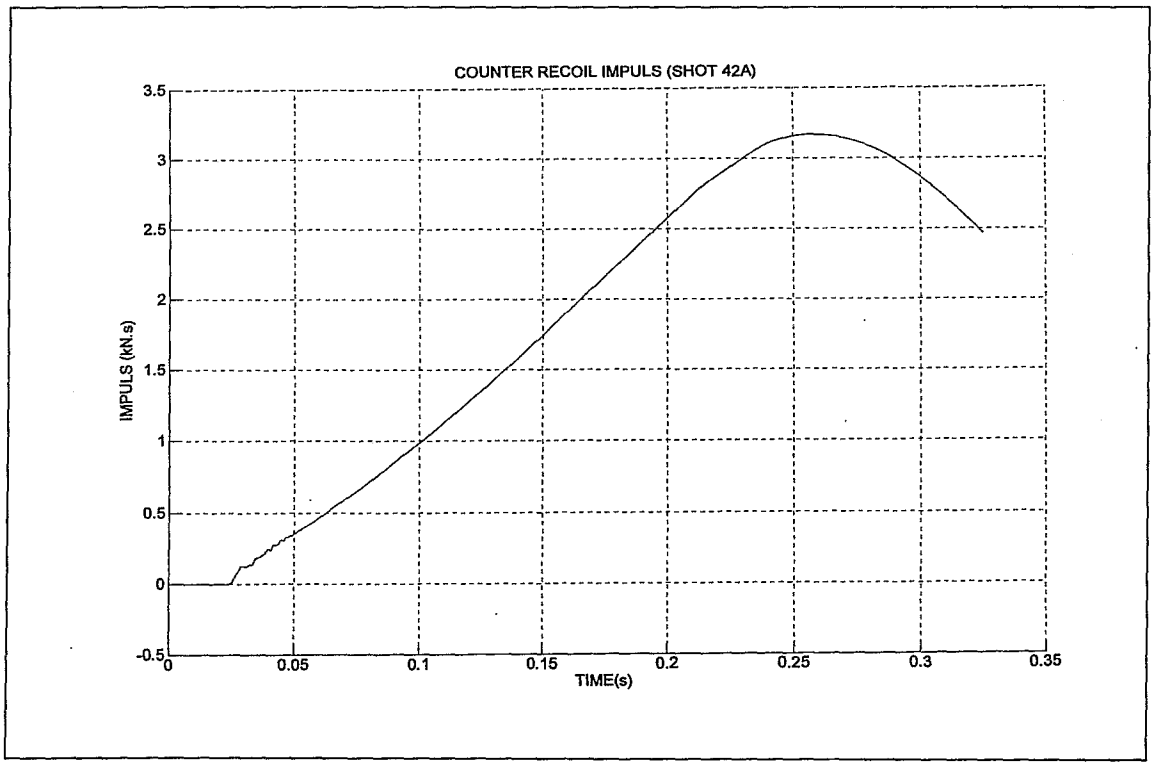

Figure J8. Counter recoil force

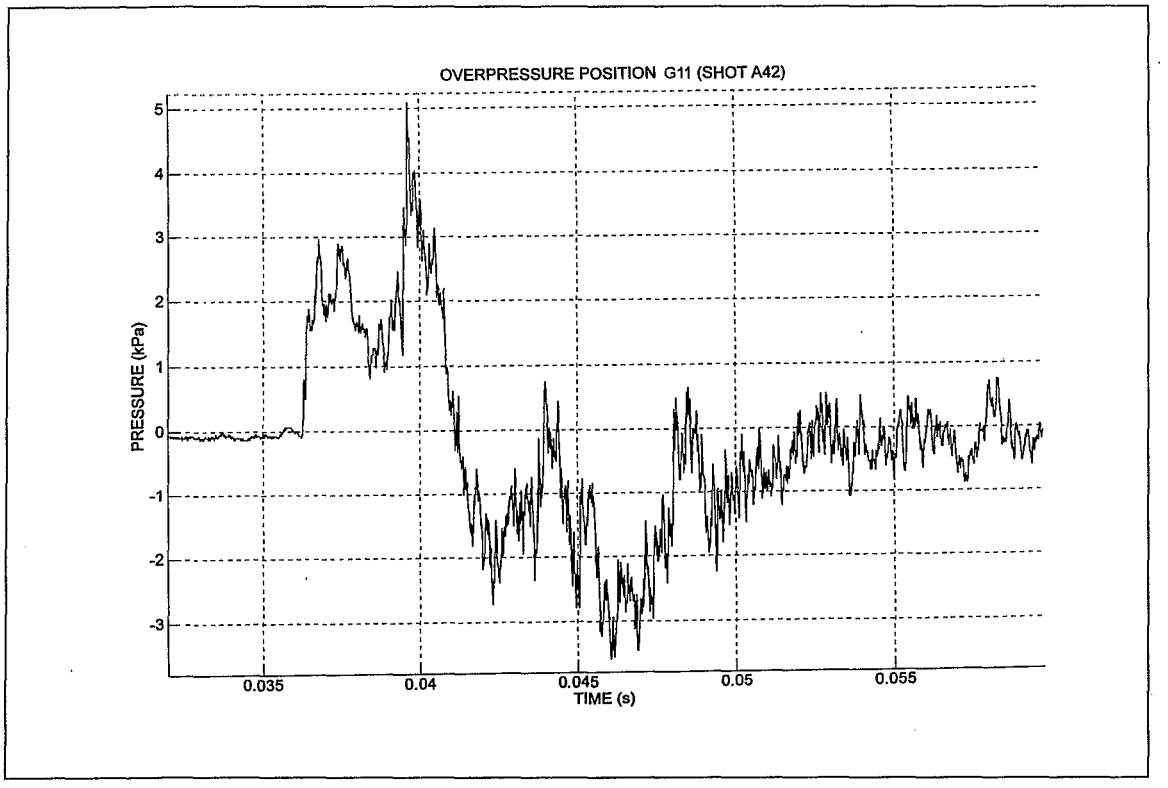

Figure J9. Overpressure position G11.

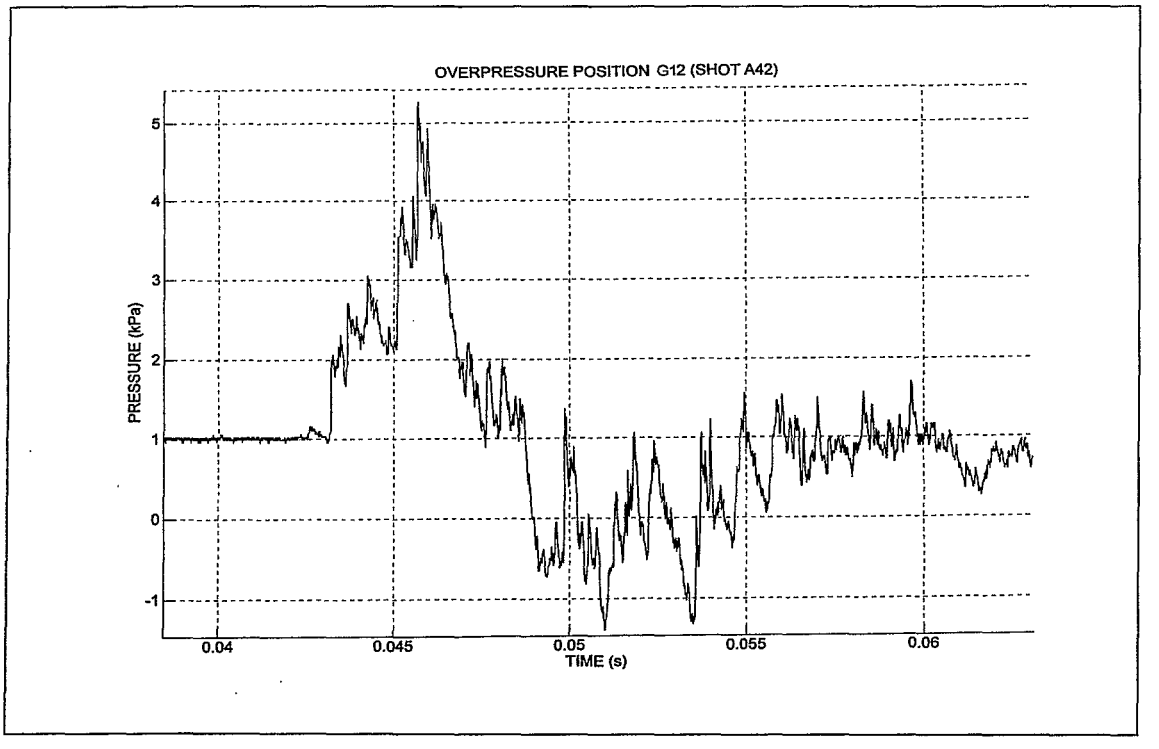

Figure J10. Overpressure position G12.

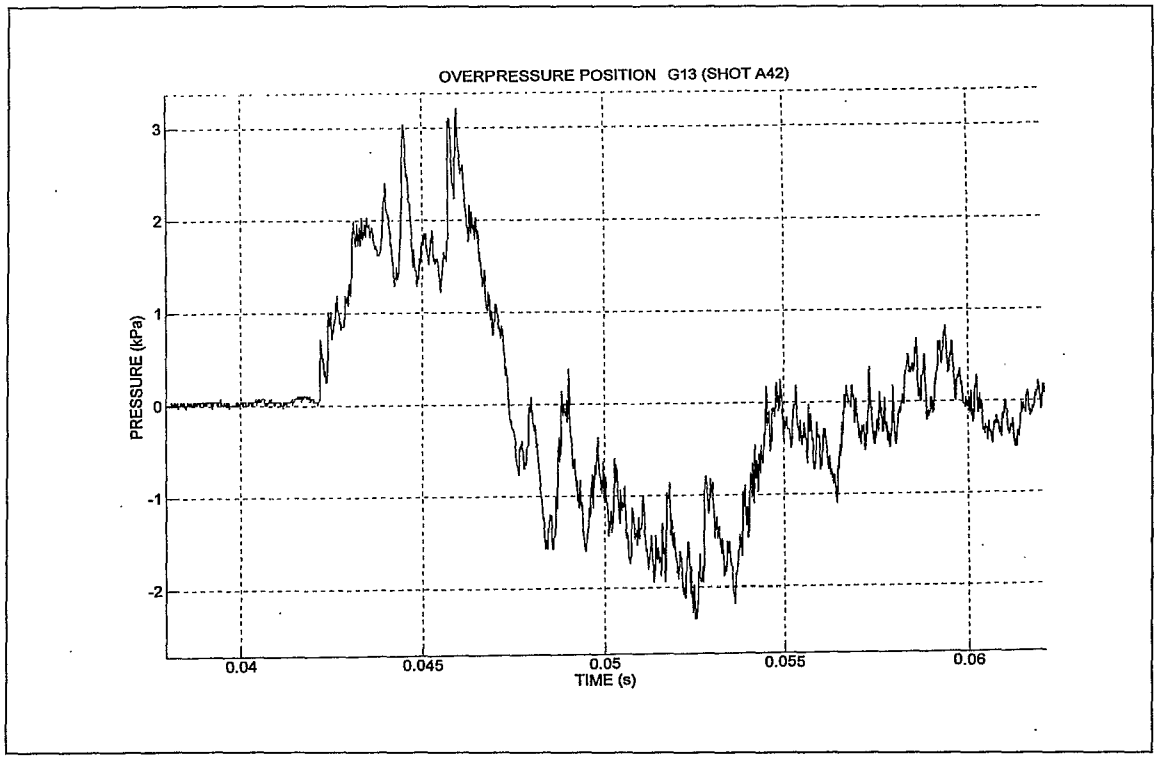

Figure J11. Overpressure position G13.

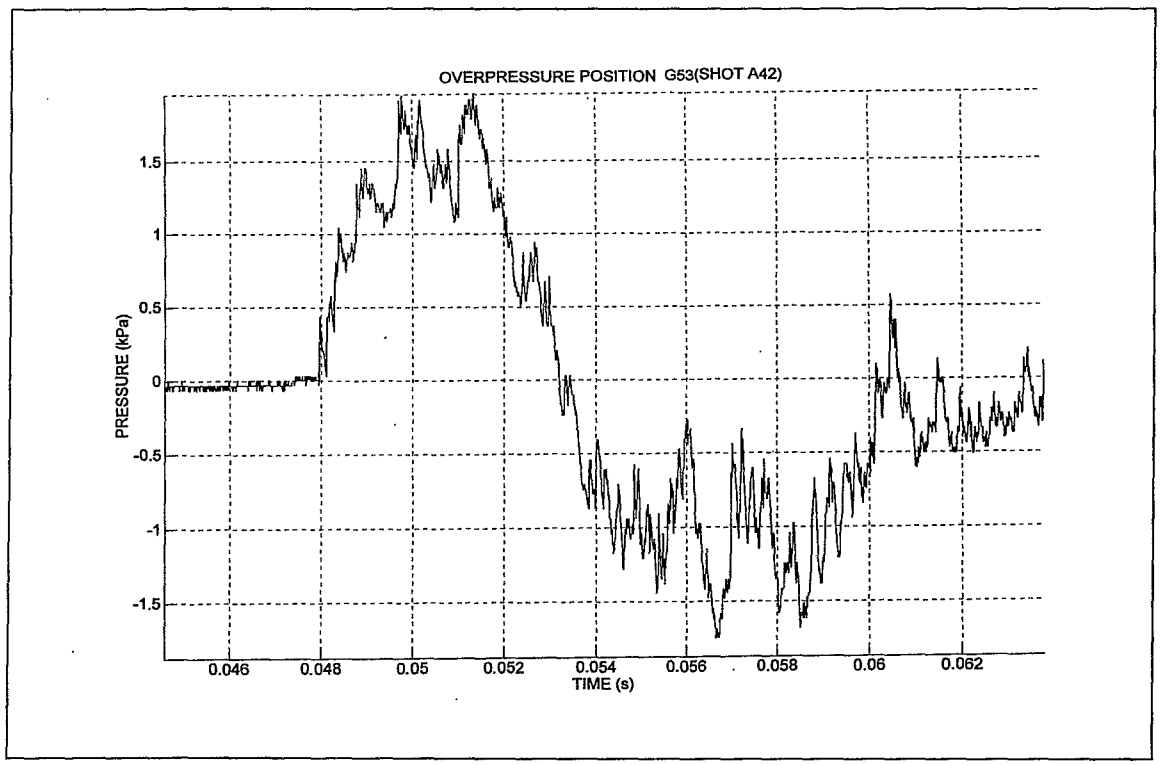

Figure J12. Overpressure position G53.

Appendix K

Traces of dynamic body movement – Phase 2.

Traces of the response of the dynamic body of versions 3 and 4 are presented. The response is illustrated in respect to the muzzle pressure decay. The graphs display the start of the dynamic body movement by the "breakwire" position.

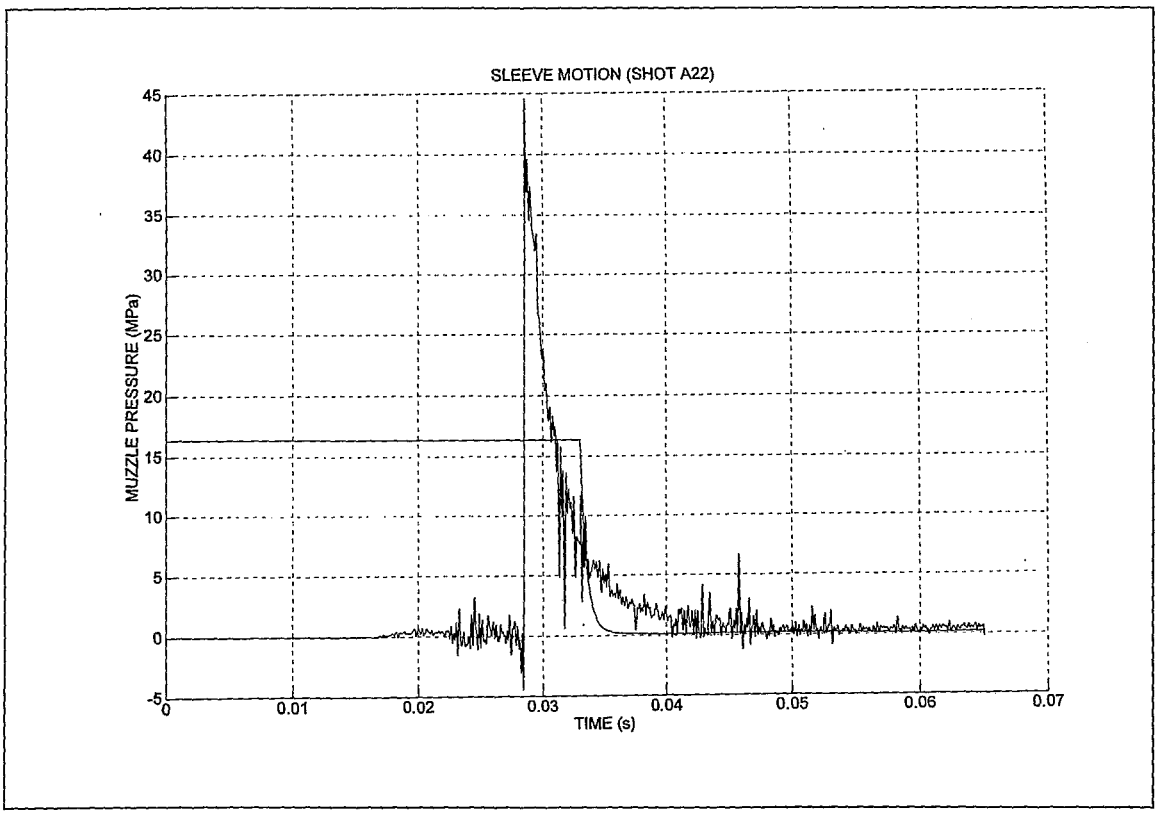

Figure K1. Dynamic body response – Version 3.

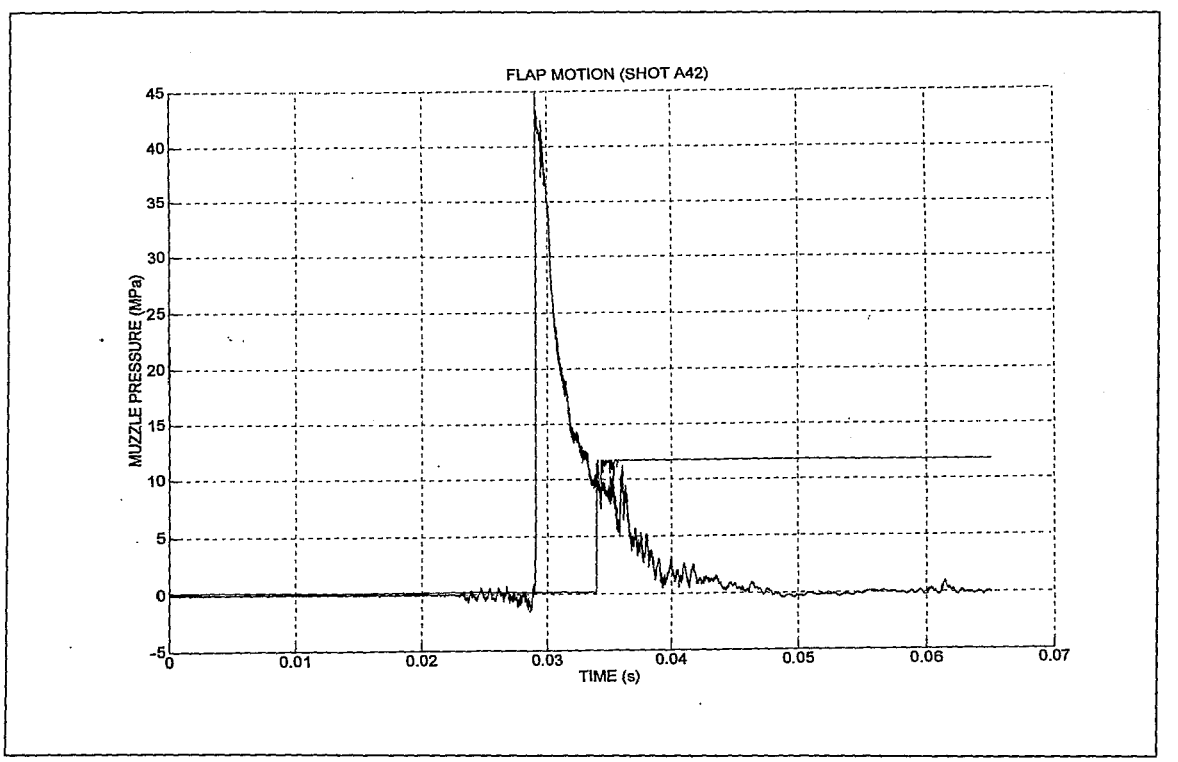

Figure K2. Dynamic body response – Version 4.